8-2014

Evaluation and Flight Assessment of a Scale Glider

Alvydas Anthony Civinskas
Embry-Riddle Aeronautical University - Daytona Beach

Evaluation and Flight Assessment of a Scale Glider

by

Alvydas Anthony Civinskas

A Thesis Submitted to the College of Engineering Department of Aerospace Engineering
in Partial Fulfillment of the Requirements for the Degree of
Master of Science in Aerospace Engineering

Embry-Riddle Aeronautical University
Daytona Beach, Florida
August 2014

Evaluation and Flight Assessment of a Scale Glider

by

Alvydas Anthony Civinskas

This thesis was prepared under the direction of the candidate's Thesis Committee Chair, Dr. William Engblom, Professor, Daytona Beach Campus, and Thesis Committee Members Dr. Hever Moncayo, Professor, Daytona Beach Campus, and Dr. Anastaios Lyrintzis, Professor, Daytona Beach Campus, and has been approved by the Thesis Committee. It was submitted to the Department of Aerospace Engineering in partial fulfillment of the requirements for the degree of Master of Science in Aerospace Engineering

Thesis Review Committee:

William Engblom, Ph.D.
Committee Chair

Hever Moncayo, Ph.D.
Committee Member

Anastaios Lyrintzis, Ph.D.
Committee Member

Yi Zhao, Ph.D.
Graduate Program Chair,
Aerospace Engineering

Anastaios Lyrintzis, Ph.D.
Department Chair,
Aerospace Engineering

Maj Mirmirani, Ph.D.
Dean, College of Engineering

for Robert Oxley, Ph.D.
Associate Vice President of Academics

8/12/2014
Date

Acknowledgements

The first person I would like to thank is my committee chair Dr. William Engblom for all the help, guidance, energy, and time he put into helping me. I would also like to thank Dr. Hever Moncayo for giving up his time, patience, and knowledge about flight dynamics and testing. Without them, this project would not have materialized nor survived the many bumps in the road.

Secondly, I would like to thank the RC pilot Daniel Harrison for his time and effort in taking up the risky and stressful work of piloting. Individuals like Jordan Beckwith and Travis Billette cannot be forgotten for their numerous contributions in getting the motor test stand made and helping in creating the air data boom pod so that test data.

Thirdly, I cannot forget the help from Jade McClanahan, Israel Mogul, Andres Perez, and Dr. Glenn Greiner for their input and insight.

Lastly, I cannot forget the people who supported me throughout this project: my family, Michael Carkin, Aliraza Rattansi, Tsewang Shrestha, Killian Marie, and Mohannad Mahdi.

“In theory, there is no difference between theory and practice. But in practice, there is.”
— Yogi Berra

Abstract

Researcher: Alvydas Anthony Civinskas

Title: Evaluation and Flight Assessment of a Scale Glider.

Institution: Embry-Riddle Aeronautical University

Degree: Master of Science in Aerospace Engineering

Year: 2014

The objective of this project is to do a flight assessment of a Phoenix K8B radio controlled glider to see what process is needed to verify its glide slope and stability characteristics. The flight test analysis, plus a computational fluid dynamics analysis, and an industry-like component build-up aerodynamic analysis were done to provide comparable estimates for the aircraft glide slope. A stability and control derivative analysis was also completed and compared using SURFACES, USAF Datcom, and MIT AVL software. The glide slope estimate and stability and control derivatives obtained from flight test data showed considerable range and uncertainty. Potential sources of noisy test data and model flaws are discussed in detail. Improvements to the flight test capability are suggested.

Table of Contents

List of Tables

Page

Table

List of Figures

Page

Figure

Nomenclature

D_{cg}: distance of center of gravity

W_T: total weight of aircraft

W_n: weight of nose section

W_t: weight of tail section

d_n: distance of nose weight measurement

d_t: distance of tail weight measurement

ID: inner diameter

OD: outer diameter

L: length

x,y,z: measurement quantities

Δx, Δy, Δz: errors associated with quantities measured

ζ: damping ratio

T: thrust

T_0: static thrusat

W: weight

S: planform area

ρ: air density at sea level

C_{L_g}: ground coefficient of lift

C_{D_g}: ground drag coefficient

a: constant with units of lb*s2/ft2

μ: runway friction coefficient

V: velocity

V_{T0}: take off velocity

g: acceleration due to gravity

List of Acronyms and Abbreviations

CFD: Computational Fluid Dynamics

DAP: Dual Aircraft Platform

UAV: Unmanned Ariel Vehicle

RC: Radio Controlled

ARFT: Almost Ready to Fly

HQ: Helmut Quabeck

CG: Center of Gravity

FBD: Free Body Diagram

APM: Ardupilot Mega

IMU: Inertial Measurement Unit

GPS: Global Positioning System

SSH: Secure Shell

IDE: Integrated Development Environment

AoA: Angle of Attack

AoY: Angle of Yaw

EFRC: Eagle Flight Research Center

NURB: Non-uniform Rational B-spline

CATIA: Computer Aided Three-dimensional Interactive Application

NACA: National Advisory Commit for Aeronautics

USAF: United States Air Force

VLM: Vortex Lattice Method

ID: Inner Diameter

OD: Outer Diameter

LE: Leading Edge

ICAO: International Civil Aviation Organization

NP: Neutral Point

RMS: Root Mean Square

1. Introduction

The objective of this project is to compare the results of the glide slope among flight-testing, computational fluid dynamics (CFD), and a conventional aerodynamic build-up approach for a scale model powered glider. This assessment is relevant because determining the accuracy will influence a designer's reliance on a particular method in predicting the glide slope of an aircraft. The motivation for this project is the Dual Aircraft Platform (DAP) configuration that relies heavily on a high lift-to-drag ratio to permit sailing type operation within the stratosphere using the least possible use of energy to stay aloft [28]. The lower the glide slope for the design translates into a higher available wind shear needed for the DAP to be an effective atmospheric satellite therefore potentially limiting the area where the DAP could be used [4]. In essence, knowing an accurate glide slope is crucial for the operating capability for the DAP [4].

Recently, both Google and Facebook acquired drone companies so that both companies could utilize these atmospheric satellites to increase access to the Internet [12, 13]. Google specifically bought Titan Aerospace for that purpose [12]. The Titan Solara can cover as much ground as 100 based towers and carry a capacity of 70lb with the Solara 50 and 250lbs with the Solara 60 model [12]. Figure 1 shows Lockheed's, Titan's, and Ascenta's concepts for atmospheric satellites, respectively.

Figure 1: From left to Right - Lockheed Martin Hale-D, Titan Aerospace Solara, and Ascenta [14 ,12 , 13]

2. Methodology

2.1. Airframe Analysis

A previous graduate student at Embry Riddle provided a design of the aircraft. It utilized a tandem wing configuration to maximize lift by using the Wortmann FX 63-137 airfoil and is shown in Figure 2 [4]:

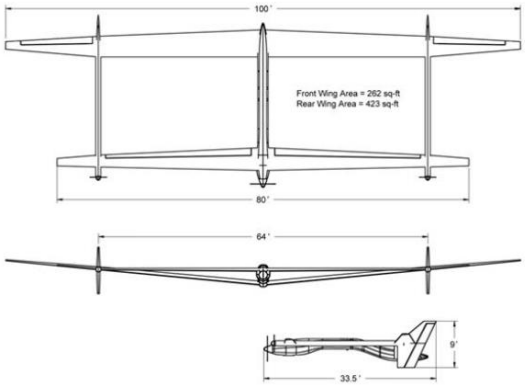

Figure 2: Previous aircraft design work [4].

Due to the limited funding available to build the unmanned aerial vehicle (UAV) from scratch utilizing carbon fiber, it was decided to find a pre-existing design on the market that satisfied the 2 m^2 wing planform area needed to satisfy the goals of the DAP program for a sub-scale aircraft. The Phoenix model K8B 6m almost ready to fly (ARFT) was chosen primarily for its wing area of 2.26 m^2 (3503 in^2) and airframe price. This model is a 40% scaled version of the Alexander Schleicher Ka 8b glider [3, 6]. This radio controller (RC) glider uses the HQ 3/15 airfoil, which the outline of the airfoil is depicted in Figure 3:

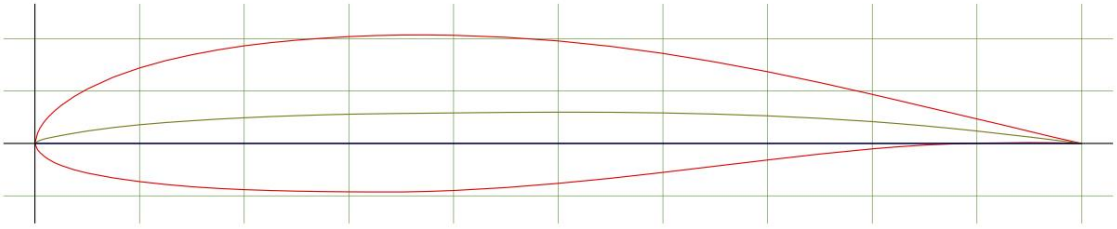

Figure 3: HQ 3.0/15.0 airfoil profile [9]

This airfoil also goes under the names of HQ 3.0/15.0 and HQ 3015. Table 1 shows the specifications of the model selected from the Phoenix Model website:

Phoenix K8b - 6m Specifications	
Wing Span	6m
Wing Area	219.4 dm^2
Length	2873mm
Wing Loading	64 g/dm^2
Flying Weight	14-18 kg
Scale	1/2.5
Wing Airfoil	HQW 3/15 [35]

Table 1: Basic Dimensions of K8b RC Glider [6]

Figure 4 shows the assembled glider.

Figure 4: Fully assembled glider

2.2 Center of Gravity Calculation

A critical piece of information for an aircraft is the location of the center of gravity (CG). To find the CG, the Computerscales AccuSet instrument pictured in Figure 5 was used:

Figure 5: Computerscales AccuSet [19]

One scale was placed below the tail section while another was placed under the cockpit. Any piece of equipment that was going to be utilized in the UAV was put into its place as and assembled as shown in Figure 6:

Figure 6: Glider on the scales

The total weight was found to be 35 lbs with a 34 lb reading on the front scale. To find the CG, the basic moment equation, as shown in equation 1, was used:

$$d_{CG}W_T = \sum_{i}^{n}(wd)_i \tag{1}$$

Figure 7 shows the free body diagram (FBD) of the glider on the weight plates:

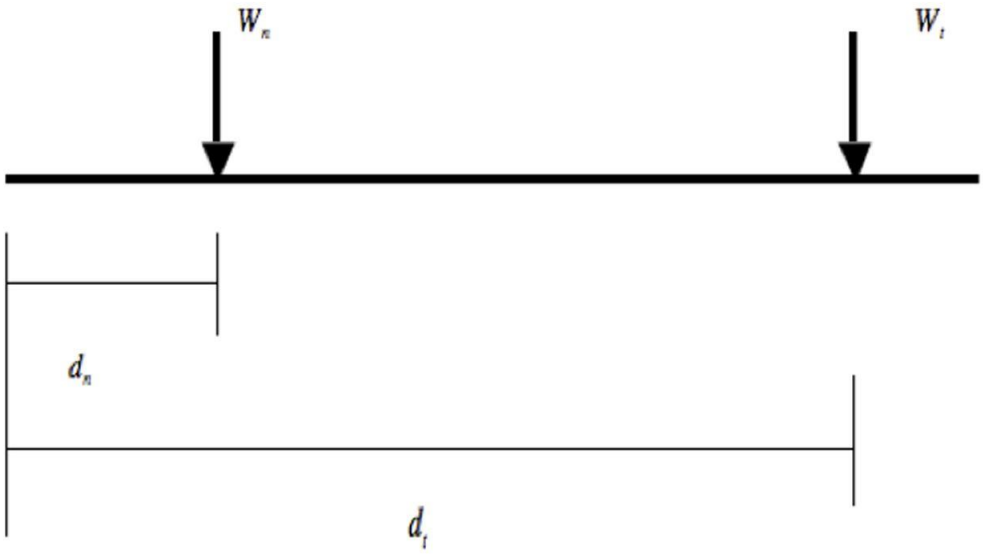

Figure 7: FBD to figure out the CG

In this case, equation 2 can be expanded into the following:

$$d_{CG}W_{TOT} = d_n w_n + d_t w_t \tag{2}$$

Plugging in the corresponding values:

$$d_{cg}(35lb) = (30in)(34lb) + (96in)(1lb) \tag{3}$$

$$d_{cg} = \frac{(30in)(34lb) + (96in)(1lb)}{35lb} \tag{4}$$

$$d_{cg} = 31.89in \tag{5}$$

The recommended CG location is 150mm from the LE with a margin of +/- 5mm. [22]. Subtracting 26 inches from 31.89 gives a distance of 5.89 inches from the LE. The mean aerodynamic chord (MAC) was found to be 14.99 in. An estimation of where the neutral point (NP) must be calculated to find the static margin. An online calculator utilizing a panel method was used to find the AC at 3.75 inches aft of the LE while the NP was 7.82 inches [25]. Finding the difference between the CG and NP and dividing that result by the MAC found a static margin of 12.88% of the MAC. Since the configuration changed with a pound of weight added to the wing of the aircraft, only a quick calculation was made to see how much the CG moved. In this case, the static margin increased to 13.25%.

2.3 Electronics Arrangement

The overall schematic of all the electronics in the UAV is shown in Figure 8.

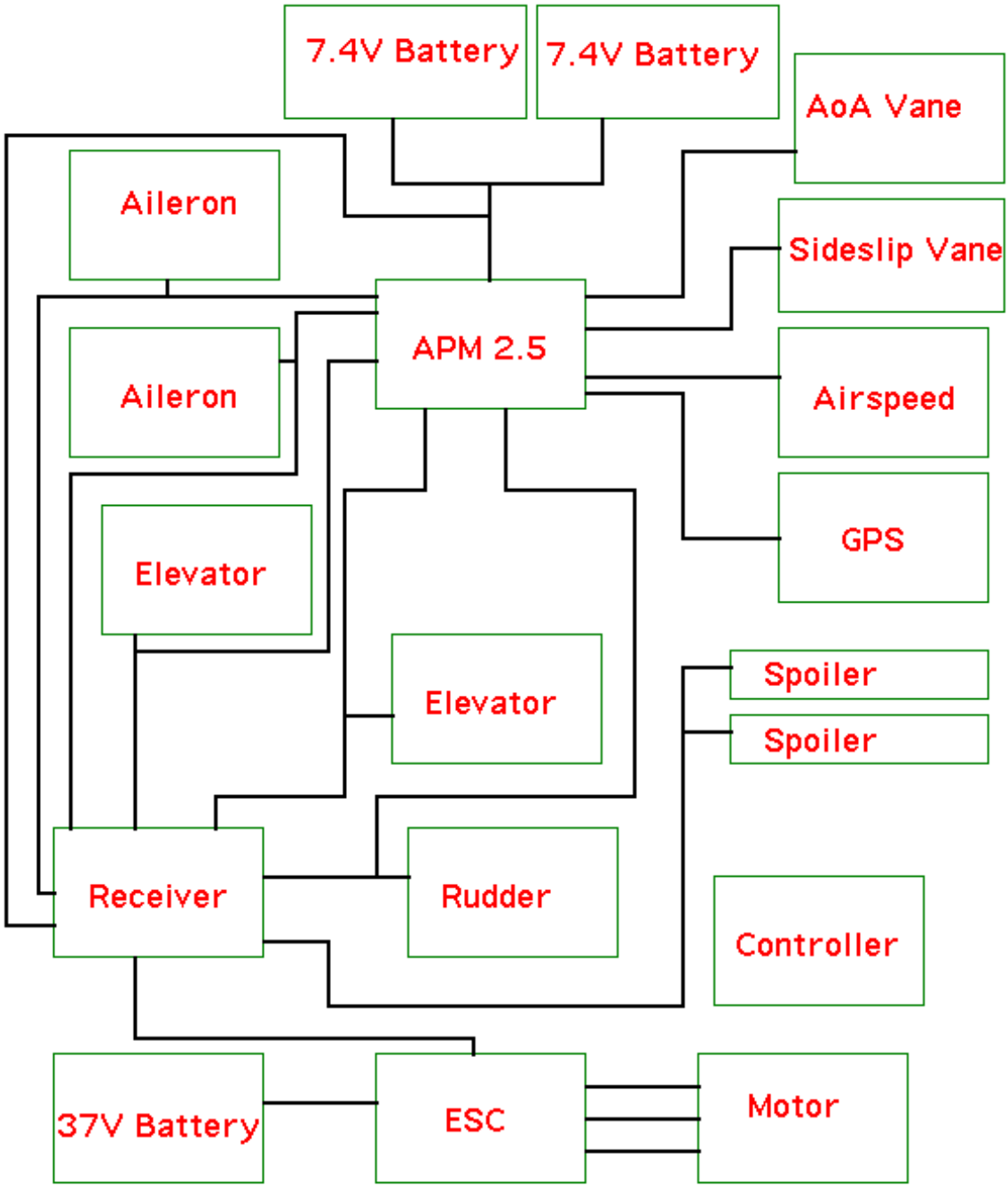

Figure 8: Electronic schematic

The servo signal had to be split using a Y-connector to send the signal to the APM 2.5. This was due to the servos drawing too much current when connecting to the APM 2.5 using all three leads and resulting in two corrupted APM 2.5 units. The parts used in the circuit are listed in Table 2:

Item Description	Model	Quantity	Function
Motor	Hacker A60-18L	1	Propulsion
ESC	Castle Creations Phoenix Edge 60HV 50V 60Amp	1	Speed control
LiPo 37.7V	Turnigy Nano-Tech 5000mah 10S LiPo Pack	1	Motor power supply
LiPo	7.4 V 2000mah	2 (in parallel)	Servo and flight computer power supply
Servo	Power HD Metal Gear Servo 60g/12.2kg/.16sec	5	Control surfaces
Spoiler	Spoilers/Air Brakes 440/16mm	2	Landing/replace flaps
Flight Computer	APM 2.5	1	Data recording
GPS	MediaTek MT3329	1	Position tracking
Airspeed Sensor	Airspeed Kit with MPXV7002DP	1	Pitot tube system
BEC	Castle Creations Castle BEC Pro V2	1	Battery Elimination Circuit
Potentiometers	963193-KIT-ND Digikey	1	Vane sensors
Receiver	User Choice	1	Receiver
Controller	User Choice	1	Transmitter

Table 2: Electronic item list

The schematic and electronic list for future configuration involving autopilot and tether are shown in Figure 9 and Table 3 respectively:

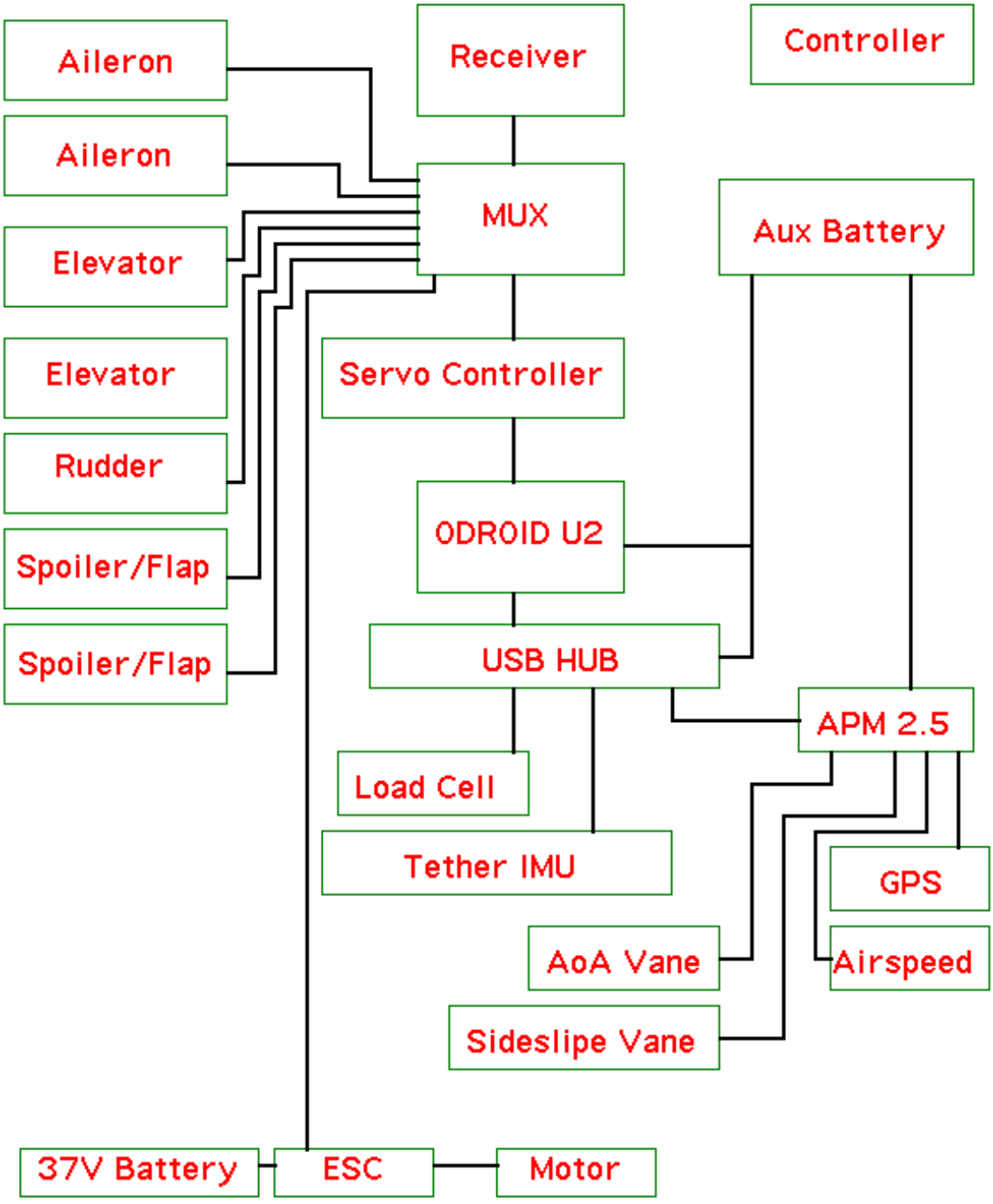

Figure 9: Upgradable electronic schematic

Item Description	Model	Quantity	Function
Motor	Hacker A60-18L	1	Propulsion
ESC	Castle Creations Phoenix Edge 60HV 50V 60Amp	1	Speed control
LiPo 37.7V	Turnigy Nano-Tech 5000mah 10S LiPo Pack	1	Motor power supply
Aux Battery		2	Servo, sensor, and flight computer power supply
Servo	Power HD Metal Gear Servo 60g/12.2kg/.16sec	5	Control surfaces
USB Hub	10 Port USB 2.0 Hub by FDL	1	USB Hub
16 Channel Servo Controller	Cytron SC16A	1	Servo Controller
ODROID U2	ODRIOD U2 - ULTRA COMPACT 1.7GHz QUAD-CORE BOARD	1	Flight computer
9 DoF IMU	9DOF Razor IMU	1	Tether IMU
Multiplexer (MUX)	Cytron 8 Channel RC RX Multiplexer	1	Switch between autopilot and manual control
Spoiler	Spoilers/Air Brakes 440/16mm	2	Landing/replace flaps
Flight Computer	APM 2.5	1	Data recording and autopilot
GPS w/ compass	uBlox LEA-6H module	1	Position tracking
Potentiometers	963193-KIT-ND Digikey	1	Vane sensors
BEC	Castle Creations Castle BEC Pro V2	1	Battery Elimination Circuit
Receiver	User choice	1	Receiver
Controller	User choice	1	Controller

Table 3: Electronic item list for autopilot and tethered configuration

2.4 Instrumentation

2.4.1 APM 2.5

The data collecting unit used for this project was the APM 2.5 loaded with a Mathworks Simulink toolbox created for the APM by previous Embry Riddle students called APM2 Simulink Blockset.

The blocks that were included were the IMU, GPS, barometer, and three analog inputs, and RC Read. For data recording, a 'Flash' block is required for data collection. The 'Serial Print Floats' block was used so that the data can be printed out as text using either Putty, an SSH secure wrapper, or the Arduino IDE at a serial baud rate of 115200. Figure 10 shows the Simulink model used for data recording:

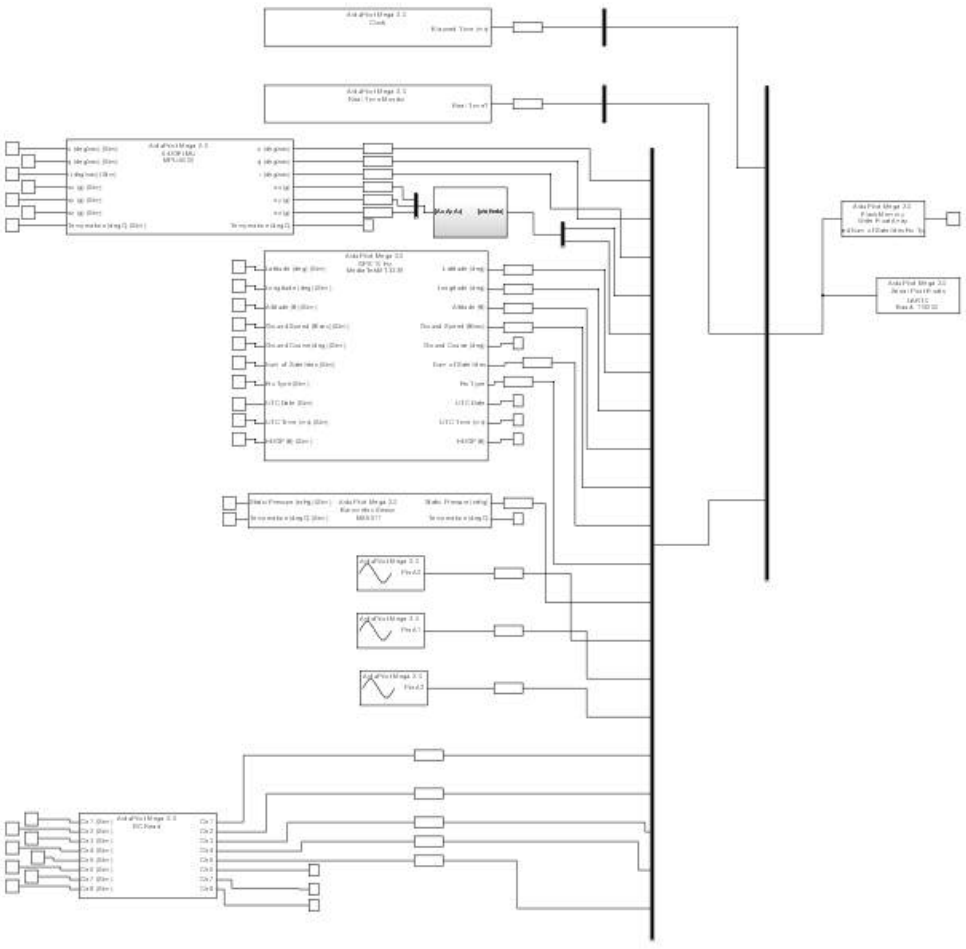

Figure 10: Overview of the Simulink wiring diagram for data recording

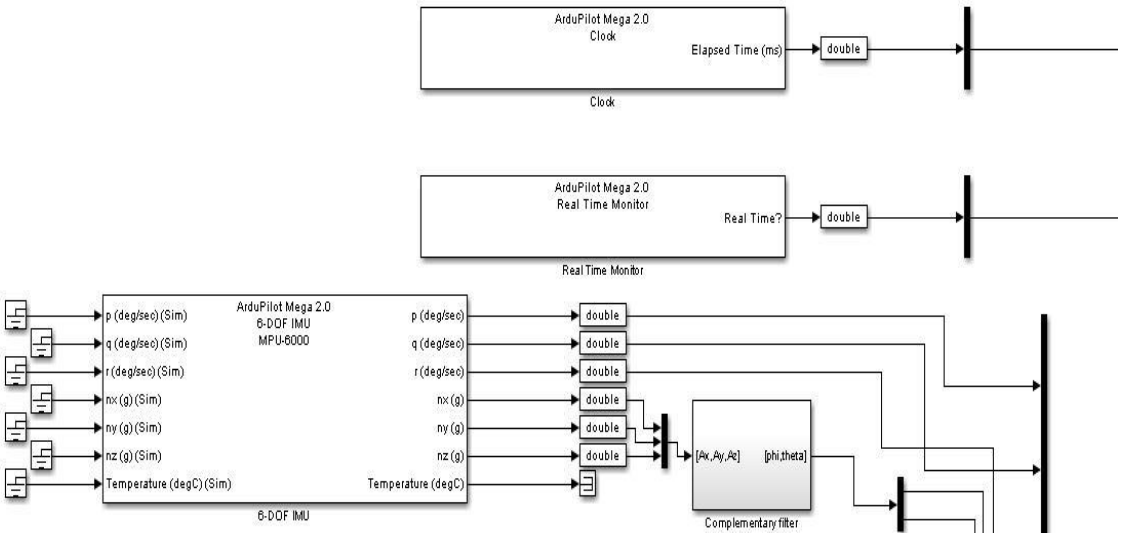

Figure 11: Blocks for clock, real time monitor, and the IMU with a complementary filter

The complementary filter was chosen because none of the sensors' data were used for navigation purposes [38]. The filter should have both accelerometer and gyro data feeding into it to calculate both phi and theta [36].

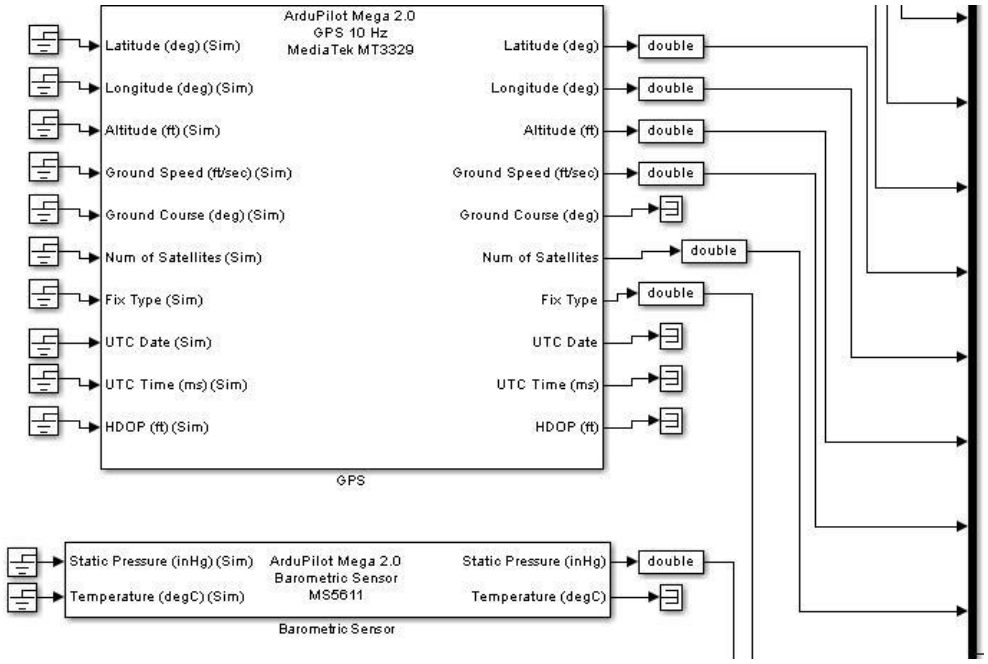

Figure 12: Part of the wiring diagram showing GPS and barometer

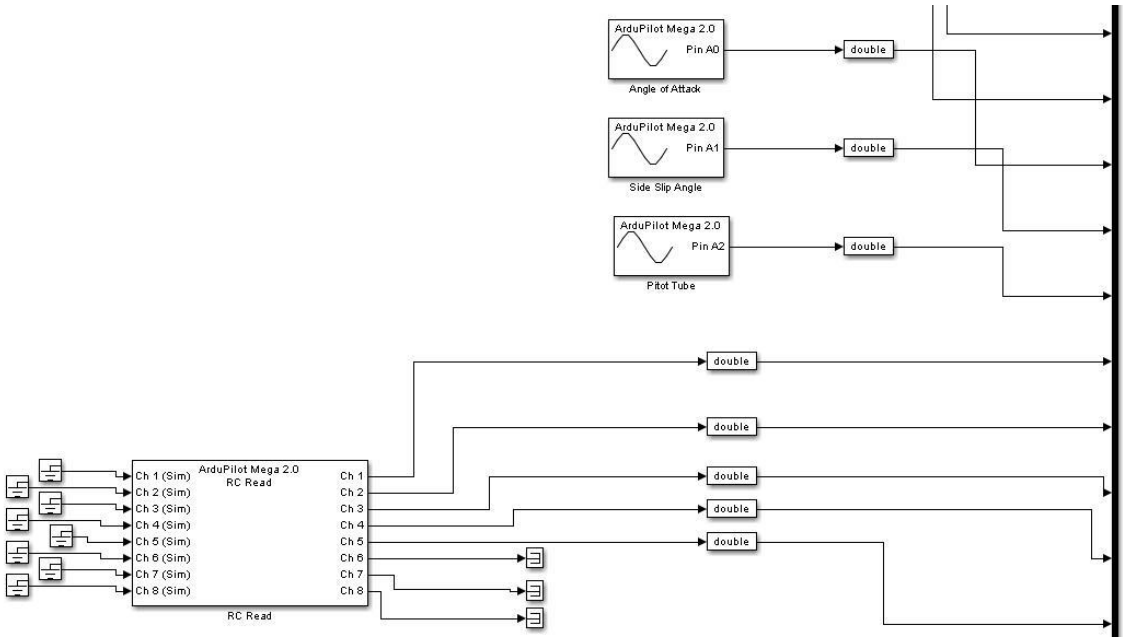

Figure 13: Part of schematic showing the three analog inputs - AoA, AoY, airspeed - and pilot inputs

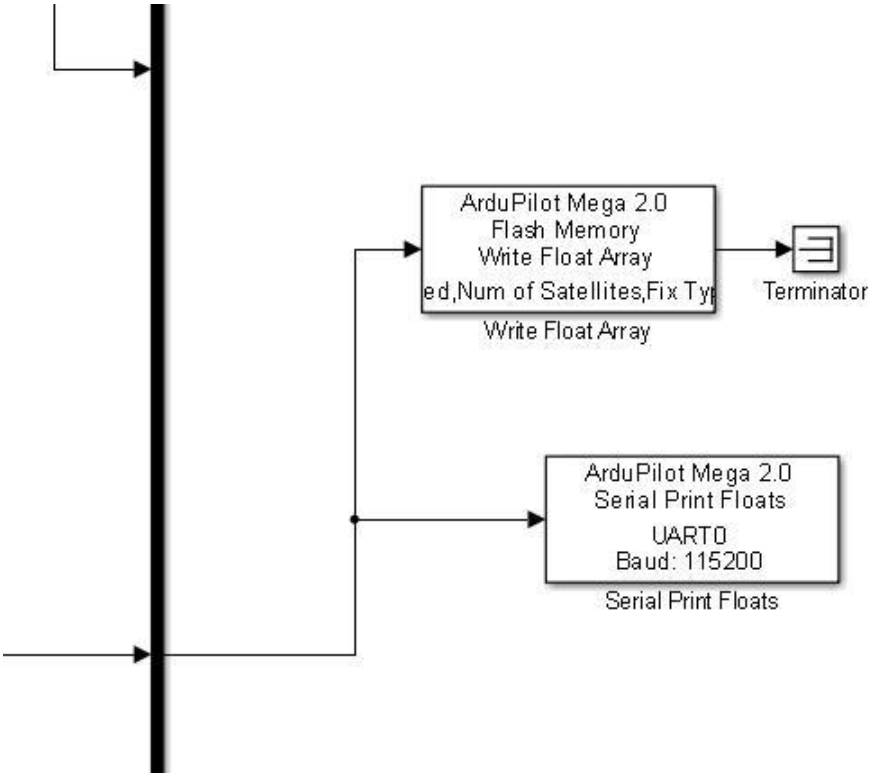

Figure 14: Blocks that print the data to IDE via serial and record data to flash memory

2.4.2 Air Data Boom

The air data boom consists of two potentiometers from CTS Electrocomponents, two 3D printed vanes, two 3D printed pieces for the boom structure, and an airspeed sensor kit from 3Drobotics that included a Pitot static tube. Figure 15 shows the pieces that make up the air data boom in the wind tunnel:

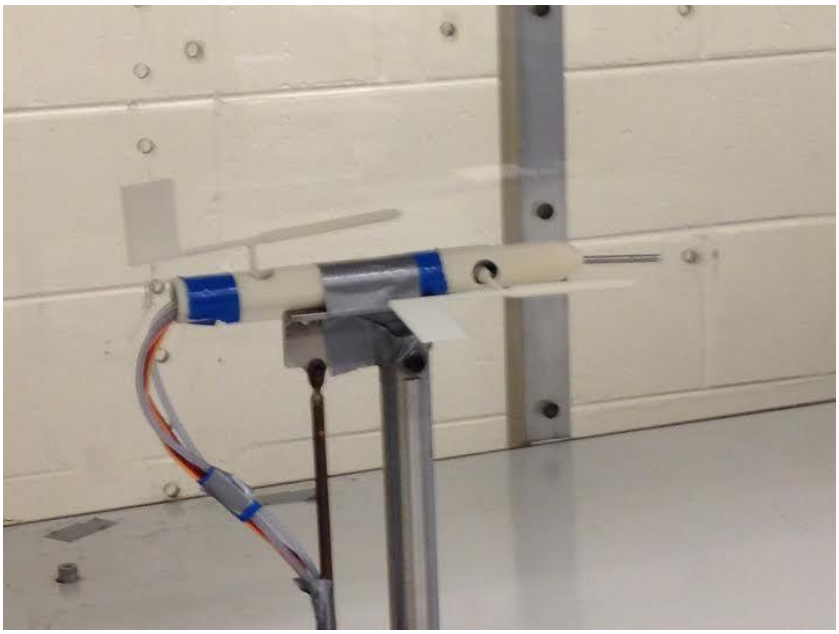

Figure 15: Air Data vane assembly with AoA vane, AoY vane, and Pitot system

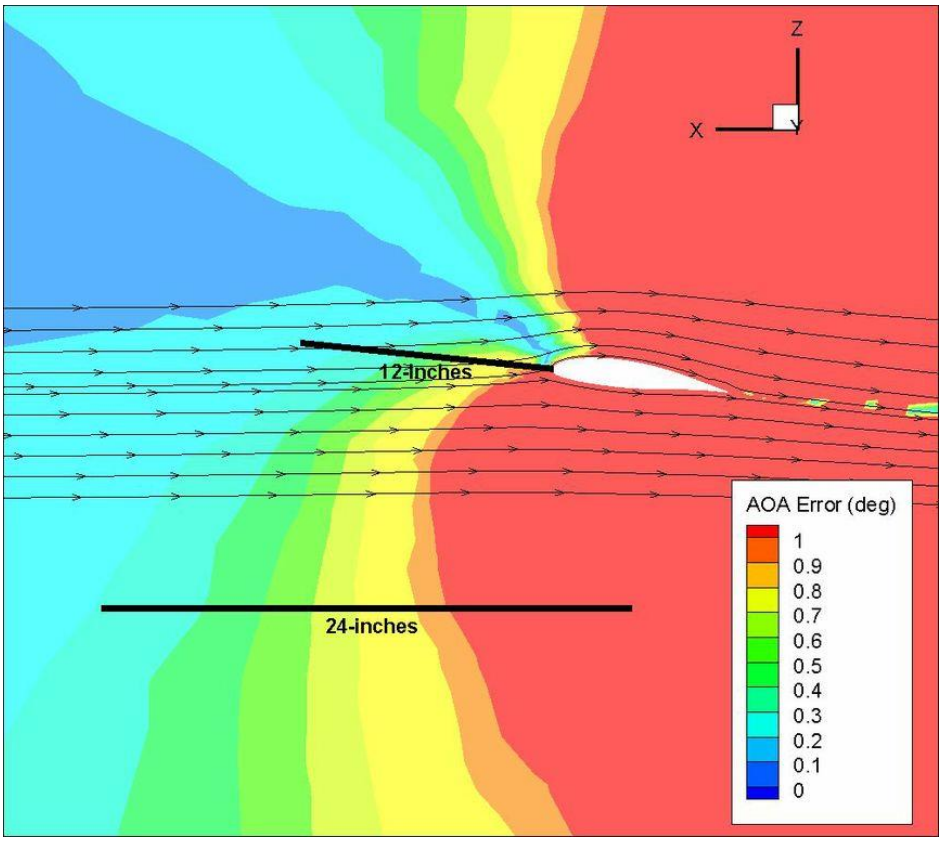

Figure 16: AoA error contour taken from a slice of the 3D wing near the wing tip [9, 37]

Figure 16 shows a CFD contour plot generated by ANSYS Fluent by taking a 2D slice taken near the wing tip from a 3D CFD showing the error associated with the angle of attack (AoA) to figure out the length of the boom [37]. To compute the error, the free stream AoA was subtracted from the local AoA [30]. As the contour shows, the longer the boom is out in front of the leading edge of the wing decreases the AoA error. A length of 24 inches gives an error of 0.1 degrees. The dimensions of the carbon fiber tube had an outside diameter of 0.625 inches, an inside diameter of.515 inches, and a length of 24 inches. Figure 17 illustrates the setup used in Embry-Riddle's wind tunnel to calibrate the vanes and pitot tube:

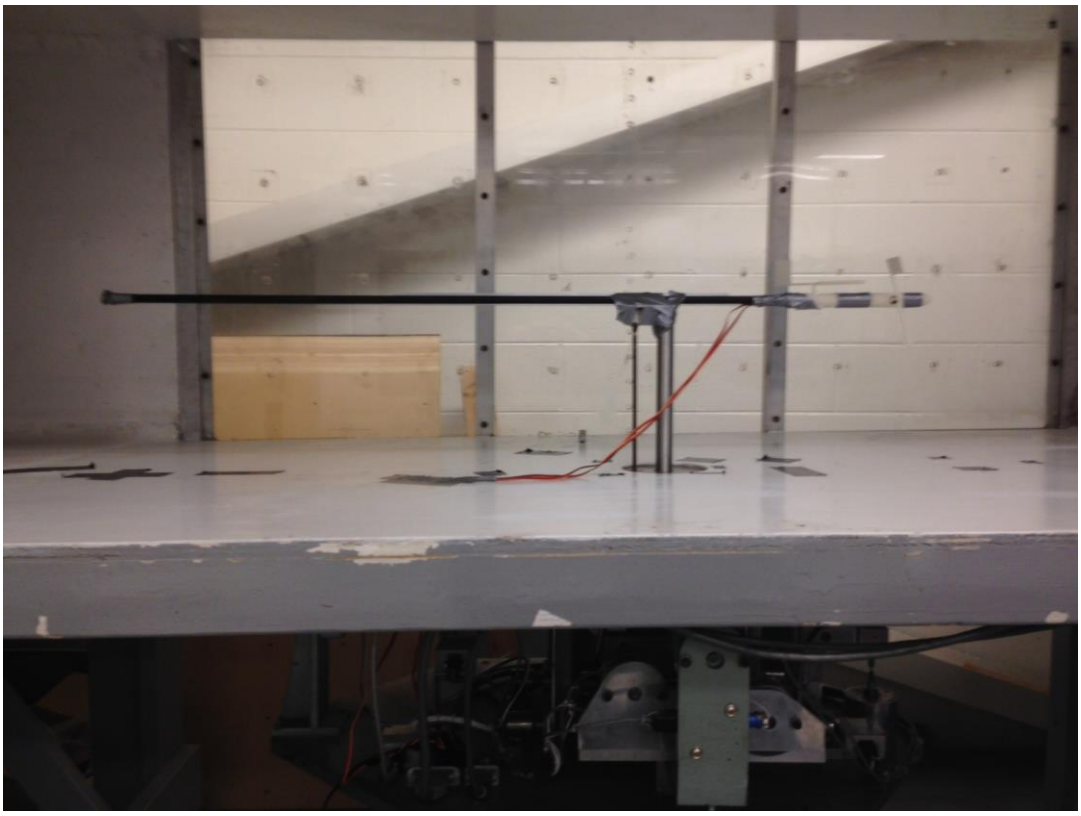

Figure 17: Calibration setup for air data boom

2.4.3 Pitot tube

The pitot tube used and tested was from an airspeed sensor kit from 3DRobotics that utilized the MPXV7002DP chip as its differential pressure sensor. It was placed at the tip of the air boom to make sure that it was away from the propeller and other downwash effects from the propeller. The sensor was then connected to the APM 2.5 via an analog input slot.

Airspeed (mph)	Output (V)
0	2.63
10	2.65
20	2.69
30	2.74
40	2.78

Table 4: Experimental data for airspeed calibration

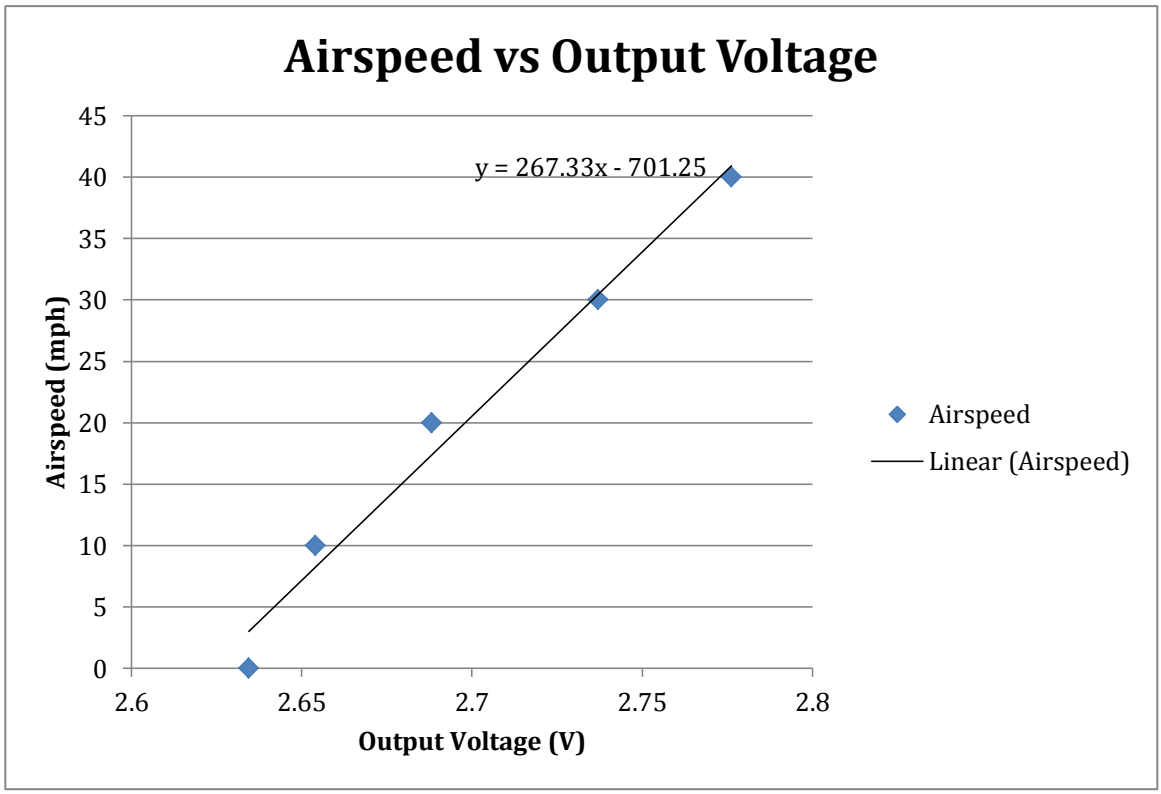

Figure 18: Graphical representation of the experimental data with the linear regression equation

2.4.4 Angle of Attack and Side Slip Vane Calibration

The AoA and angle of yaw (AoY) sensors are just potentiometers with vanes that are glued onto the tabs. The data collected in Table 5, Table 6, Figure 19, and Figure 20 had the wind tunnel speed set at a constant 10 mph. A positive angle for the AoA vane indicated that the nose was pitching up. For the AoY, a positive angle meant the nose yawed to the right.

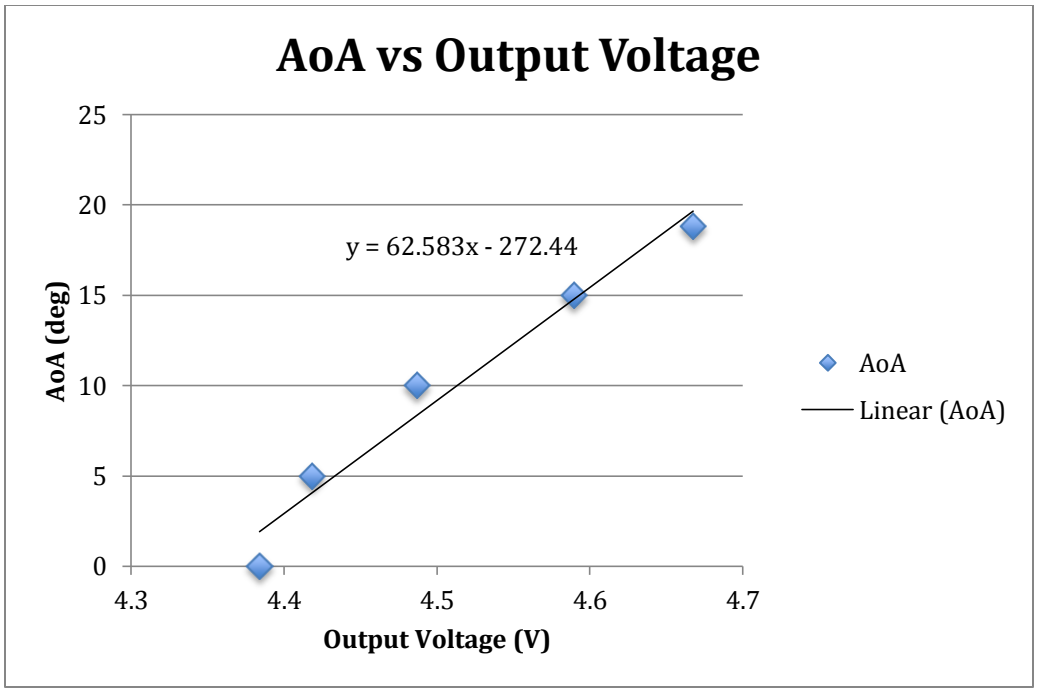

Figure 19: Graphical representation of the experimental data with the linear regression equation

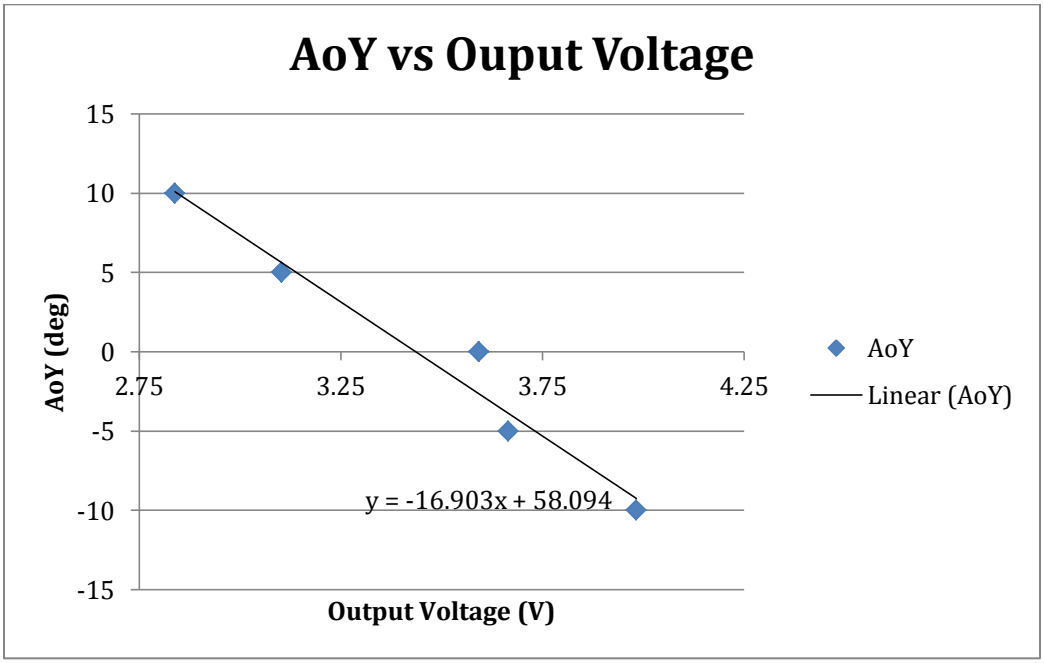

Figure 20: Graphical representation of experimental data with regression line

AoA (alpha)	Output (V)
0	4.38
5	4.42
10	4.49
15	4.59
18.8	4.67

Table 5: Experimental data for AoA calibration

Side Slip/Beta (deg)	Output (V)
-10	3.98
-5	3.67
0	3.59
5	3.10
10	2.84

Table 6: Experimental data for AoY calibration

However, the airspeed should have been set to 25 mph because the vanes were designed for that velocity [36].

2.4.5 Air Data Boom Pod

The air data boom pod was made out of Styrofoam and fiberglass chop mat. The first step in the process was to trace an outline of the tip of the wing. Then the Styrofoam block was sanded down into the desired shape as shown in Figure 21 and Figure 22:

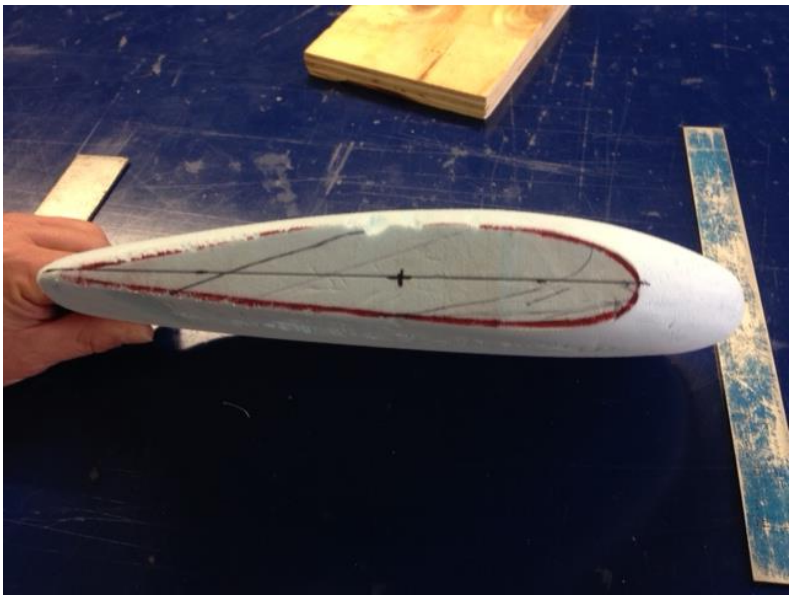

Figure 21: Side view of air data boom pod with wingtip outline

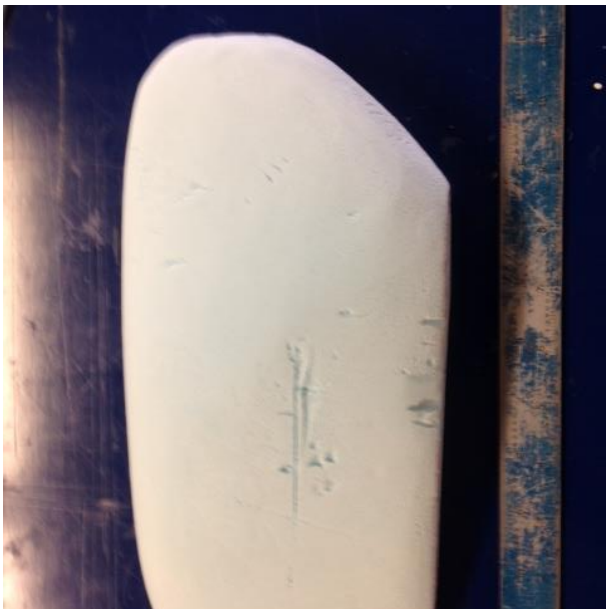

Figure 22: Top view with a 12 inch ruler for reference

The next step was to use a hot wire tool in Figure 23 and cut the Styrofoam pod into two pieces:

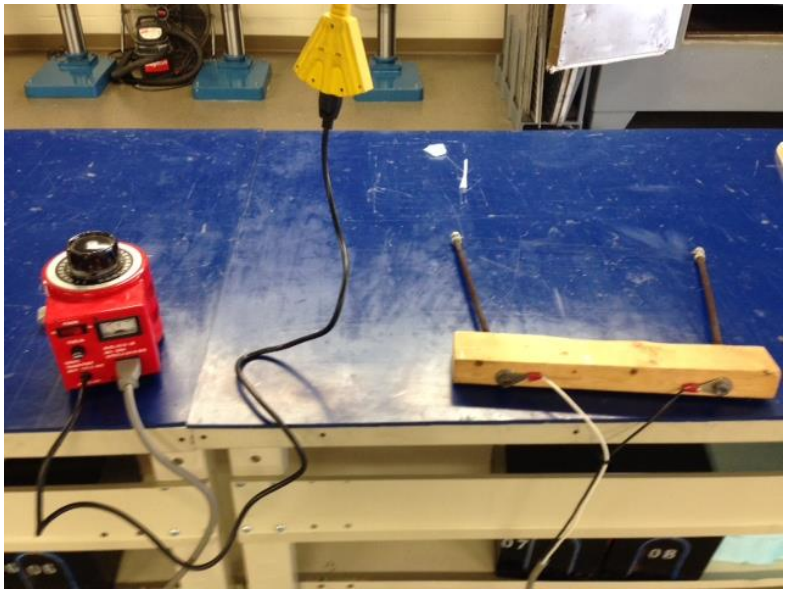

Figure 23: Hot wire tool

The fiberglass pieces were then laid on top of each piece of the mold once layer at a time and vacuum bagged before they were placed into the oven as Figure 24 and Figure 25 show:

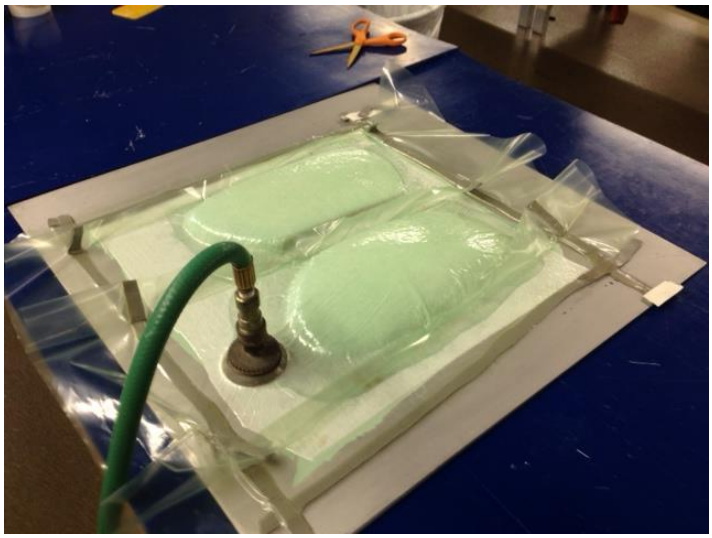

Figure 24: Vacuum bagging air data pod

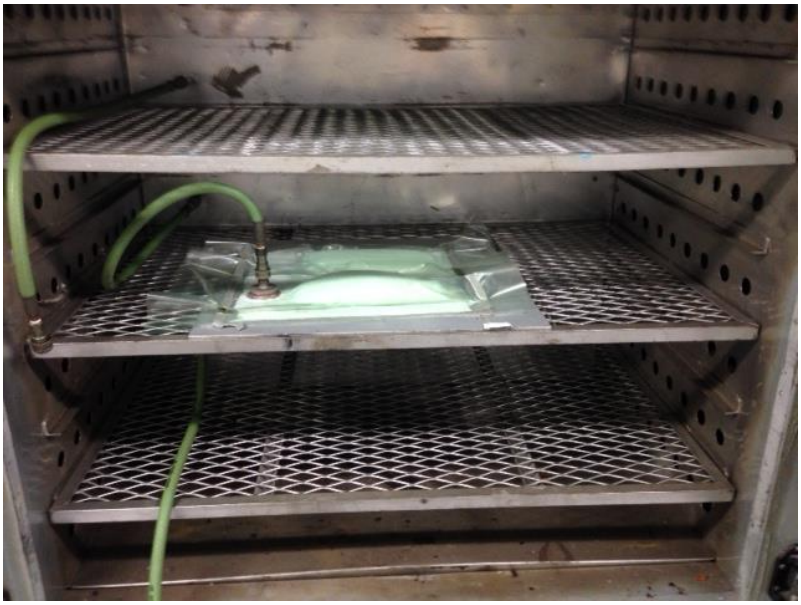

Figure 25: Air data pod vacuum bagged in oven

Lines were drawn to map out where wingtip would be placed as shown in Figure 26:

Figure 26: Mapping of the inside the air data boom pod

The wingtip area was cut out, as shown in Figure 27, so that the pod could fit on the wingtip by putting the two pieces together as shown in Figure 28:

Figure 27: Both halves of the air data pod

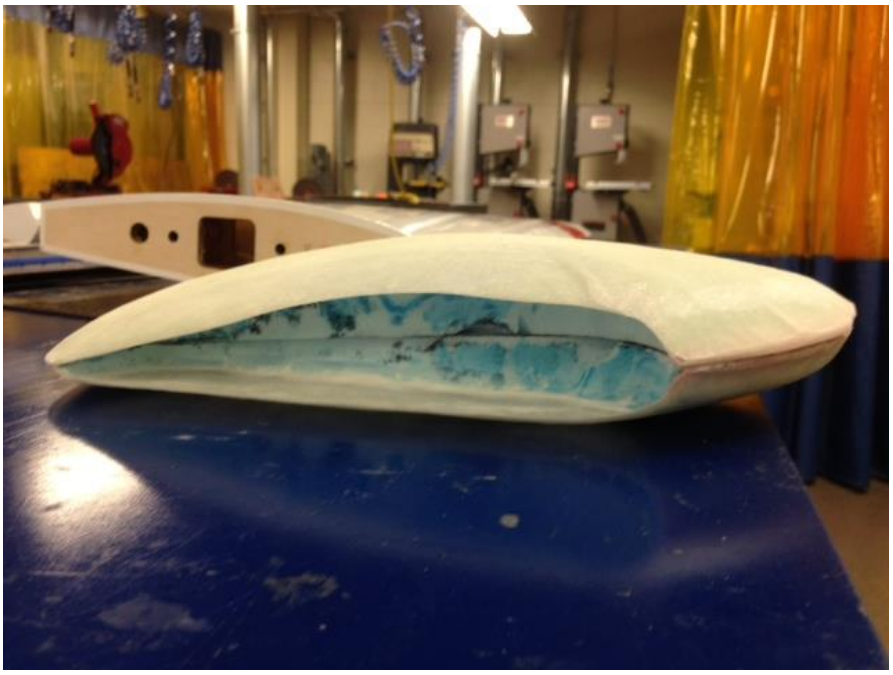

Figure 28: Side view of air data pod

The next step was to make sure that the pod was aligned with the wing at the same pitch angle of 7 degrees and at the same yaw angle by using a right angle in Figure 29:

Figure 29: Aligning air data boom pod

To make sure that the boom was parallel to the fuselage, the glider had to be leveled as shown in Figure 30 and Figure 31 show:

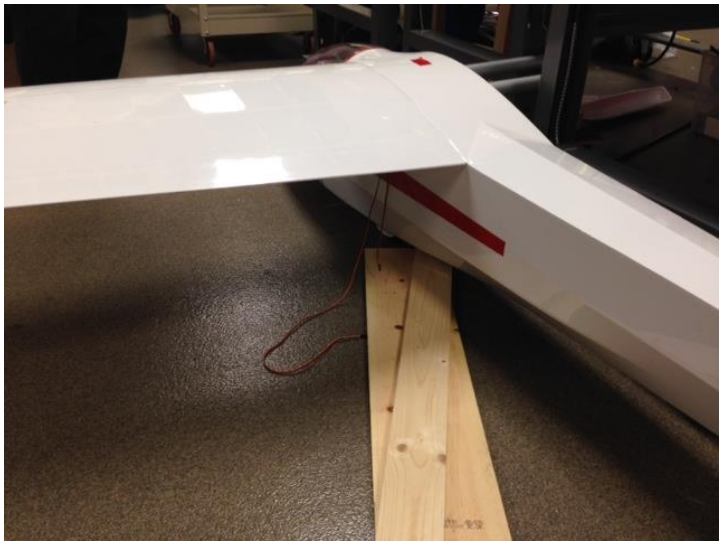

Figure 30: Leveling the glider

Figure 31: Leveling wing for aligning the air data pod

A piece of fishing line was taped to the half span of the wing. The fishing line was made parallel to the wing tube connectors so that a reference 90-degree angle could be made as shown in Figure 32 as a red line in the pod. A space was carved out where the carbon

fiber tube and airspeed sensor were placed along with any wires from the AoA and AoY vanes.

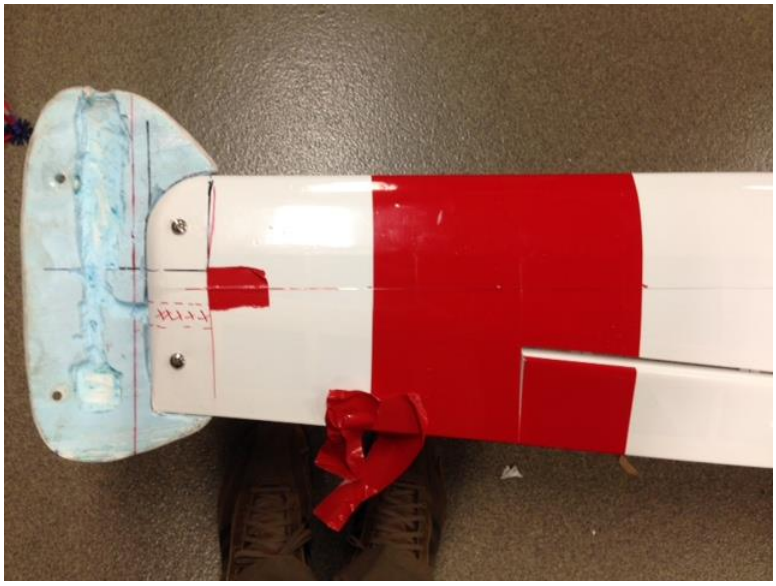

Figure 32: Aligning the air data boom pod

The last step is to put all these pieces together and mount the pod onto the wingtip as shown in Figure 33:

Figure 33: The assembled air data boom on the wingtip of the glider

2.4.6 GPS

The GPS used for data collecting was the MediaTek MT3329. This was used to capture the location of the UAV and the ground speed. The GPS was checked by cross checking the lateral and longitudinal coordinates at a known location. The performance of the GPS chip can be found in from its data sheet as shown in Table 7:

Performance Characteristics	
Position Accuracy	3m 2D-RMS
Velocity Accuracy	0.1 m/s
Acceleration Accuracy	0.1 m/s^2
Timing Accuracy	100 ns RMS

Table 7: Specifications of the MediaTek MT3329 GPS without any type of augmentation [41]

2.5 Computational Fluid Dynamics (CFD) Model

For the purposes of obtaining estimates for the mass moment of inertias and for CFD analysis, a surface model of the RC glider was created by using the FARO PlatniumArm 3D laser scanner at Embry Riddle's Eagle Flight Research Center (EFRC) [3]. The arm has an accuracy of +/- 0.029mm [3].

Figure 34: The laser 3D scanner Faro arm [3]

The first step is to make sure that the object that is to be scanned must not move while the FARO arm is in use to avoid redoing the scan [3]. Once the object is secured, a thin layer of fine powder must be sprayed so that the laser can pick up the surface [3]. Since the glider had a reflective surface, any area that is not covered with the powder will not be read by the laser [3]. The software that was used to collect the cloud points and then create the NURB surfaces was Geomagic Studios [3]. An example of the post processing using the vertical tail section is depicted in Figure 35 and Figure 36:

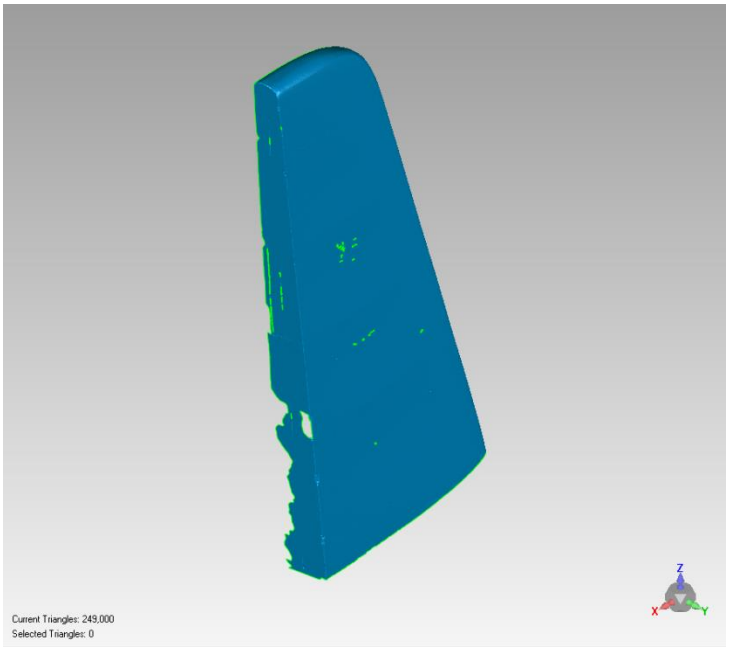

Figure 35: 3D laser scan of the vertical tail section [3]

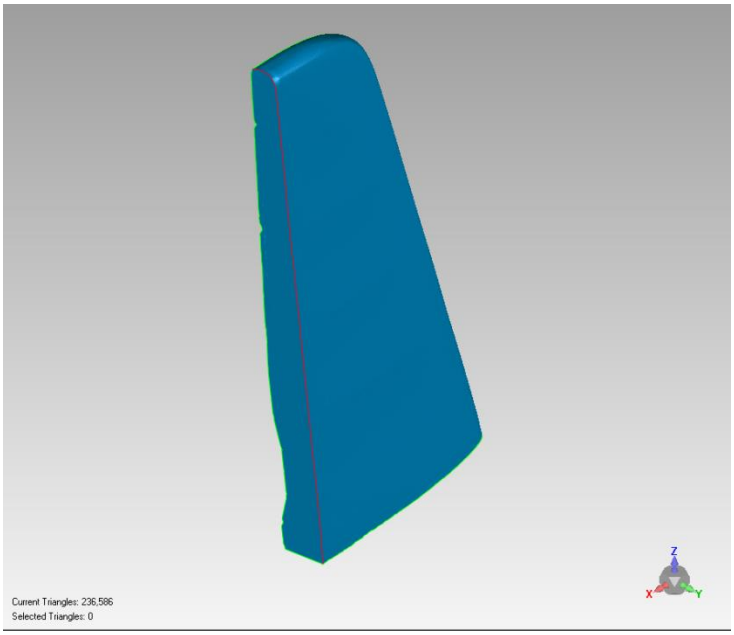

Figure 36: Post processing of completed model for the vertical tail [3]

Since the airfoil of the wing was known, it was decided that scanning the wing was not necessary [3]. Instead, CATIA was used to extrude the airfoil into the wing with the associated dimensions in Table 8 [3]:

Wing Measurements (in)	
Base Chord	20.50
Tip Chord	7.75
Wing Span	113.375

Table 8: Wing measurements [3]

It should be noted that a 1/8 inch rounded trailing edge was created to match the dimension on the glider [3]. The tip of the wing was approximated due to the complex shape [3].

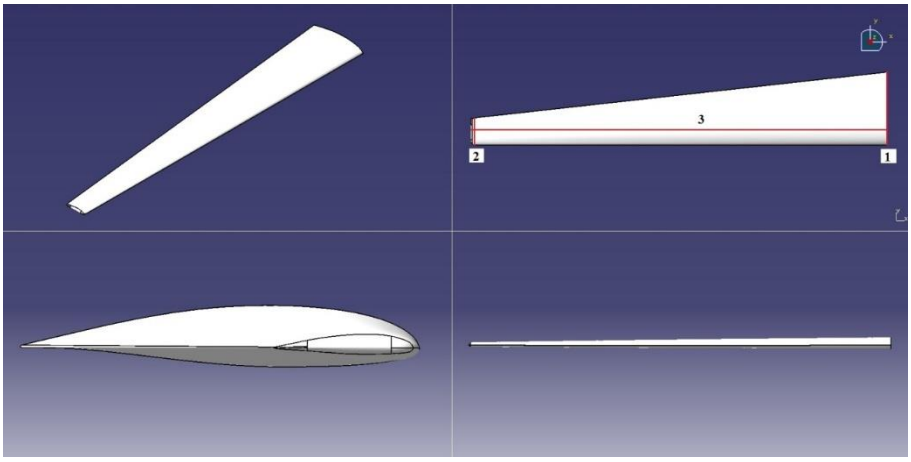

Figure 37:CATIA model views of the wing [3]

Once the fuselage, horizontal tail, and vertical tail were scanned and converted to surfaces, they were assembled into one model [3]. It can be seen in Figure 38 that the vertical tail does not properly fit the model [3]. It is likely that the calibration setting on the FARO arm was not set correctly [3]. The incidence angle of the wing root chord was measured to be 7 degrees [3].

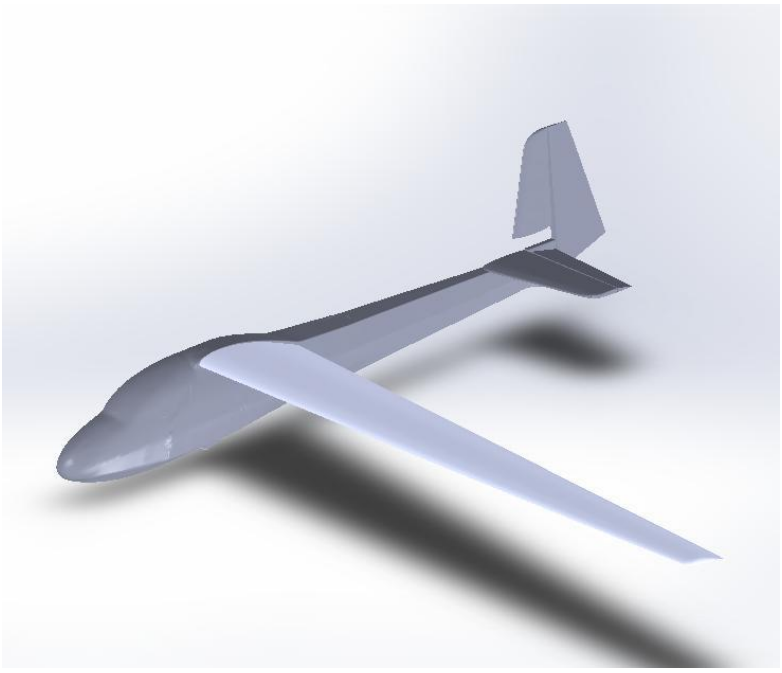

Figure 38: Completed model for CFD [3]

2.6 3D Computational Fluid Dynamics (CFD) Analysis

The importance of determining the glide slope using CFD is that the aerospace industry uses CFD to determine the lift to glide ratio since it is cheaper than experimentation [39,42]. Also, Embry-Riddle does not have a wind tunnel to accommodate a scale glider of this size to determine the glide slope.

A 3D CFD analysis was done by Dr, Engblom utilizing a 6 million-cell grid and the assembled surface geometry in Pointwise with the CFD analysis was done by utilizing ANSYS Fluent to find the predicted glide slope [9].

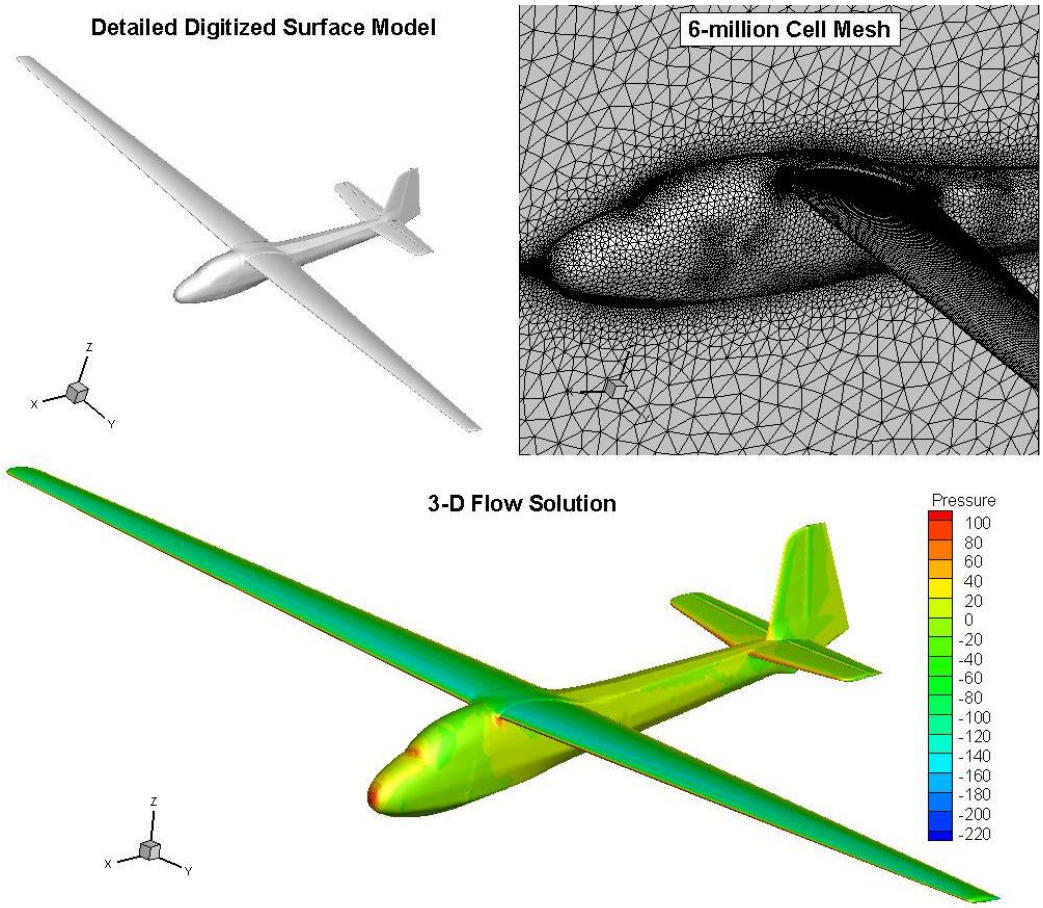

Figure 39: 3D CFD grid [9]

The 3D CFD model predicted a C_L of .71 and a C_D of .044. This gives an L/D of 16.3 at a wing alpha of 4 degrees. This is below the glide slope of 25 that was desired [37].

2.7 Component Build-up (Industry) Approach

A conventional approach to calculate the glide slope of an aircraft is to look at an airfoil's lift and drag coefficient for each individual component and assume negligible interactions among the components [9]. The performance for the finite wings in this assessment are made based on XFOIL airfoil data at Reynolds number of 300,000 and the affect of induced drag [9].

SAIL AIRCRAFT CONFIGURATION			
Wing Area	2.2	m2	
Wing Span	6.0	m	(19.7 ft)
AR	16.4		
Mass	13.6	kg	(30 lbm)
MAC	0.367	m	
Wing Efficiency	0.98		

Table 9: Aircraft geometry [9]

FLIGHT CONDITIONS		
Velocity	13.0	m
RHO	1.2	kg/m^3
Viscosity	2.0E-05	N-s/m
RE	286000.0	

Table 10: Flight Conditions [9]

TAIL and FUSELAGE CONTRIBUTION		
Horiz Tail Area	0.33	m^2
Vert Tail Area	0.220	m^2
Fuse Wetted Area	1.65	m^2
Fuse Cross-Sect Area	0.1	m^2
Horiz Tail C_D	0.012	Ref to above
Vert Tail C_D	0.012	Ref to above
Fuse C_f	0.004	Ref to above
Fuse C_D	0.040	Ref to above
Horiz Tail C_D	0.0018	Ref to Wing Area
Vert Tail C_D	0.0012	Ref to Wing Area
Fuse Frict C_D	0.003	Ref to Wing Area
Fuse Nose C_D	0.002	Ref to Wing Area
Extra C_D	0.005	Ref to Wing Area

Table 11: Tail and fuselage contribution values [9]

Standard formulas for the induced drag and skin friction drag created by the fuselage, vertical and horizontal tails are added to the 2-D XFOIL drag estimate. An extra 0.005 of drag was added to account for any other protuberances. These values for C_D were added together to get the total drag so that the glide slope could be calculated using the C_L from data generated by Xfoil [10].

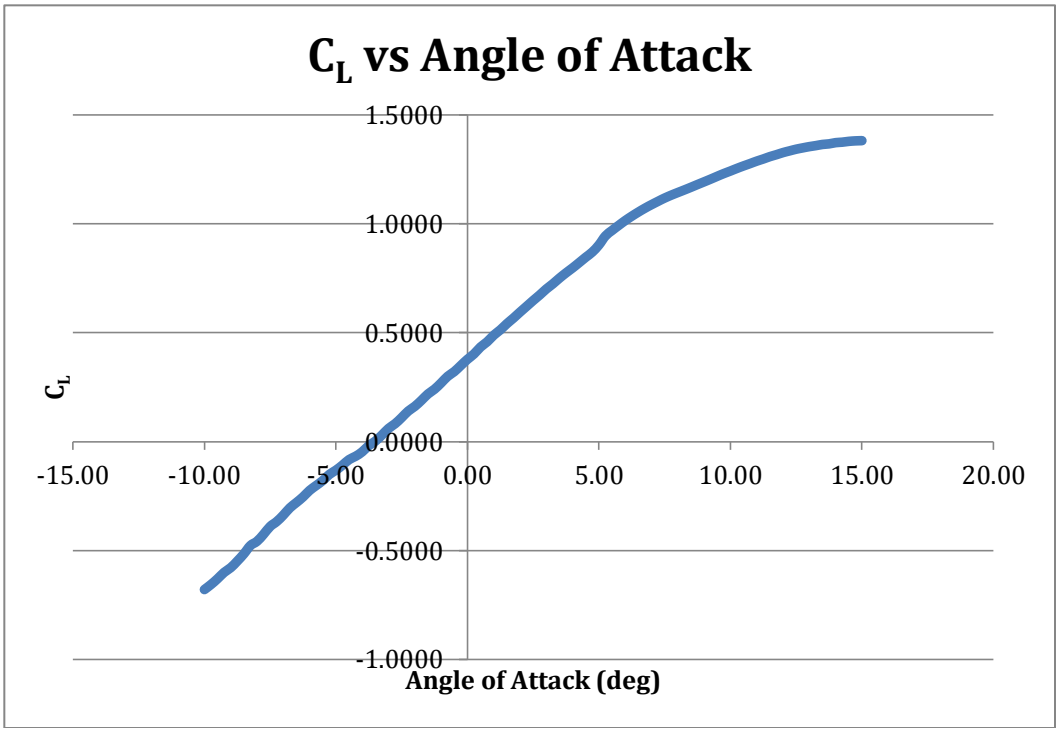

Figure 40: Coefficient of lift versus angle of attack

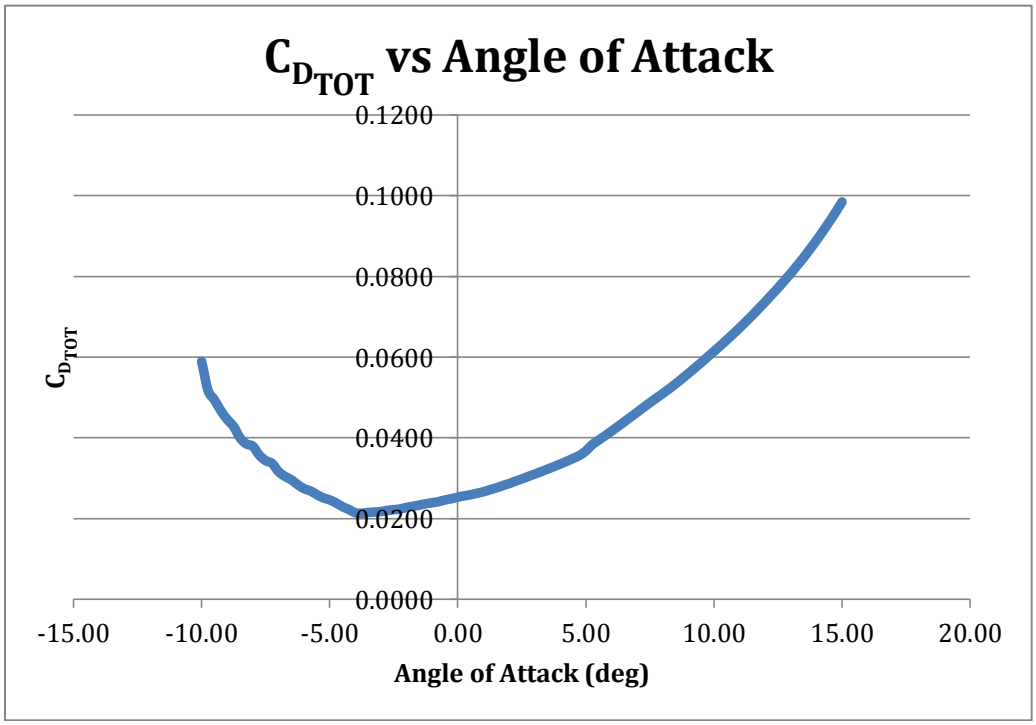

Figure 41: Drag coefficient for the whole aircraft versus angle of attack

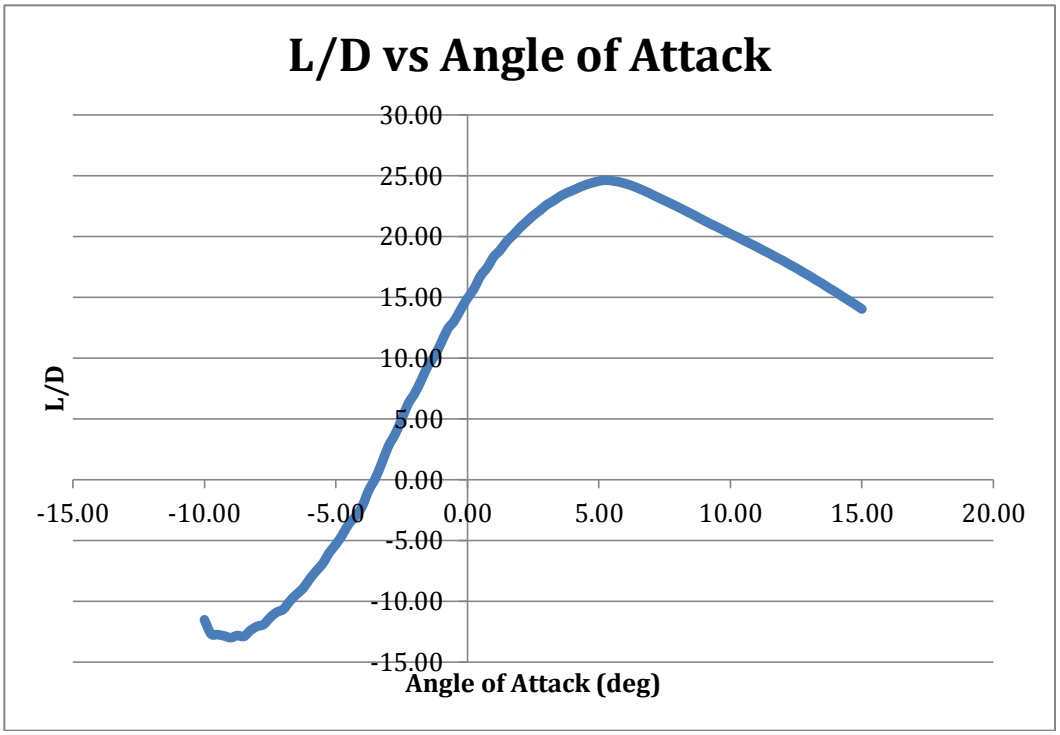

Figure 42: Lift to drag ratio versus angle of attack

The maximum glide slope was found to be 23.79. This value is larger than the 16.63 found from using CFD and closer to the desired value of 25. However, both approaches make assumptions about the geometry and flow conditions like a constant, idealized flow from one direction and ignoring the imperfections of the scale glider model that make an accurate estimation from these two methods unreliable.

2.8 Aero and Stability Characteristics from Computer Models

2.8.1 SURFACES

The first and main,Vortex Lattice Method (VLM) program that was used was SURFACES. Figure 43 through Figure 45 show the model that was created and used in SURFACES to estimate the inertias and stability derivatives.

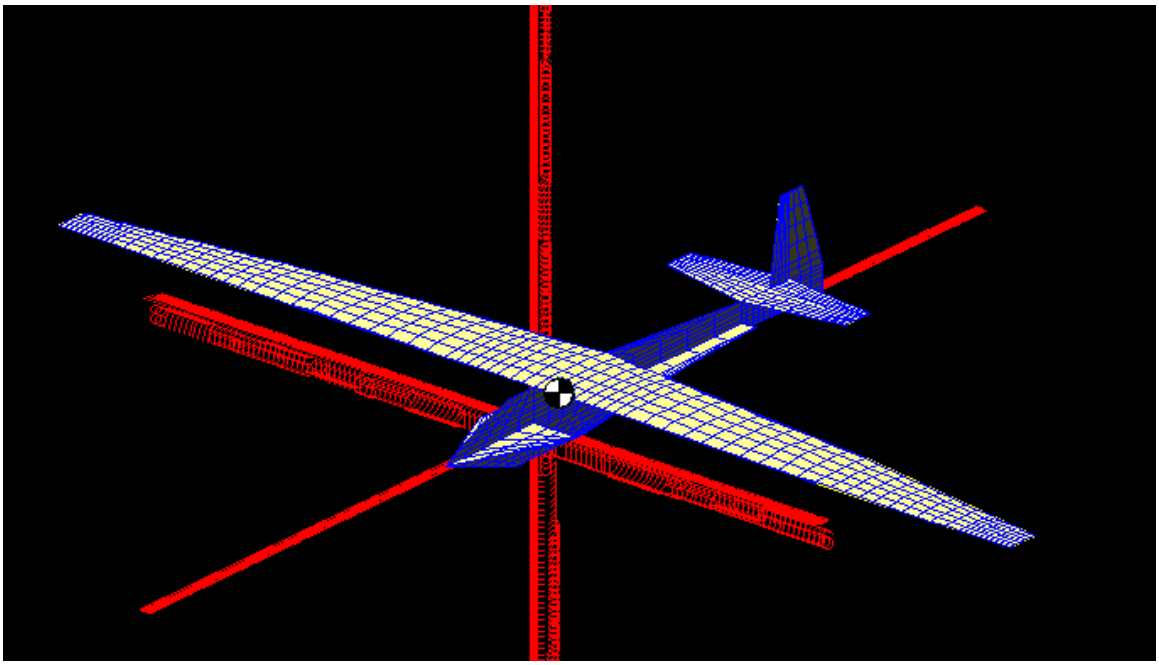

Figure 43: Isometric view of SURFACES model

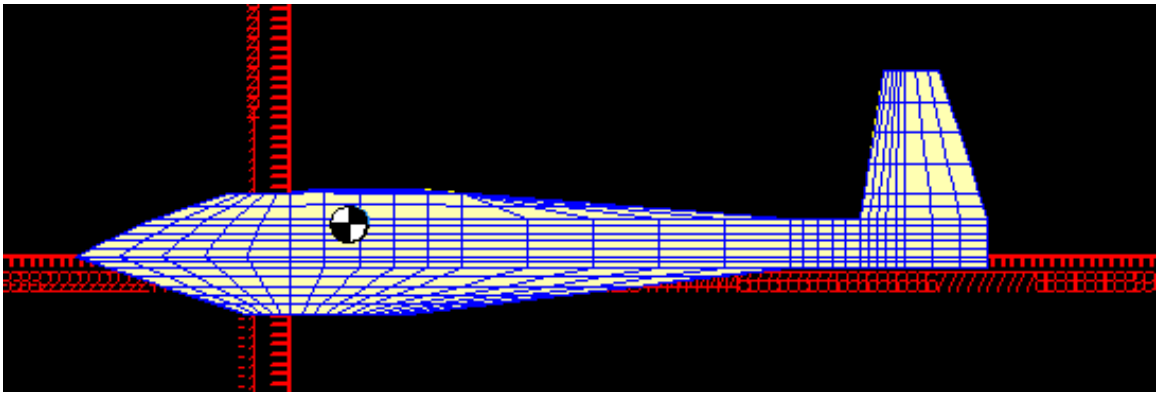

Figure 44: Side view of SURFACES model

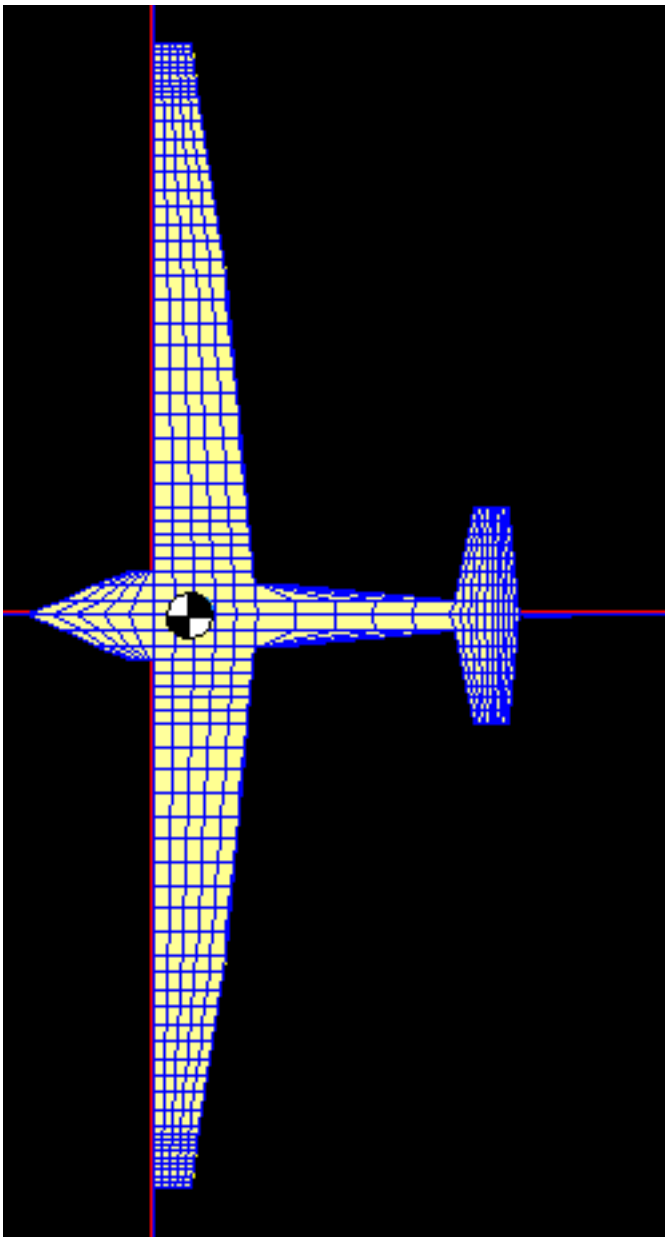

Figure 45: Top view of SURFACES model

Table 12 through Table 14 show the reference values used in SURFACES:

Reference Geometry	
Reference Chord (MAC), Cref	1.28 ft
Cref start location, Xref	0.00 ft
Reference Span, Bref	19.4 ft
Reference Area, Sref	23.6 ft^2
Wetted Area, Swet	47.85 ft^2

Table 12: Reference geometry value used in SURFACES

Acceleration Z-dir	-32.174 ft/s^2
Reference Weight, Wref	35 lbf
Xcg	0.59 ft
Ycg	0.00 ft
Zcg	0.32 ft
Xneu	0.61 ft

Table 13: Reference information used in SURFACES

As Table 13 shows, the distance of the CG in the x-direction is 7.08 in (.59ft) which is 1.19 inches further back than the CG predicted using the Accuset scale system. Table 14 shows the inertias calculated by SURFACES:

Inertias (slug*ft^2)	
Ixx	11.41
Iyy	4.88
Izz	16.02
Ixy	0
Ixz	0.31
Iyz	0

Table 14: Inertias calculated by SURFACES

2.8.2 AVL

The second VLM program that was used was developed by MIT. It is an extended VLM method to calculate the flight dynamics of rigid aircraft of an arbitrary configuration [5]. The inertias and CG location used in AVL were transferred from SURFACES to AVL by using an AVL MASS file and using the model as shown in Figure 46 through Figure 48:

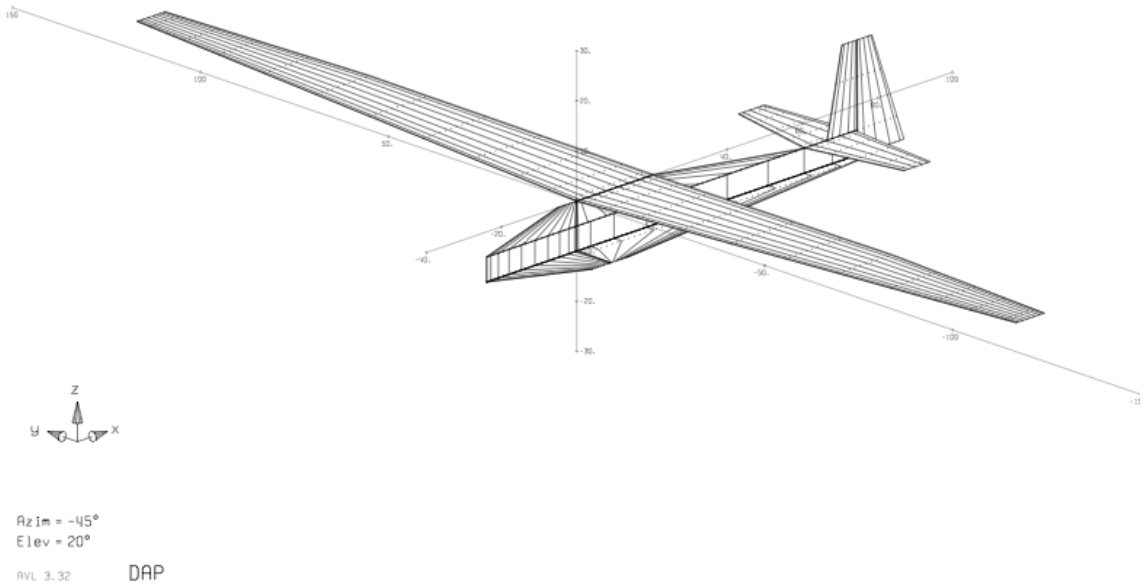

Figure 46: Isometric view of AVL model

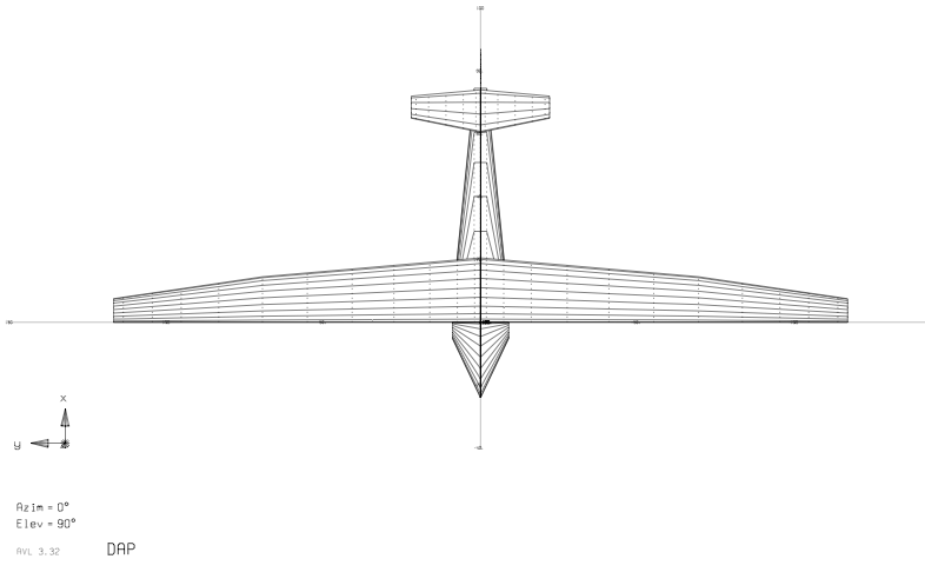

Figure 47: Top View of AVL model

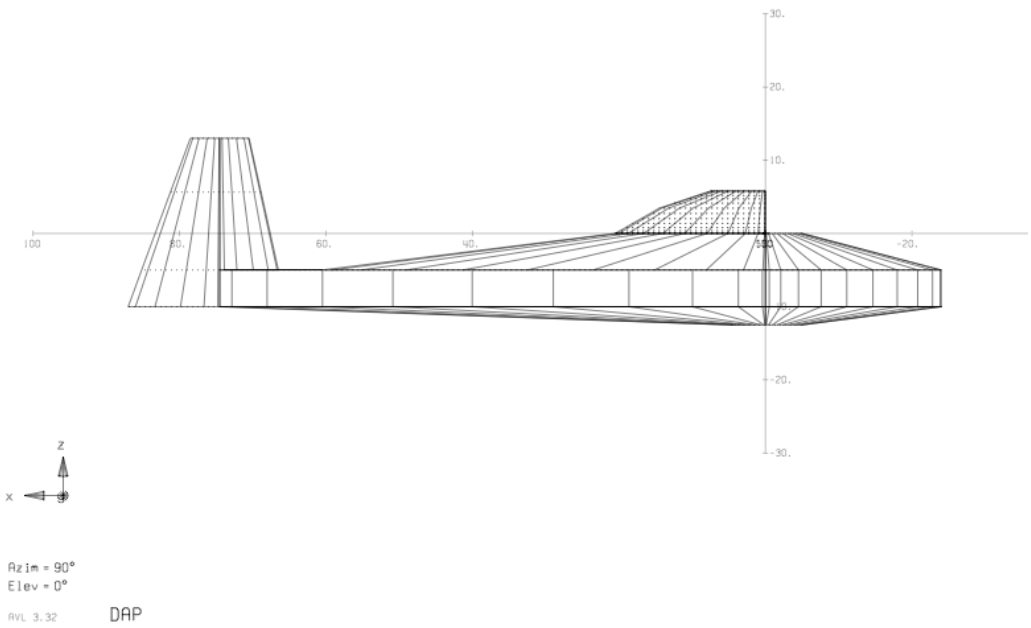

Figure 48: Side View of AVL model

2.8.3 USAF Digital Datcom

The last program that was used to estimate the stability characteristics of the glider was the United States Air Force's (USAF) Digital Datcom. Figure 49 through Figure 52 show a model of the glider generated by Datcom using a MATLAB script file that was developed by Professor Greiner and Jafar Mohammed in 2008.

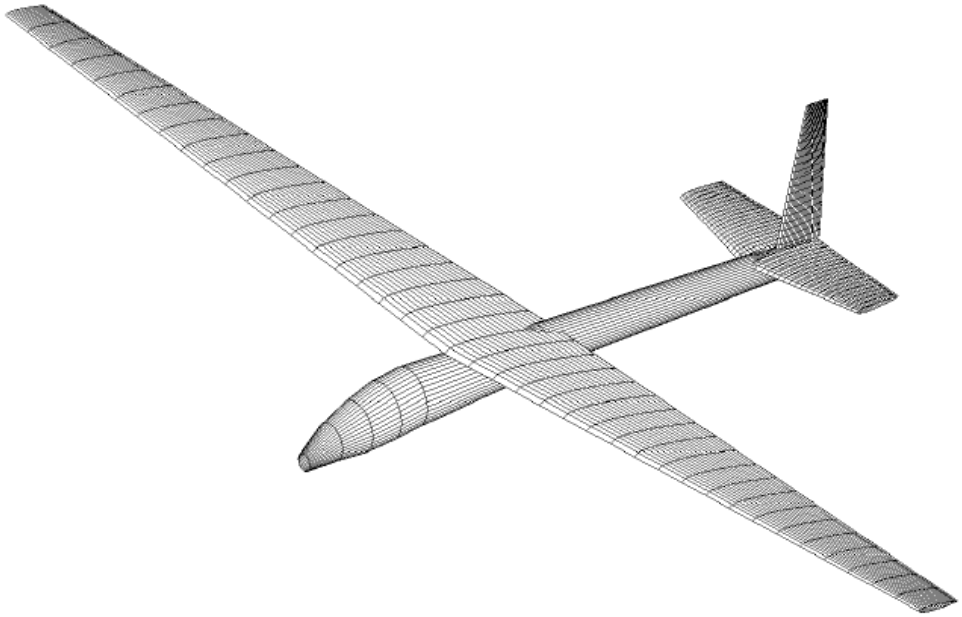

Figure 49: Isometric view generated by MATLAB

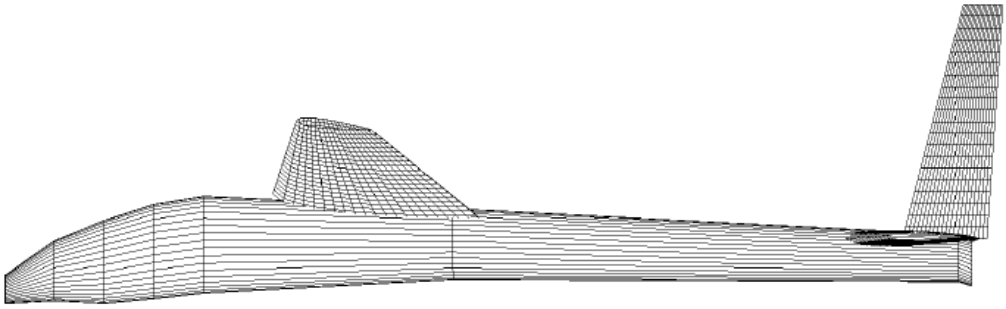

Figure 50: Side View generated by MATLAB

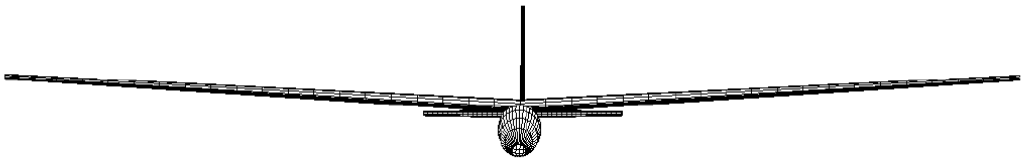

Figure 51: Front View generated by MATLAB

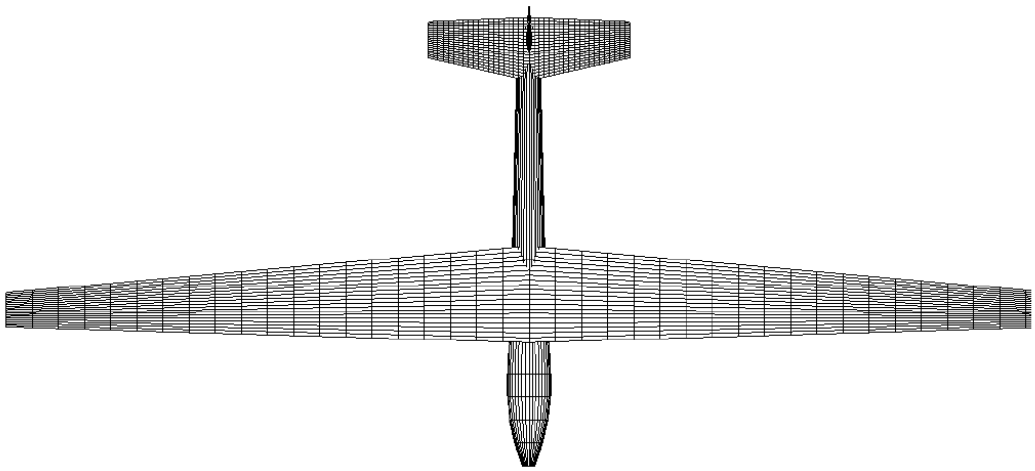

Figure 52: Top View generated by MATLAB

It should be noted the HQ 3.0/15.0 airfoil was not used but rather the NACA 6 series airfoil 63(2)-615, which is similar to the HQ airfoil [9]. Evaluation of rudder input was not available in the software. The graphs generated by Datcom can be found in Appendix B from the same MATLAB script made possible by Dr. Greiner and Jafar Mohammad.

The table in Appendix F compares the stability derivatives generated by all three software packages. Any stability derivative that was on the scale of 10^-5 was deemed to small and therefore, zero.

2.8.4 MATLAB/Simulink Model

An optimization program was planned, but due to noisy flight data and issues with optimization convergence, as shown in Appendix E, a decision was made to analyze the dynamic modes of the aircraft - the phugoid, short period, and Dutch-roll. Unfortunately, only the short and phugoid modes were evaluated but the Dutch-roll mode was found to be highly unstable based on the derivatives obtained and shown in Appendix D.

The model used to figure out the modes of the aircraft is shown in Figure 53:

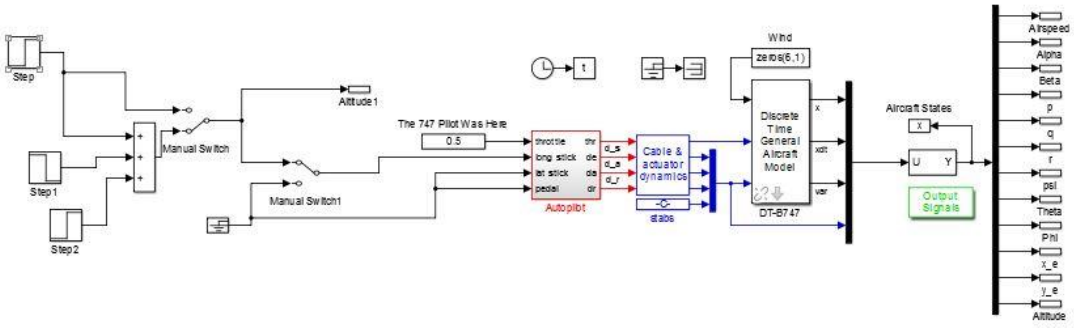

Figure 53: Simulink model for figuring out the aircraft response

The first task is to input zero signals into each direction to see if the model is stable – to see damped oscillations in the longitudinal direction, but zero dynamic behavior in the lateral direction. These time history figures are provided in Appendix D along with a table of stability derivatives that were found to make the model stable. The two blocks whose contents that were modified to make the model stable are shown in Figure 54:

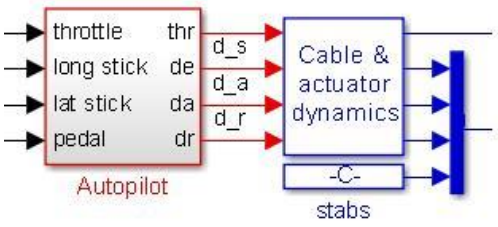

Figure 54: Blocks that need to be changed

Inside the Autopilot block, shown in red in Figure 54, the user must change the gains to one and negative one as shown in Figure 55:

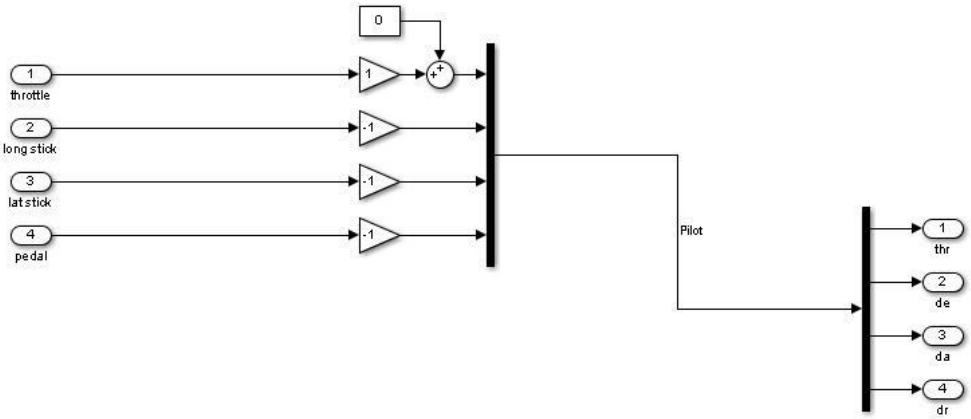

Figure 55:Inside Autopilot Block to change all the gains to the appropriate values

Inside the blue 'Cable & Actuator Dynamics' block, the 'Force' gain had to be changed so that the altitude oscillation leveled off, as shown in Appendix D. In this case, the 'Force' gain was set to 20.385 N because the altitude was at level flight as shown in Appendix D for the trimmed condition.

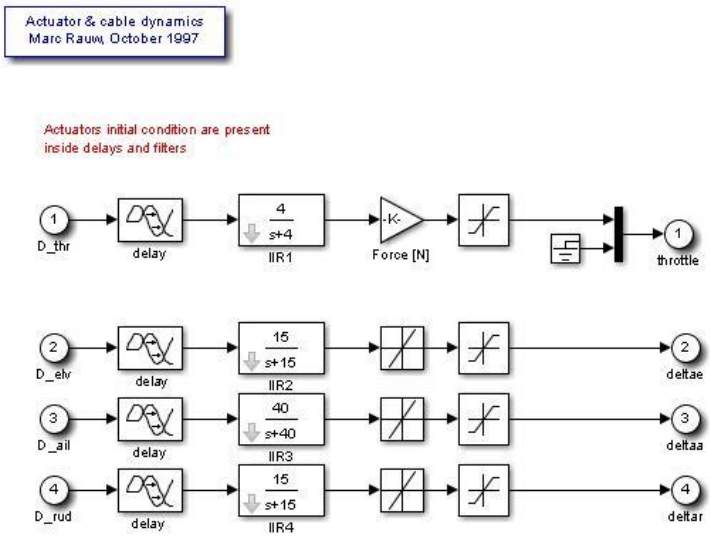

Figure 56: Inside the Cable & Actuator Dynamics block to change the force gain so that the altitude is trimmed for level flight

After these changes, a step function was introduced into the pitch direction. Figure 57 shows the step function in radians that was used to excite the response in the model:

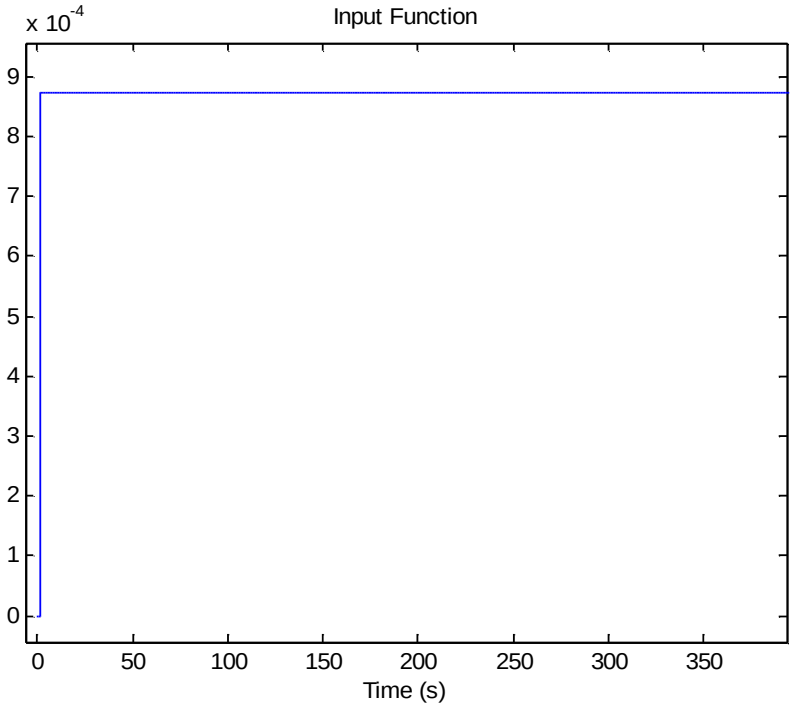

Figure 57: Step function input in radians

Figure 58 shows an example of how both alpha and q responded to a step response input function from Eric Watkiss from the Naval Postgraduate School [21]:

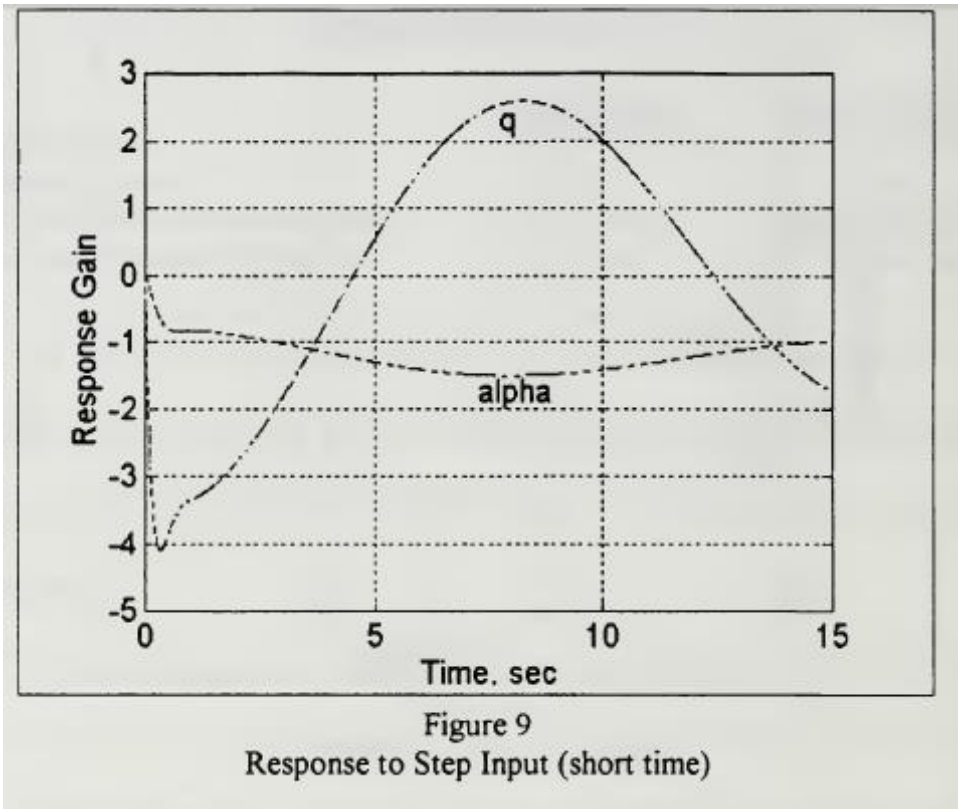

Figure 58: An example of how alpha should respond to a step function [20]

Figure 59 and Figure 60 show the response of alpha while the airspeed response is shown in Figure 61 for the MATLAB model using the stability derivatives in Appendix D:

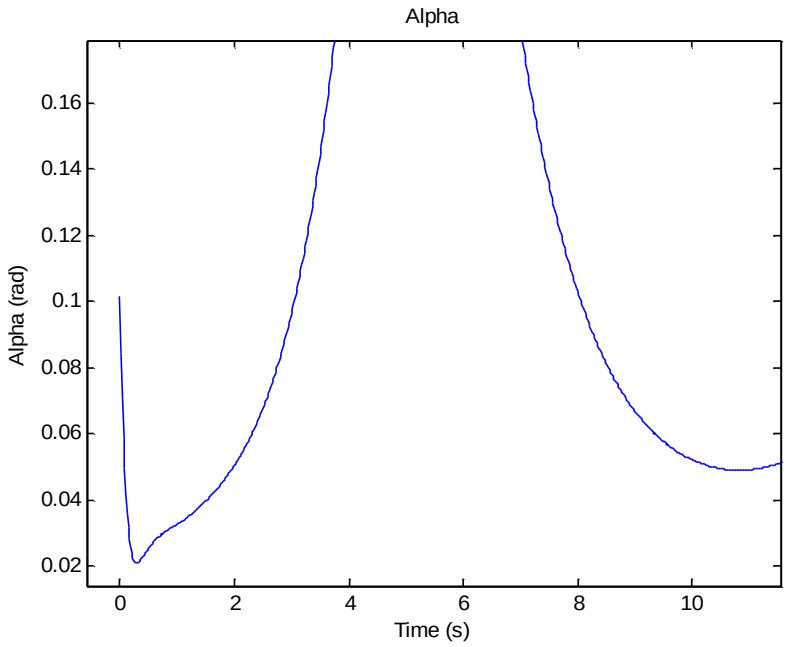

Figure 59: Alpha response of the Simulink model to the step function input at one second

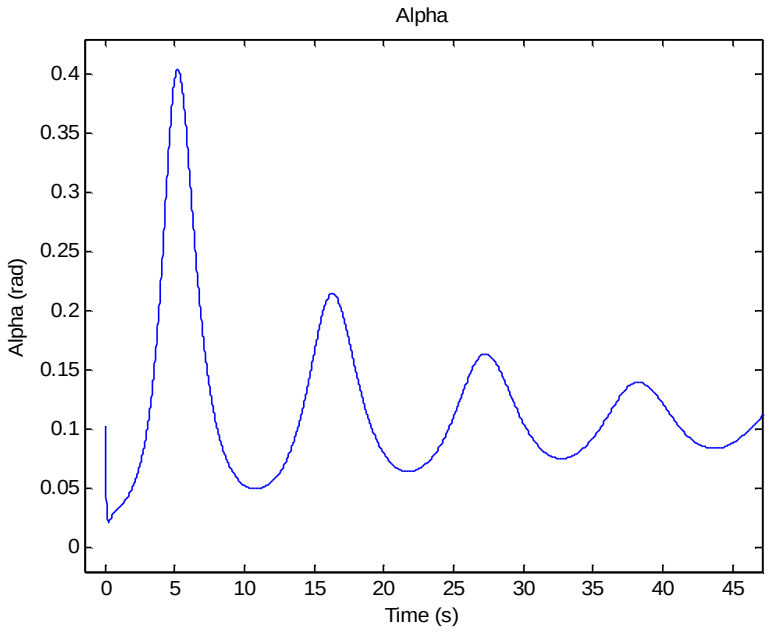

Figure 60: A longer time period response to the step function input for alpha

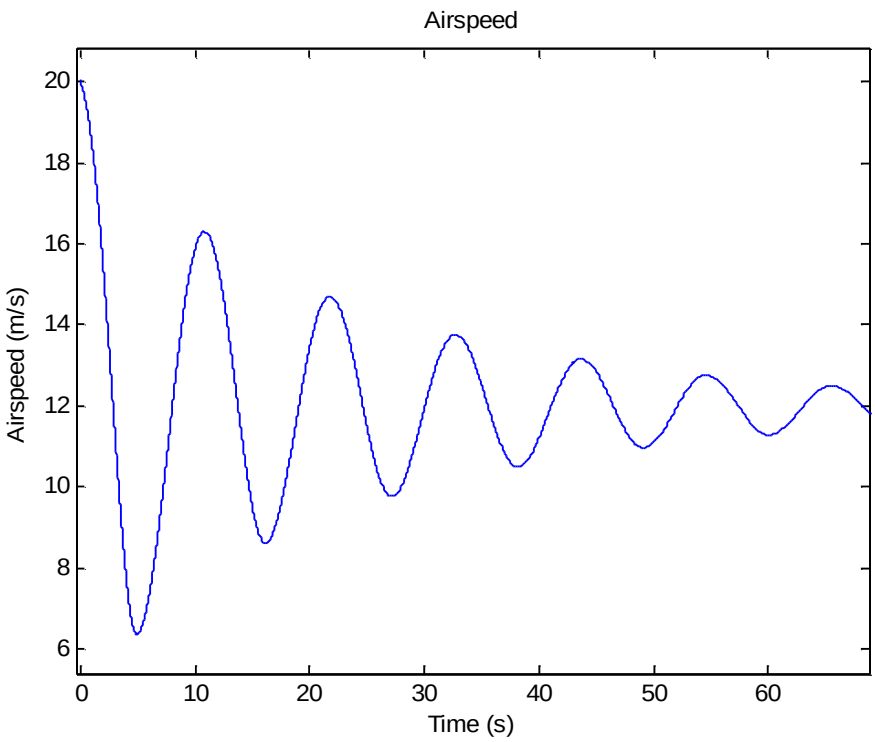

Figure 61: Airspeed response from step function input

Both the long and short periods' damping ratio were found by using the exponential decay equation shown as equation 6 by using the peak-to-peak values [24]:

$$\zeta = \frac{ln\frac{y}{y_0}}{2\pi n} \tag{6}$$

where y is the final peak value at n cycles starting from an initial peak of y_0. The phugoid was found from using values from the airspeed, and the short period was found from alpha. However, the short period could not be determined using the peak-to-peak method because it was not obvious what value the oscillation decayed to. The damping ratios for both modes are listed in Table 15 along with the frequencies:

Mode	Frequency (Hz)	Damping ratio, ζ
Long period (Phugoid)	.09066	-0.01637
Short period	Could not be determined	Could not be determined

Table 15: Damping ratios for both modes using the stability derivatives in Appendix D

The doublet function and responses are provided in Appendix D, but the responses appear to behave similarly to that of the step function.

It should be noted that any time the configuration of the aircraft changes, this process must be repeated – change SURFACES, Datcom, AVL, re-trim the aircraft in the Simulink model by changing the stability derivatives, and then figure out the damping ratio and frequencies for the short period and phugoid modes. Only after this process can the flight test data be optimized.

2.9 Motor Testing

Motor testing was done at Embry Riddle's wind tunnel to determine the nominal thrust of the Hacker A60-18L electric brushless motor by utilizing the tunnel's force sensor. The amount of thrust and the aircraft weight determines what type of takeoff technique is used.

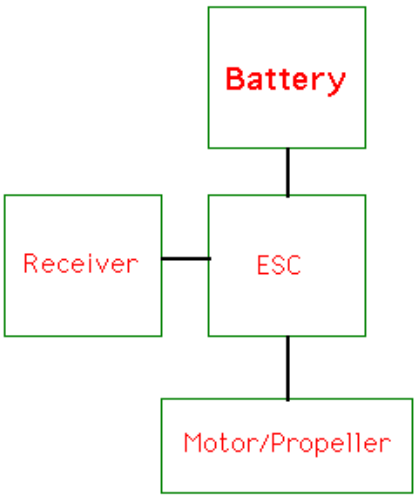

Figure 62: Electronic Schematic for propeller testing

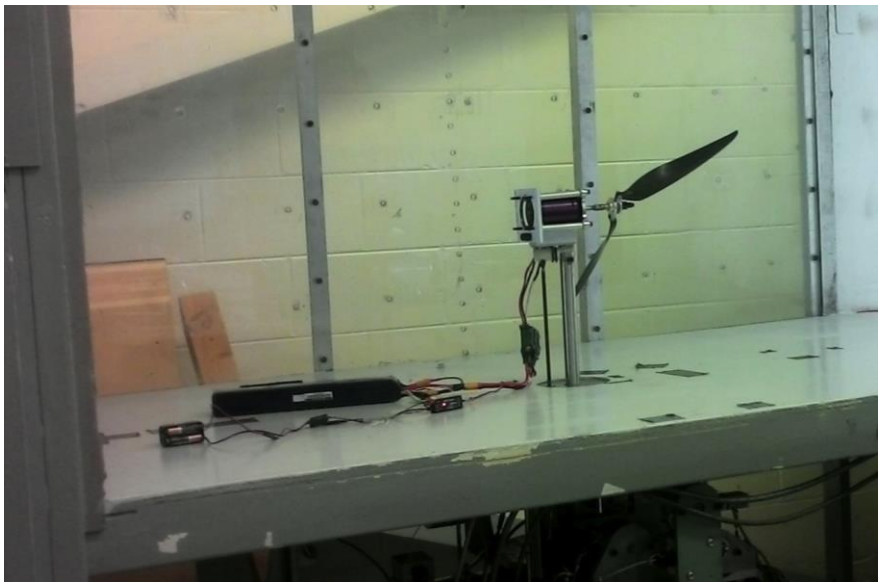

Figure 63: Experimental setup in the wind tunnel

As Table 16 and Figure 64 show, the three bladed configuration increases the thrust by 3.81 lbf compared to the two bladed configuration at full throttle and assuming a linear throttle curve:

	2 blades	3 blades
0	10.52 lbf	14.33 lbf
15	9.83 lbf	13.47 lbf
30	7.82 lbf	11.43 lbf

Table 16: Experimental data for motor testing

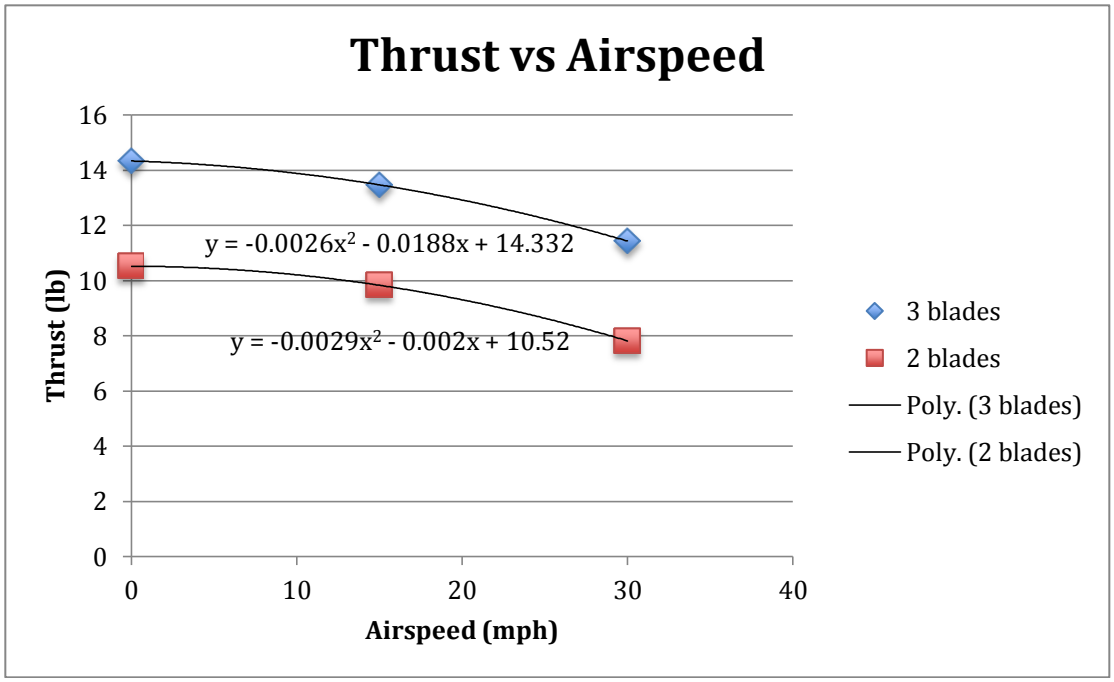

Figure 64: Graphical representation of experimental data

2.10 Flight Test

2.10.1 Takeoff

The first thing to do is to consider all the options for take off for a glider – bungee system, winch, aero tow by another aircraft or vehicle, dolly, conventional self launch system (SLS), and combination systems like SLS and dolly [31, 33, 43]. Each offers their advantages and disadvantages, but the main details that need to be considered are weight, cost, time to prepare, complexity, and flying conditions like headwind, crosswind, and length of runway.

The next value to find is the take off speed by using equations 7 and 8 [32]:

$$V_{TO} = 1.2V_{Stall} \tag{7}$$

where

$$V_{Stall} = \sqrt{\frac{W}{1/2\rho S C_{L_{max}}}} \tag{8}$$

using a maximum C_L of 1 from the build up component data in section 2.7, a wing area, S, of 23.68 ft^2, a weight, W, of 36 lbf, and a density, ρ, of 0.002377 $slug/ft^3$ as shown in equation 9:

$$V_{Stall} = \sqrt{\frac{36lbf}{1/2(0.002377\ slug/ft^3(23.68\ ft^2)(1)}} \tag{9}$$

The stall velocity, V_{Stall}, was found to be 36.36 ft/s (24.79 mph) while the takeoff velocity, V_{TO}, was found to be 43.63 ft/s (29.75 mph). The next detail to figure out was the take off ground distance using equations 10 through 12 [32]:

$$S_{TO} = \frac{1}{2B} ln \frac{A}{A\text{-}BV_{TO}^2} \tag{10}$$

where A and B are the following

$$A = g\left(\frac{T_0}{W} - \mu\right) \tag{11}$$

$$B = \frac{g}{W}\left[\frac{1}{2}\rho S\left(C_{D_g} - \mu C_{L_g}\right) + a\right] \tag{12}$$

The runway coefficient, μ, value was taken as 0.02, which is below the International Civil Aviation Organization's (ICAO) poor rating for what is called the runway friction coefficient [34]. To find the C_{D_g} and C_{L_g} equations 13 and 14 were used [32]:

$$C_{D_g} = \frac{D}{1/2\rho S V^2} \tag{13}$$

$$C_{L_g} = \frac{W}{1/2\rho S V^2} \tag{14}$$

where the drag, D, was found by using the following equation 15 [32]:

$$D = \frac{W}{L/D} \tag{15}$$

where the lift –to-drag ratio was 16.63 to assume the worst case scenario. The next step was to use equation 16 to find the constant *a* [32]:

$$T = T_0 - aV^2 \tag{16}$$

The static thrust, T_0, was found to be 14.332 lb while the thrust, T, at the take off velocity can be found by using the polynomial regression from Figure 64:

$$T = -0.0025V^2 - 0.0188V + 14.332 \tag{17}$$

Using the take off velocity, the thrust was found to be 11.56 lb. Rearranging and solving equation 16 with the previous values, the constant, a, was found to be 0.003132. Using the known values for all the variables, the take off distance was found to be 98.98 ft.

Take off was decided to be accomplished by using a bungee system made out of the items in Table 17 and shown in Figure 65 due to its simplicity and advantages of the least amount of added weight from landing gear and issues like ground clearance for the propellers:

Item	Quantity
16” Universal Spiral Anchor	1
¼” x 100’ All purpose poly rope	1
3/8” OD x ¼” ID x 10’ latex tubing	9
1 ½” Steel Rings – 2 pk	1
Steel ring	1

Table 17: Items in bungee launch system

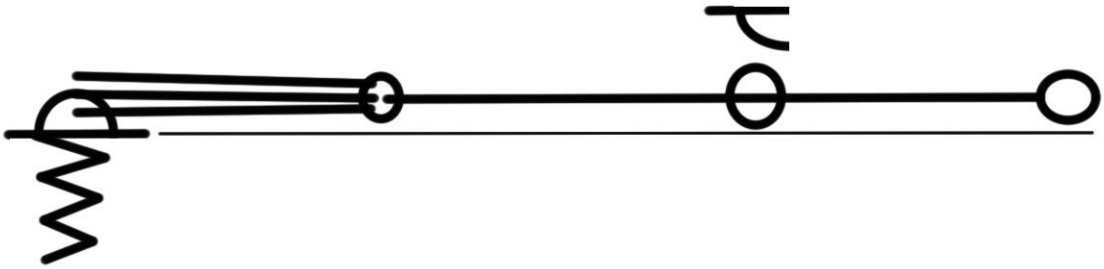

Figure 65: Bungee system diagram for takeoff

The anchor was screwed into the ground with one end of the surgical tubing tied to the anchor. The other end of the tubing was tied to a steel ring. One end of a poly rope was tied to the first steel ring. Two steel rings were then tied in the configuration shown in Figure 65. A hook was attached to the glider so that when the bungee system was pulled, the glider was placed into the middle steel ring as shown in Figure 65.

2.10.2 Maneuvers

The maneuver used in flight-testing for this project was the doublet. The doublet is a proven experimental method for finding the dampening ratio and natural frequency [40]. The maneuver was performed in the roll, pitch, and yaw directions [2]. The maneuver consists of the pilot getting the plane into level flight, then moving the stick to one direction, then moving the stick to the other direction, and then back to level flight [2]. This was done multiple times for each direction. Figure 66 though Figure 68 show the doublet for each direction:

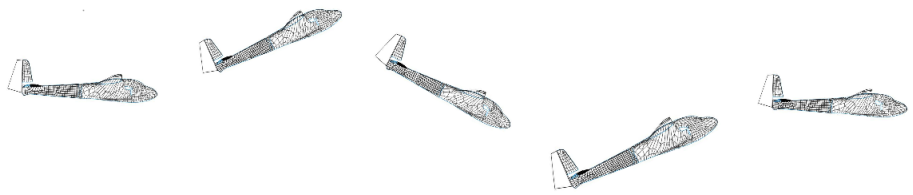

Figure 66: Pitch doublet

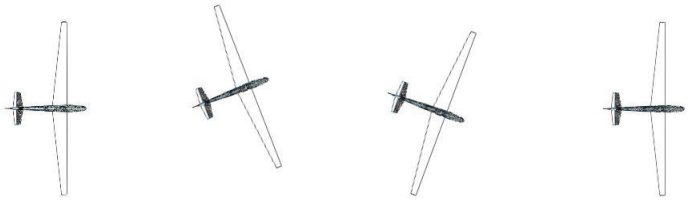

Figure 67: Yaw doublet

Figure 68: Roll doublet

The fourth maneuver was just an unpowered glide to gather data on the glide slope.

2.10.3 Data

Three sets of data were taken on two different days – April 30th and May 8th 2014. On May 8th 2014, there were two sets of flight data due to pilot concern for the safety of the aircraft during the first flight test of the day. All of the data collected can be found in Appendix A. The pilot inputs for each control surface in Appendix A had to be converted from a pulse signal to degrees by utilizing the linear regression lines in Appendix C for the respective sets of data from a surface deflection test. It was also assumed that the left aileron was just the inverse of the right in both signal and deflection. This assumption was made because the optimization program in MATLAB does not allow for two inputs for the roll direction.

3. Results

3.1 Stability Results Comparison

The table in Appendix F compares the stability and aerodynamic characteristics that were generated by Surfaces, Datcom, and AVL with flight-testing. From the table in Appendix F, two to three VLM methods produced matching characteristics for the lift coefficient, drag coefficient, and side force derivative. The table located in Appendix E shows the optimization attempt using the Latin Hypercube method in Simulink, but started to diverge. Unfortunately, the flight data was not suitable to find the actual stability derivatives due to noise and the use of an incorrect complementary filter block in the Simulink data-recording model for finding phi and theta [23, 36]. Another probable cause could be the use of inertias from SURFACES instead of using the swing method [36].

3.2 Glide Slope Comparison

The data used for finding the glide slope was taken from the flight test done on April 30th 2014. The reason was that the AoA vane worked properly and measured reasonable values for AoA. As shown in Appendix A, the angle of attack is consistently at 5 degrees. This was due to the carbon fiber tube setting at this angle while the epoxy was curing. The angle of attack data from the other two data sets do not make sense since both show that the neutral angle of attack is close to -50 and -220 degrees as shown in Appendix A for the flight test data sets for May 8th 2014.

The glide slope from the test flight was found by using the ratio between the airspeed and sink rate using equation 18 [8]:

$$\frac{L}{D} = \frac{v_{airspeed}}{v_{sk}} \tag{18}$$

An average airspeed was found by using the April 30th flight test data from Appendix A. To find the sink rate, the data had to be converted from 'in Hg' to 'Pa' so the barometric formula shown in equation 19 was used find the altitude in feet [7]:

$$P_h = P_0 e^{-\frac{mgh}{kT}} \tag{19}$$

By dividing the difference in altitude by the time it took to sink, a sink rate can be used with the airspeed to find the glide slope. Figure 69 through Figure 70 show the selected altitude that was used to find out the sink rate:

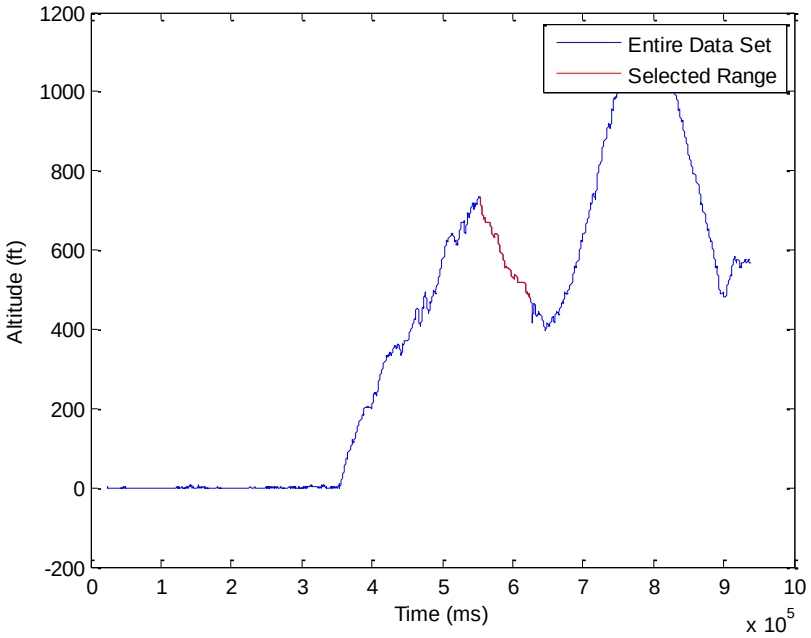

Figure 69: Selected altitude

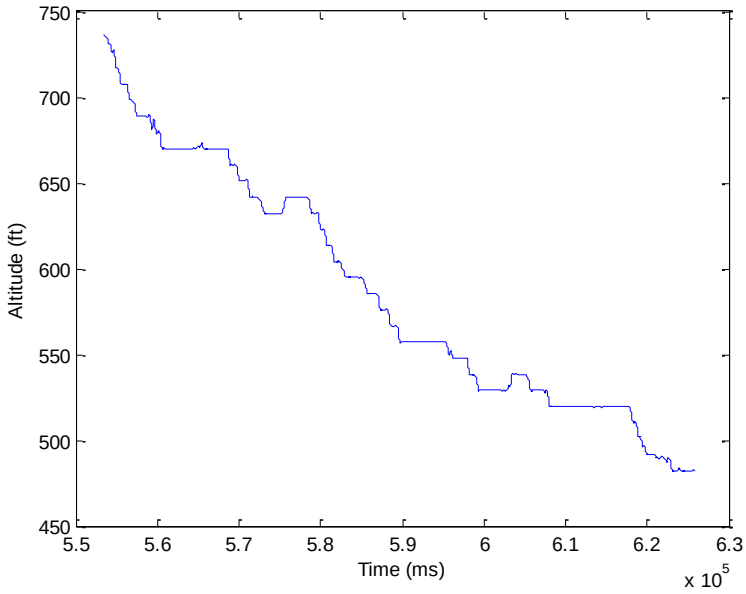

Figure 70: Selected altitude close up

Figure 71 shows a comparison of the ground speed and airspeed versus time in the selected time range.

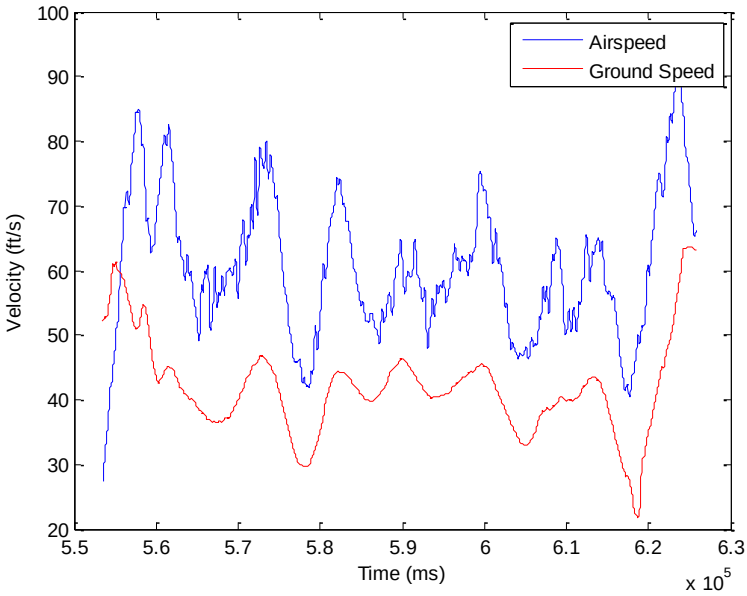

Figure 71: Air speed and ground speed

This is an important consideration since going against the wind would increase the airspeed and therefore lift. The wind direction was found by using equation 20 [29]:

$$v_{ground} = v_{wind} + v_{air} \tag{20}$$

A negative wind velocity would mean that the glider was going into the wind.

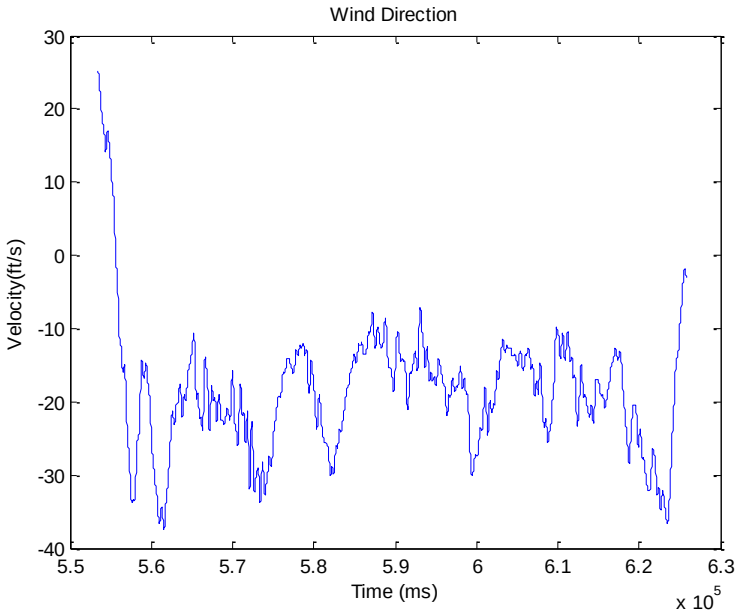

Figure 72: Wind speed from the difference of airspeed and ground speed

It is also important to look at the pilot inputs and angles of attack are during this interval:

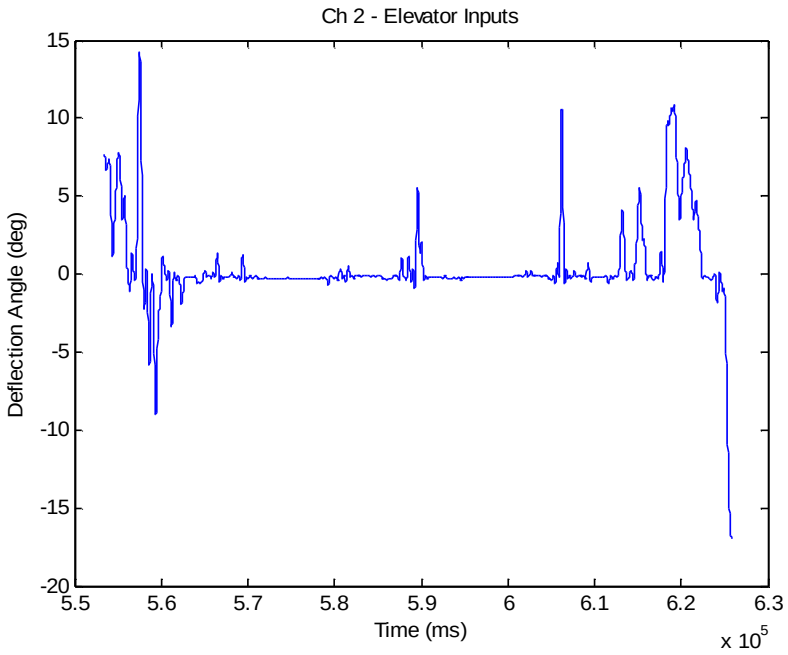

Figure 73: Pilot inputs

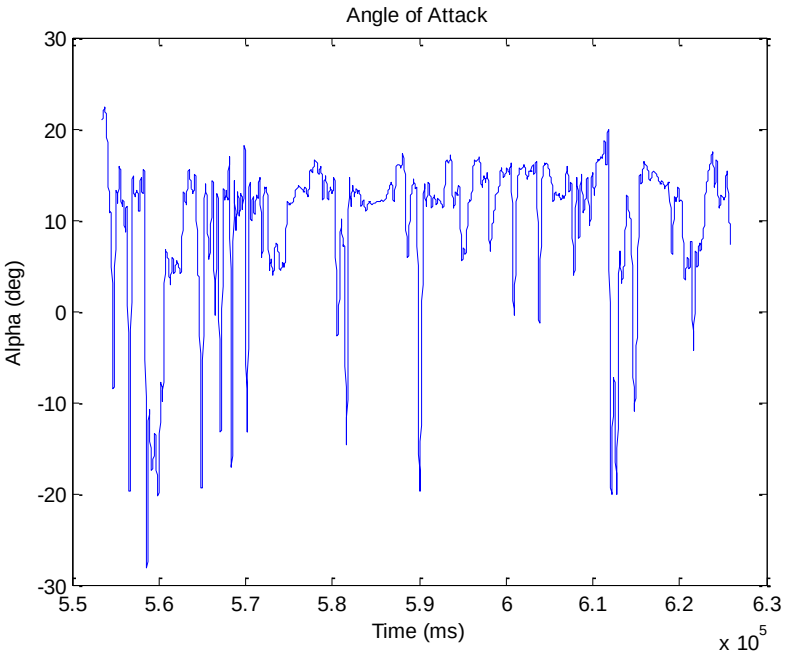

Figure 74: Measured angle of attack

The glide slope for this glider was found to be 17.233 on April 30th 2014. However, if the data is taken between 5.8386e5 ms and 6.2388e5 ms, the glide slope is 22.0744. The data used to find this glide slope is shown in the following graphs:

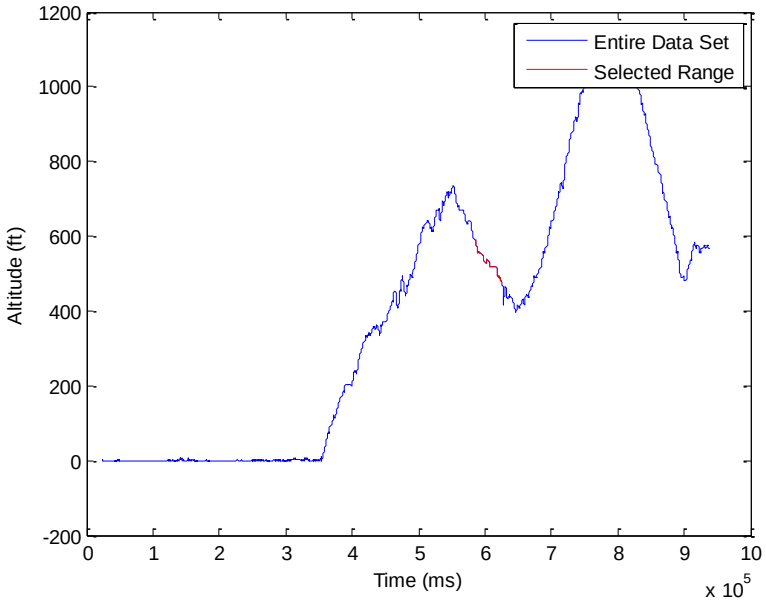

Figure 75: Selected altitude

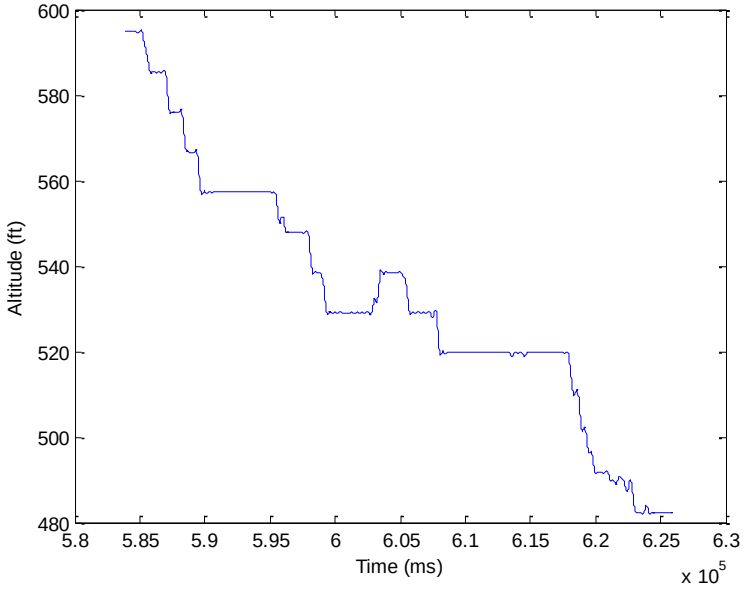

Figure 76: Close up of selected altitude range

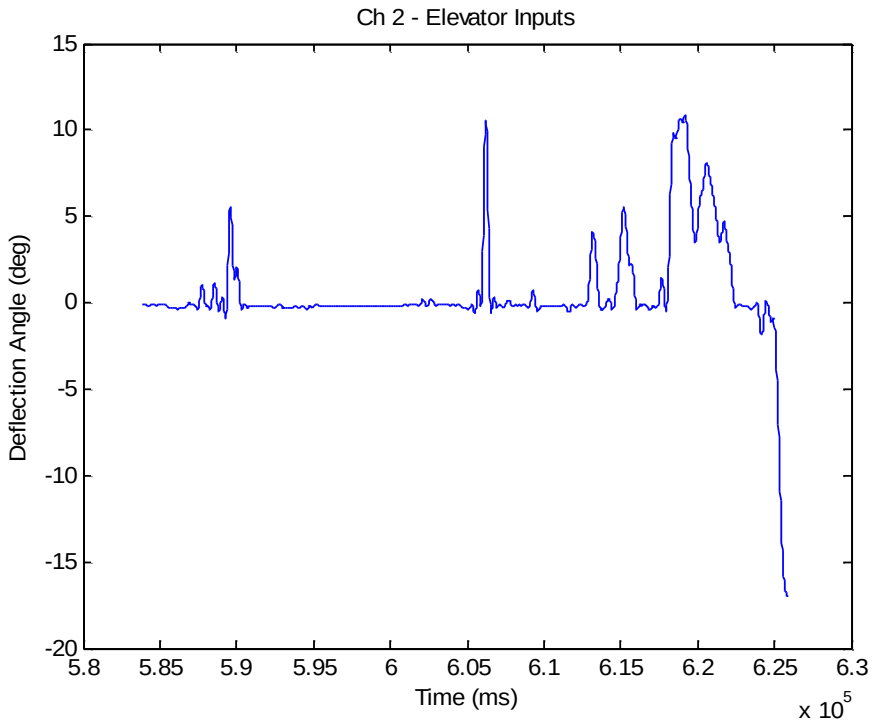

Figure 77:Pilot Inputs

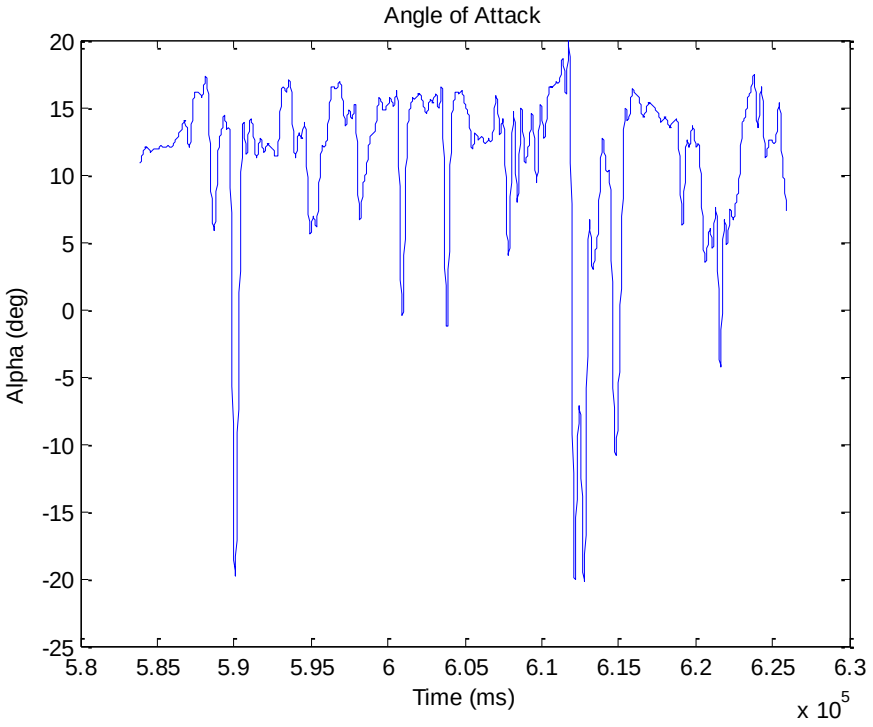

Figure 78: Measured angle of attack

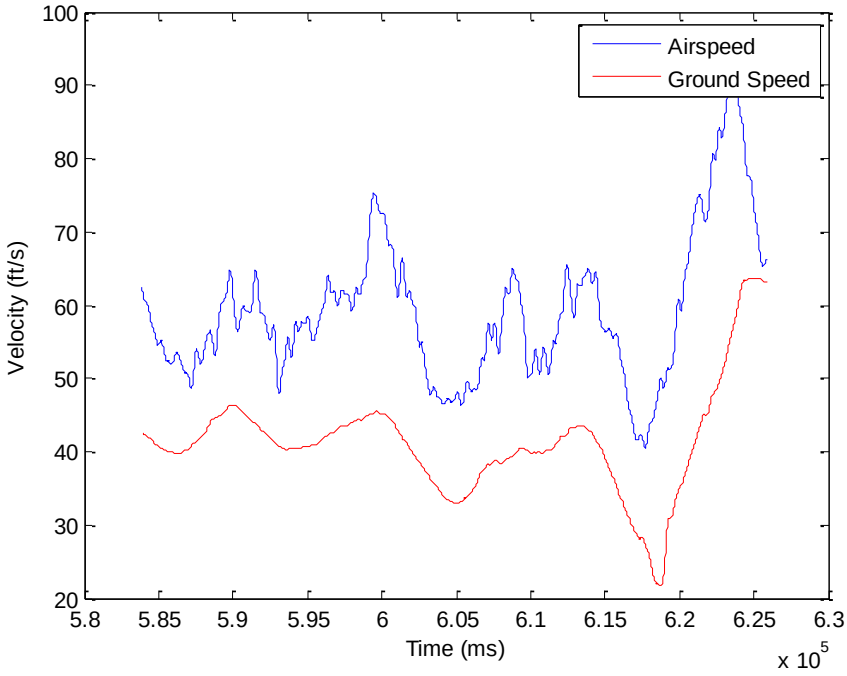

Figure 79: Air speed and ground speed comparison

If we compare the two data sets, it becomes clear that the L/D ratio can vary greatly.

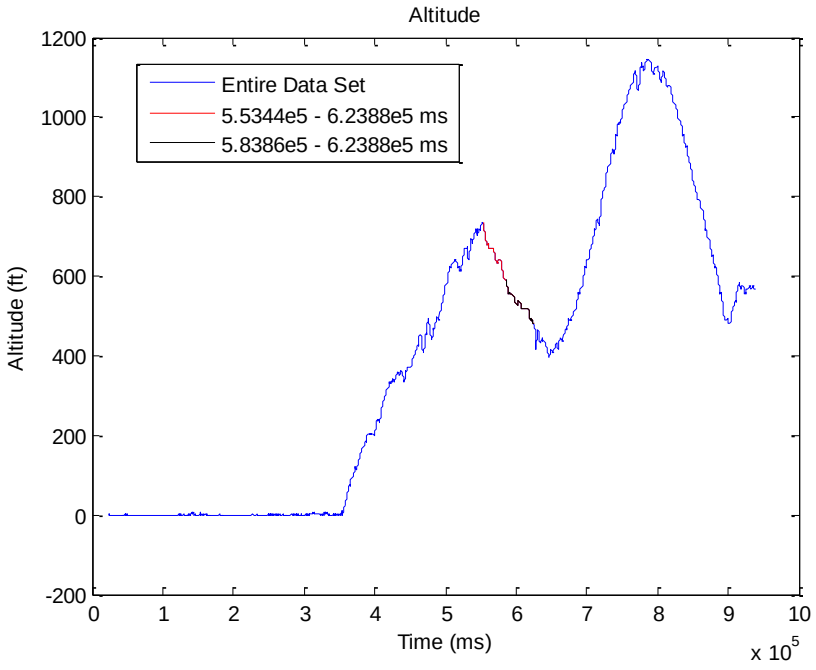

Figure 80: Comparison of selected ranges

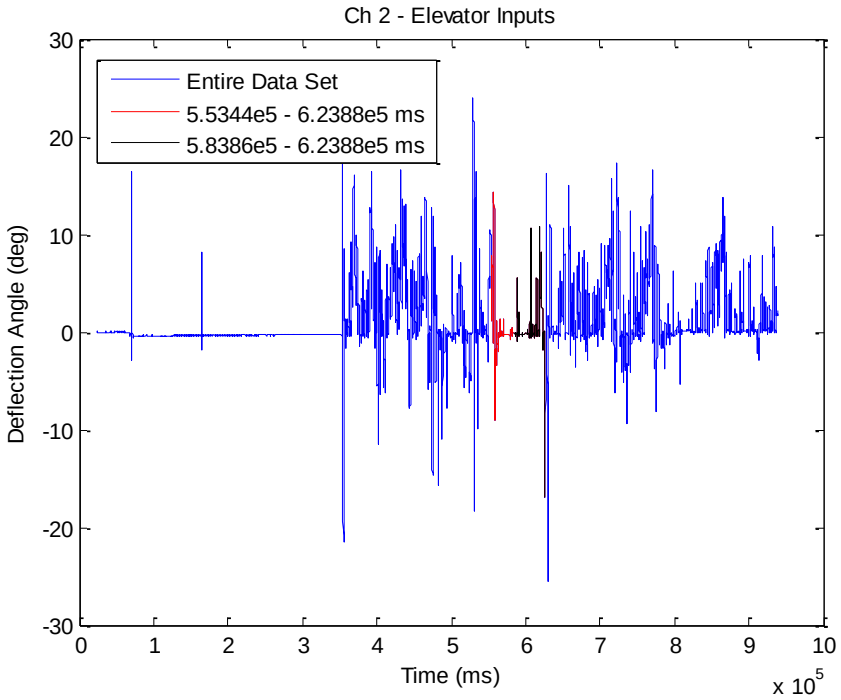

Figure 81: Comparison of pilot inputs for selected ranges

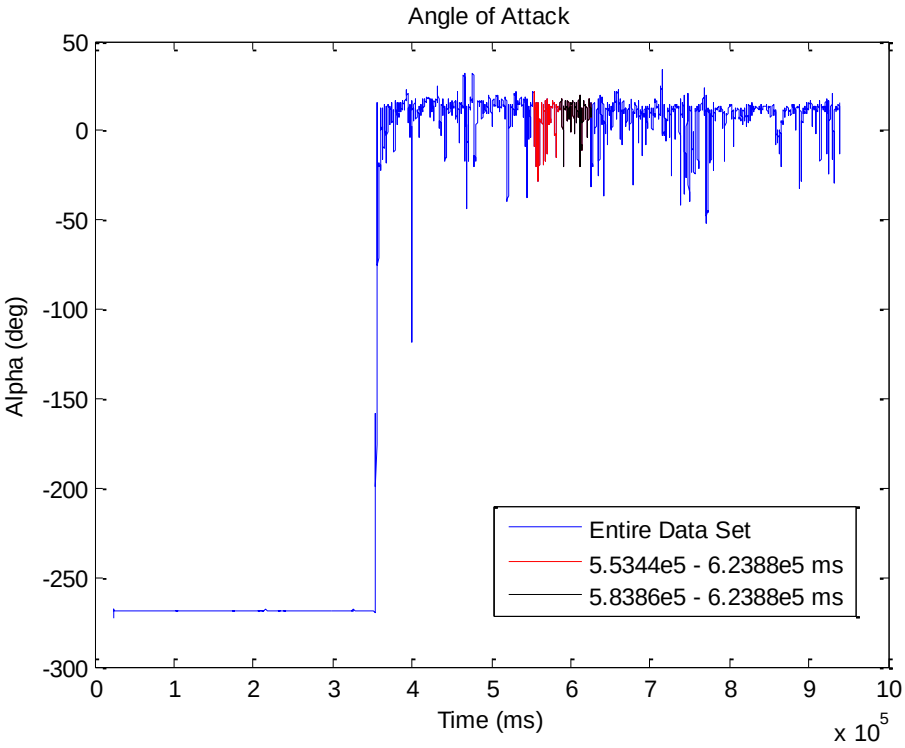

Figure 82: Comparison of angle of attack among selected ranges

However, this number cannot be used because, due to no accelerometer data in the y-direction, a constant acceleration due to gravity cannot be assumed. Also, the data up to this point went through a Butterworth filter to clean out any noise and was generated by the second script in Appendix G. It should be noted that the filter does alter the numerical value.

Another method had to be used to figure out the glide slope using the first script in Appendix G. This included incorporating the error in the barometer and airspeed sensors. To get the total error from both the barometer and airspeed sensor, equation 22 is utilized when either multiplying or dividing two numbers with errors [1]:

$$z = \frac{x}{y} \tag{21}$$

$$\frac{\Delta z}{z} = \frac{\Delta y}{y} + \frac{\Delta x}{x} \tag{22}$$

The airspeed sensor was bought from 3DRobotics and had the MPXV7002 Series chip from Freescale Semiconductor with an error of +/- 6.25% V_{FSS} [18]. The error can be found by using the given transfer function, equation 23, of the chip located in the data sheet [18]:

$$V_{out} = V_s * \left(0.2 * P(kPa)\right) + 0.5 \pm 6.25\% V_{FSS} \tag{23}$$

The V_{out} was found by using the voltage values from Figure 18 to find the pressure in kilopascals. Since only a certain range is used within the chip's operating condition, a

ratio can be found by using the difference of pressure used in the actual measurement and the difference of the total operating range of the chip and then multiplying this number by 6.25% to find an error of +/-0.4074 ft/s [17]. Finding the error for the barometer was much simpler since it was given in the data sheet for the M5611-01BA03 Barometric Pressure Sensor from Measurement Specialties [16]. This number is +/- 1.5 mbar, which converts to +/- 0.0738 in Hg [16]. The error was found by taking the first error free reading and then subtracting it from the same reading with the error included. This was found to be +/- 8.2274 ft. To find the instantaneous velocity, the equation for the vertical position was found by using a regression line in terms of time. The regression line for the selected range using a first order polynomial fit was found to be the following:

$$y(t) = -3.1372t + 2360.1 \tag{24}$$

The selected region is shown in Figure 83:

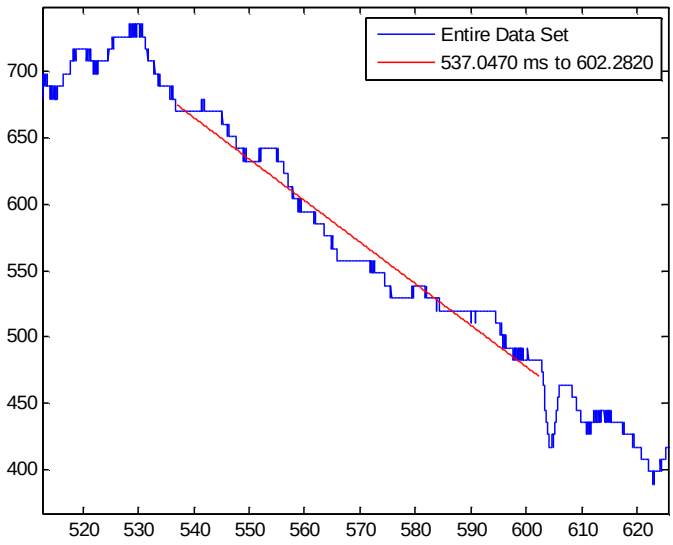

Figure 83: Linear regression line for selected range

Taking the derivative gives a constant velocity of -3.1372 ft/s. The first glide slope ratio data point was found to be 6.9451 using an airspeed of 71.4846 ft/s and a sink rate of 3.1372 ft/s. An error of 0.2537 ft/s was found for the sink rate by taking the difference of altitude with the error included and dividing by the time range [15]. This was the only way to figure out an average error just using the barometer error. The sink rate is always negative number unless it is being used to calculate the glide slope. Inserting the information into equation 22 to get equation 25:

$$\frac{\Delta z}{6.9451} = \frac{0.4074\ ft/s}{71.4846\ ft/s} + \frac{0.2537\ ft/s}{-3.1372\ ft/s} \tag{25}$$

Solving for Δz, the error associated with the L/D ratio is +/- 0.7914, which can be shown in red error bars in Figure 84 for the instantaneous L/D ratio:

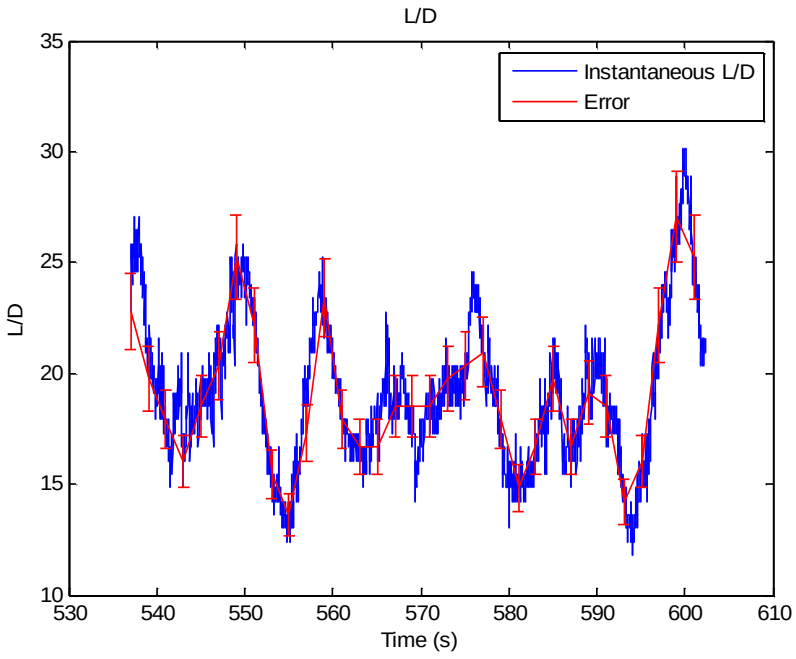

Figure 84: Instantaneous L/D with error bars

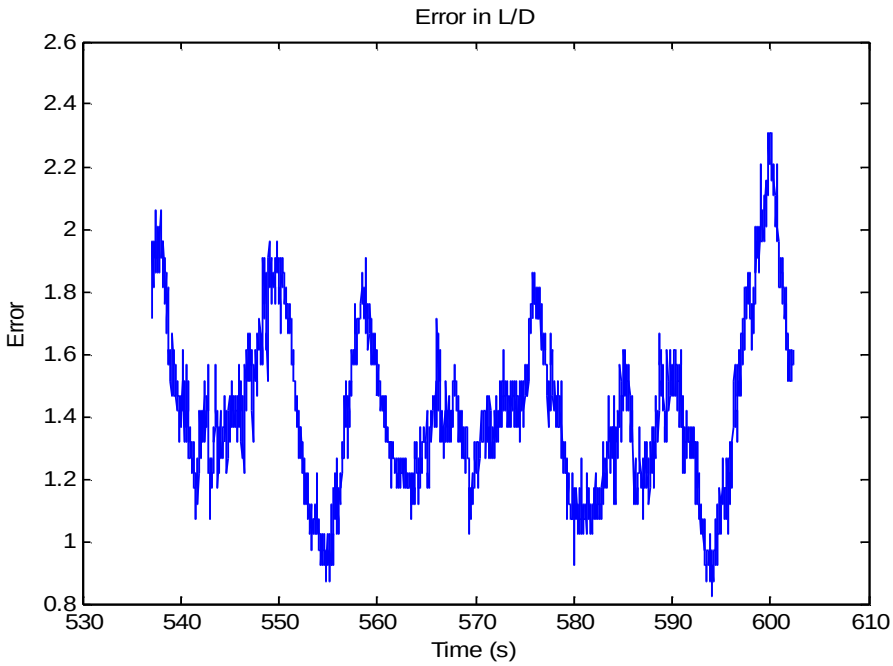

Figure 85: Error in L/D

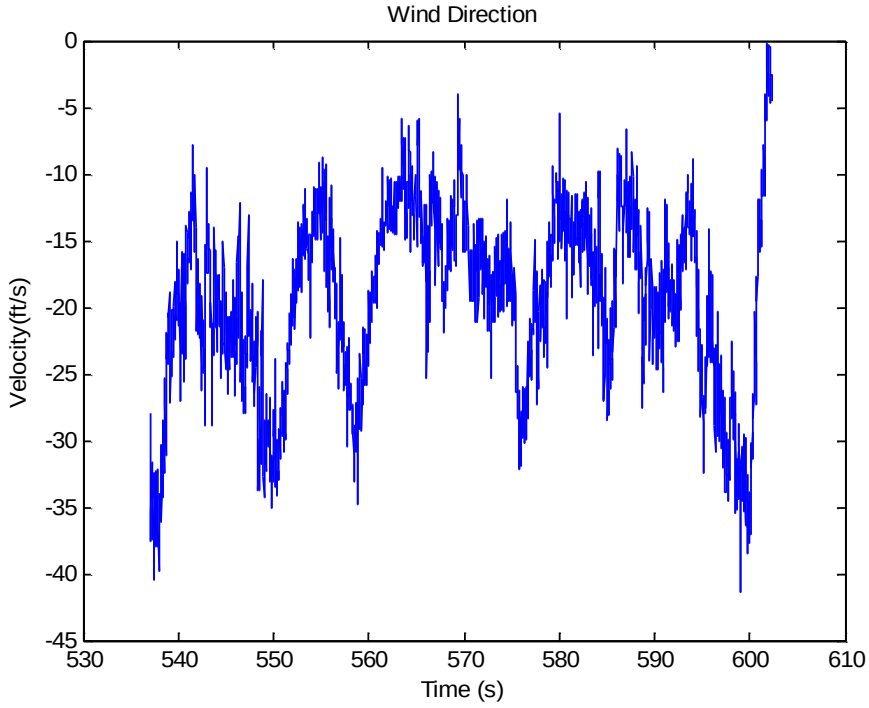

Figure 86: Wind direction by taking the difference of air and ground speed

However, plotting the residuals show that there is a non-random error as shown in Figure 87. This means that the model chosen, or a polynomial fit order of one, does not fit the data even though the confidence level is at 95.67% [22].

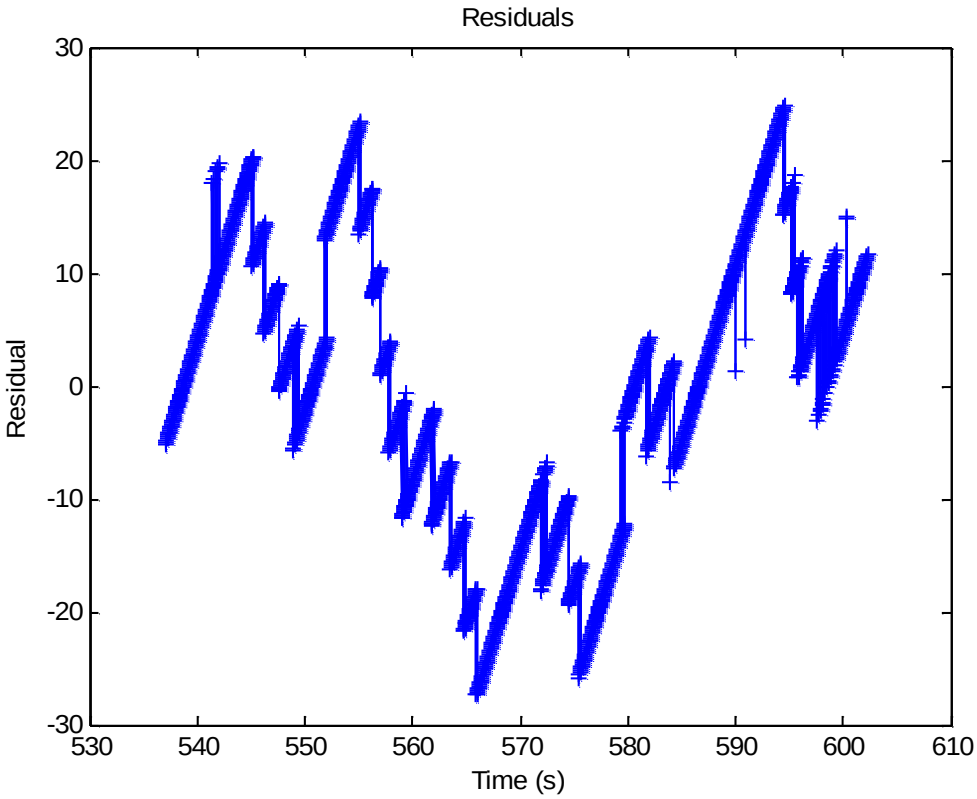

Figure 87: Residuals to tell how well the linear regression line fits the model

The data was then reanalyzed to the new value for both L/D ratio and a new error. By increasing the power of the polynomial to two, the average glide slope changes to 21.2520. However, this L/D has a variable error associated with it where the minimum error is +/- 0.4915 and a maximum of +/- 8.4866.

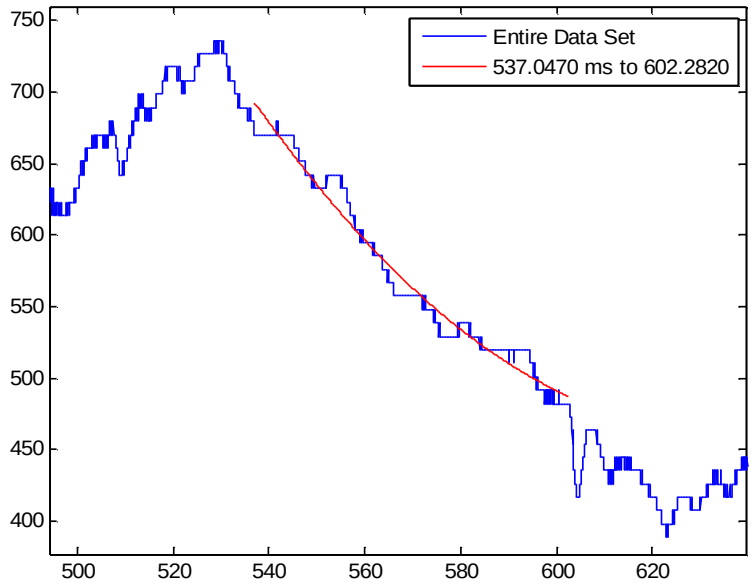

Figure 88: Same selected altitude range but with a 2nd order polynomial fit regression line

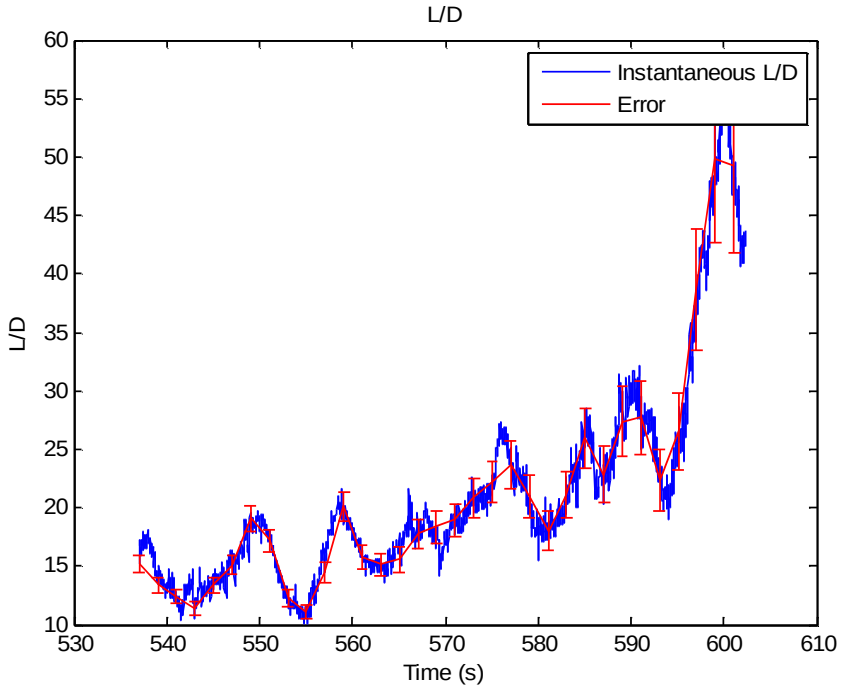

Figure 89: Instantaneous L/D with error bars

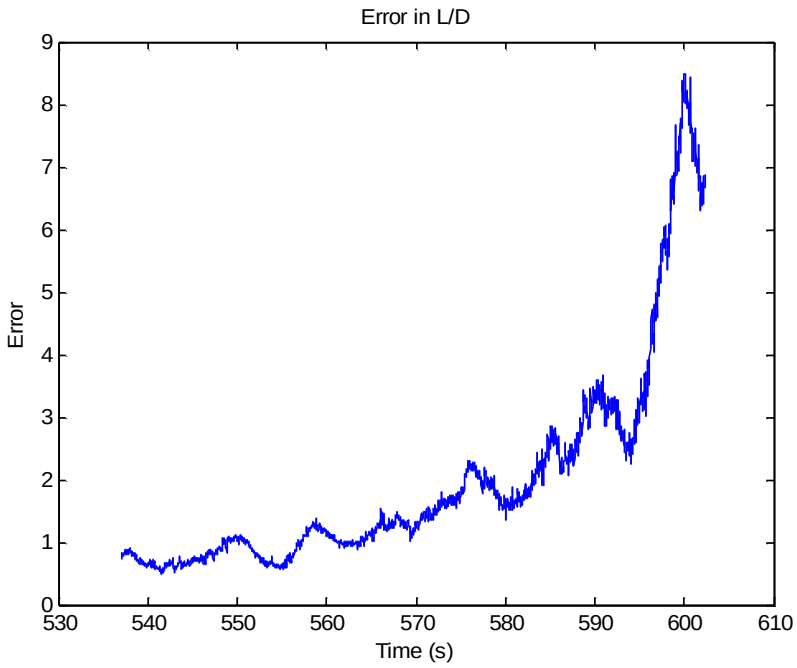

Figure 90: Error in L/D

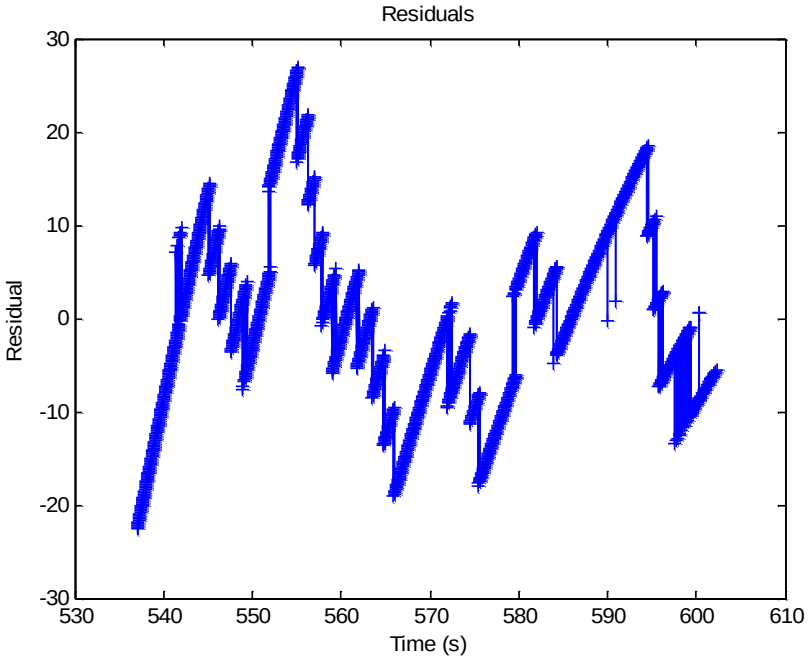

Figure 91: Residual plot for the 2nd order polynomial fit regression

Nonetheless, a predictive behavior of the residuals, as shown in Figure 91, persists. This means that the polynomial fit chosen still does not fit and that a variable has not be accounted for [22].

The average glide slope was found to be between 19.1617 for a polynomial fit order of one and 21.2520 for an order of two. However, the average errors associated with both glide slopes need to be found by using the rules for addition as shown in equations 26 and 27 [1]:

$$z = x + y \tag{26}$$

$$\Delta z = \Delta x + \Delta y \tag{27}$$

The average glide slopes become 21.2520 +/- 1.99 and 19.1617 +/- 1.4196.

4. Conclusion

As Table 18 shows, the flight test gave a lift to drag ratio between the two other methods but biased towards the industry build up method.

L/D – Glide Slope Comparison		
Flight Test	CFD 3D	Industry
19.1617 +/- 1.4196 – 21.2520 +/- 1.99	16.63	23.79

Table 18: Glide slope comparison

For the CFD method, it is expected for the glide slope to be low because CFD over predicts the drag due to artificial viscosity coupled with the omission of realistic imperfections that come with the glider [31]. The industry build up method assumes that the glider has less drag by making assumptions about the geometry of the fuselage and vertical tail. However, both methods assume a constant wind direction in the horizontal direction.

Nonetheless, the results are inconclusive for what the real glide slope is from the flight test data due to the presence of wind because there was no way to measure the influence of an updraft caused by a thermal, a down draft, or a vertical component of a gust. Another issue that hindered the analysis was to correctly select the maneuver time range that would capture the real glide slope.

5. Future Work

There are many things to improve upon within this project. The most important issue is to upgrade and add more instrumentation to get an accurate measurement of the glide slope. Some suggestions for new instrumentation, but not a complete list, would include the following:

- Variometer

  The variometer is an important piece since it measures the rate of descent or ascent. This will give an instantaneous measurement of the vertical velocity so that a polynomial fit would not have to be used. This sensor coupled with a ground station would make finding thermals easy to keep aloft for longer periods. This would help in figuring out the speed polar for the glider [27]. A digital variometer could be implemented using a complimentary filter to fuse the barometric vertical velocity and vertical acceleration readings [38].

- Real-time telemetry sent to pilot

  It was difficult to make sure that the glider was flying level from the ground until the data was analyzed. Knowing the angle of attack in real time or having autopilot would save a lot of time instead of analyzing the angle of attack data after landing. This would also allow testing of the L/D at different angles of attack.

- Strain gauges or accelerometers to measure the wing deflection

  By knowing the instantaneous deflection of the wings, a deeper understanding of its dynamics and design can be examined [26]. One important dynamic behavior to avoid is when does fluttering occur.

- Better air data boom

  A redesign of the air data boom structure is needed because time is wasted when recalibrating when the potentiometers for the AoA and AoY vanes are replaced. The design needs to incorporate a holder so that the potentiometer could be placed in a more accessible position. Also, designing a wing with a place where the boom could be threaded in using a threaded rod and access point would improve the measurements and any logistical issues. A wind tunnel test should be done to determine the size of the vanes to improve the measurements for AoA and AoY.

- Inertia

  A contraption will have to be built so that a scale glider could swing and the inertias found by using the swing method [20].

- Motor Testing

  A new test should be done to look at the efficiency of different blade configurations and throttle position.

References

[1] Linberg, Vern. *Uncertainties and Error Propagation. Part I of a manual on Uncertainties, Graphing, and the Vernier Caliper*. RIT, 1 July 2000. Web. 21 June 2014.

[2] Alvydas Civinskas (student) in discussion with professor Moncayo, January 2014.

[3] McClanahan, Jade. Numerical Evaluation of Glider Aerodynamic Performance.

[4] Mckee, Kyle. "Novel Airframe Design for the Dual-Aircraft Atmospheric Platform Flight Concept. MS Thesis." Embry Riddle Aeronautical University, 2012. Print.

[5] "AVL" MIT. MIT. N.d, n.p. Web.<http://web.mit.edu/drela/Public/web/avl/>

[6] "GL04 - Ka-8b ELECTRIC 6000 ARF 1/2.5 SCALE." *Phoenix Model*. Phoenix Model, n.d. Web. Jan. 2014. <http://phoenixmodel.com/Product.aspx?ProductId=295>.

[7] "Barometric Formula" *Hyperphuysics*. Georgia State University, n.d., n.p. Web. 17 June 2014. <http://hyperphysics.phy-astr.gsu.edu/hbase/kinetic/barfor.html>

[8] Federal Aviation Administration. *Chapter 3: Aerodynamics of Flight.* FAA. PDF File.

[9]"HQ 3.0/15 AIRFOIL." *Airfoil Tools*. N.p., n.d. Web. Jan. 2014. <http://airfoiltools.com/airfoil/details?airfoil=hq3015-il>.

[10] "Lift & Drag Polars." *Airfoil Tools*. N.p., n.d. Web. Jan. 2014. <http://airfoiltools.com/airfoil/details?r=polar/index/#xfoil>.

[11] Drela, Mark. "Xfoil - Subsonic Airfoil Development System." *MIT*. MIT, 11 Dec. 2000. Web. <http://web.mit.edu/drela/Public/web/xfoil/>.

[12] Coxworth, Ben. Solar-powered UAV could fly in the upper atmosphere for 5 years at a time. Gizmag. Web. 20 June 2014. <http://www.gizmag.com/solara-uav-atmospheric-satellite/28886/>

[13] Chapman, Matthew. Facebook buys UK-based drone company Ascenta to 'beam' internet from sky. Marketing Magazine. Web. 20 June 2014. <http://www.marketingmagazine.co.uk/article/1287644/facebook-buys-uk-based-drone-company-ascenta-beam-internet-sky>

[14] Quick, Darren. Lockheed Martin's HALE-D airship takes to the air. Gizmag. Web. 20 June 2014. <http://www.gizmag.com/lockheed-martin-hale-d-airship/19360/>

[15] *Error Analysis*. University of Tennessee of Martin. N.d., n.p. Web. <http://www.utm.edu/staff/cerkal/Lect4.html>

[16] Measurement Specialties. *MS5611-01BA03 Barometric Pressure Sensor, with stainless steel cap.* Measurement Specialties. PDF File.

[17] Honeywell. *Pressure Transducer Accuracy in Application.* Honeywell. PDF File.

[18] Freescale Semiconductor, Inc. *MPXV7002 Series.* Freescale Semiconductor, Inc. PDF File.

[19] Longacre. Computerscales Accuset II Basic System. N.d., Longacre. Web. <http://www.longacreracing.com/products.aspx?prodid=7143>

[20] Watkiss, Eric John. *Flight Dynamics of an Unmanned Aerial Vehicle* Monterey, CA: US Naval Postgraduate School. 1994. PDF File.

[21] National Institute of Standards and Technology. *Are the model residuals well-behaved?* N.d., NIST. Web. <http://www.itl.nist.gov/div898/handbook/pri/section2/pri24.htm>

[22] Phoenix Model. *Instruction Manual: K8B*. Print.

[23] Alvydas Civinskas (student) in discussion with professor Moncayo, June 2014

[24] Thompson, David E. "Harmonic Response of Second Order Systems" University of Idaho, 2006., n.p. Web. 30 June 2014. <http://www.engr.uidaho.edu/thompson/courses/ME330/lecture/SecondOrderSystems.html>

[25] "Aircraft Center of Gravity Calculator" n.p. Web. 5 Julty 2014. <http://adamone.rchomepage.com/cg_calc.htm>

[26] Qiao, Yuqing. "Effect of Wing Flexibility on Aircraft Flight Dynamics." MA Thesis. Cranfield University, 2012. Web. 9 July 2014.

[27] Federal Aviation Administration. *Chapter 5: Glider Performance.* FAA. PDF File.

[28] Engblom, William A. "Development of an Atmospheric Satellite Concept Based on Sailing." *AIAA SciTech: 52nd Aerospace meeting. National Harbor, Maryland 13-14 January 2014.* n.p.

[29] Ohlson, Dawn. *The Mathematics of Aircraft Navigation.* Royal Academy of Engineering. n.d. PDF File.

[30] Alvydas Civinskas (student) in discussion with professor Engblom, July 2014.

[31] Espritmodel *Sailplane Takeoff Dolly 1/3 Scale*.Web. <http://www.espritmodel.com/sailplane-takeoff-dolly-1-3-scale.aspx>.

[31] Virginia Tech. *Performance*. Virginia Tech. PDF File.

[33] Federal Aviation Administration. *Chapter 7: Launch and Recovery Procedures and Flight Maneuvers.* FAA. PDF File.

[34] International Civil Aviation Organization. *Study Note 2, Appendix, Checklist of AMD 37 Revisions* 2014. *Microsoft Word* file

[35] "Phoenix Models K8b – 3.5m ARFT" *Hyperflight UK*. Hyperflight UK. n.d. Web. Aug 2014. <http://www.hyperflight.co.uk/products.asp?code=PM%2DK8B%2D3M>

[36] Alvydas Civinskas (student) in discussion with professor Moncayo, August 2014

[37] Alvydas Civinskas (student) in discussion with professor Engblom, June 2014

[38] Higgins, Jr., Walter T. "A Comparison of Complementary and Kalman Filtering." *IEEE Transactions on Aerospace and Electronic Systems.* 3 (1975): 321-325. Web.

[39] Fatica, Massimiliano and Antony Jameson. *Using Computational Fluid Dynamics for Aerodynamics.* Stanford University. PDF File.

[40] Yechout, Thomas R., Steven L. Morris, David E. Bossert, and Wayne F. Hallgren. *Introduction to Aircraft Flight Mechanics: Performance, Static Stability, Dynamic Stability, and Classical Feedback Control.* Reston, VA:American Institute of Aeronautics and Astronautics, Inc. 2003.

[41] MEDIATEK. *MEDIATEK-3329 Datasheet.* MEDIATEK. PDF File.

[42] Zuo, Wangda. Introduction of Computational Fluid Dynamics.

[43] Alvydas Civinskas (student) in discussion with Daniel Harrison (RC pilot), June 2014

Appendix:

A. Flight Test Data

a. April 30th 2014

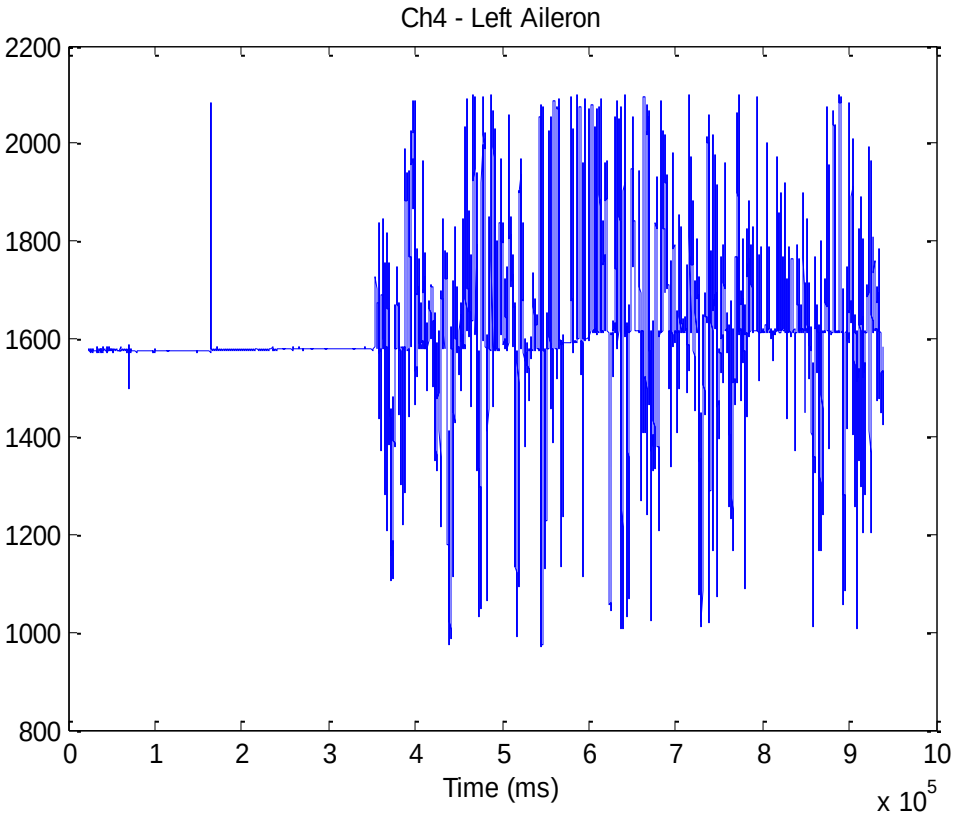

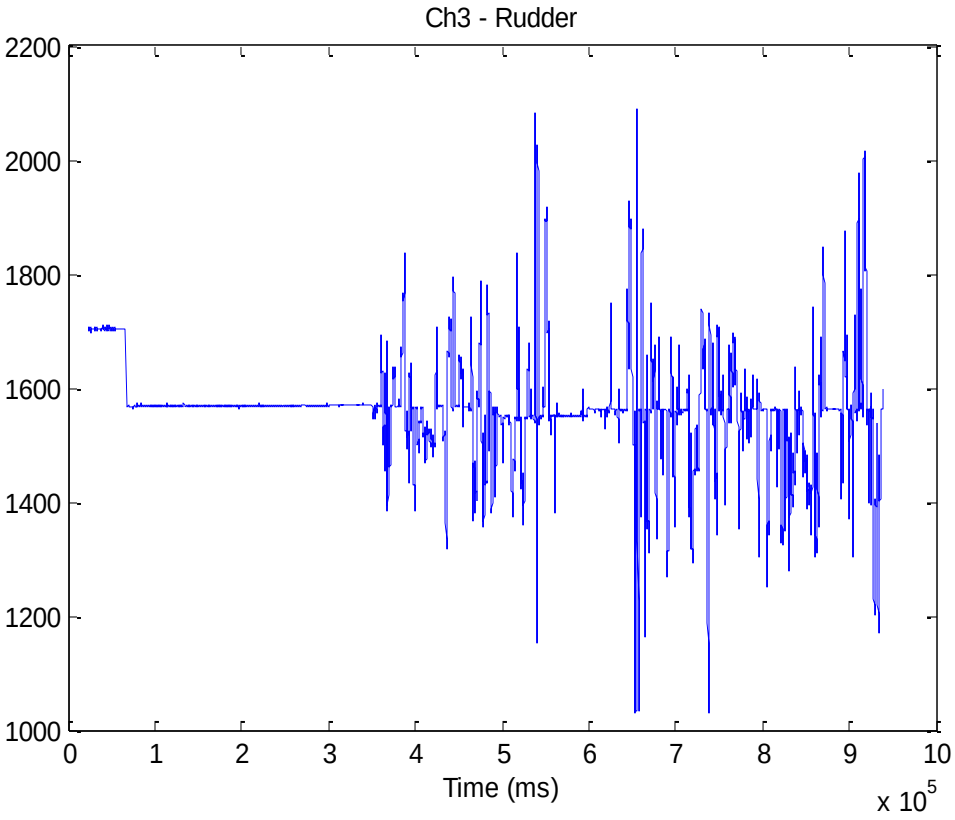
Ch3 - Rudder
2200
2000
1800
1600
1400
1200
1000
0
1
2
3
4
5
6
7
8
9
10
Time (ms)
x 10^5

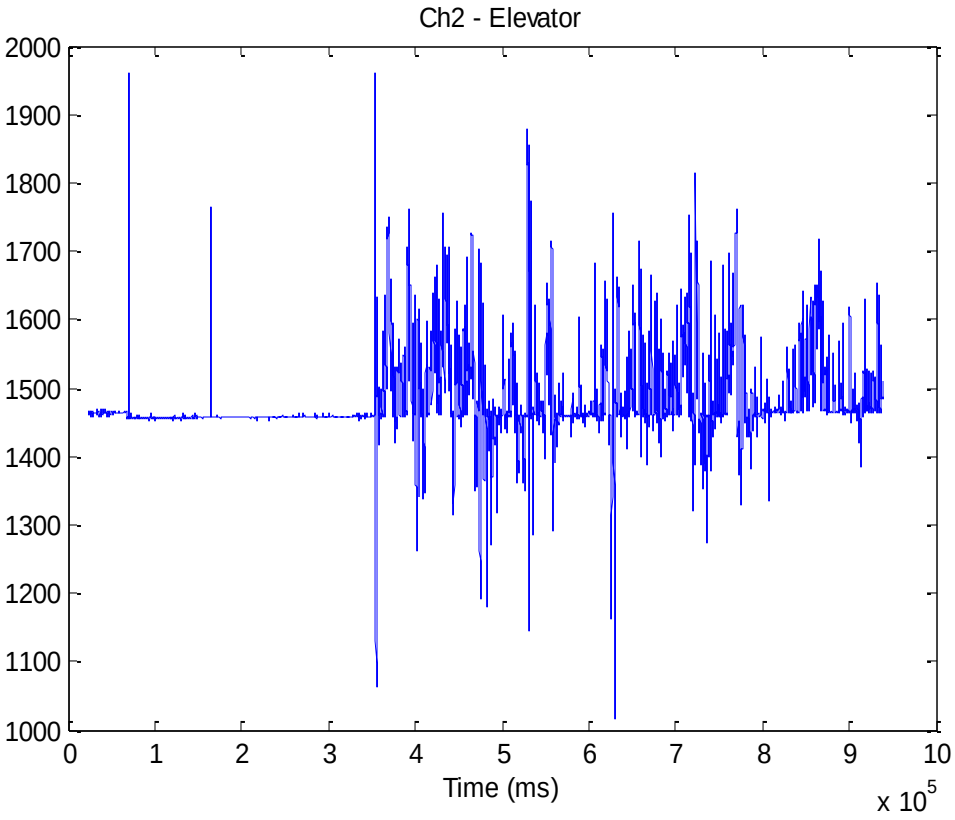
Ch2 - Elevator
2000
1900
1800
1700
1600
1500
1400
1300
1200
1100
1000
0
1
2
3
4
5
6
7
8
9
10
Time (ms)
x 10^5

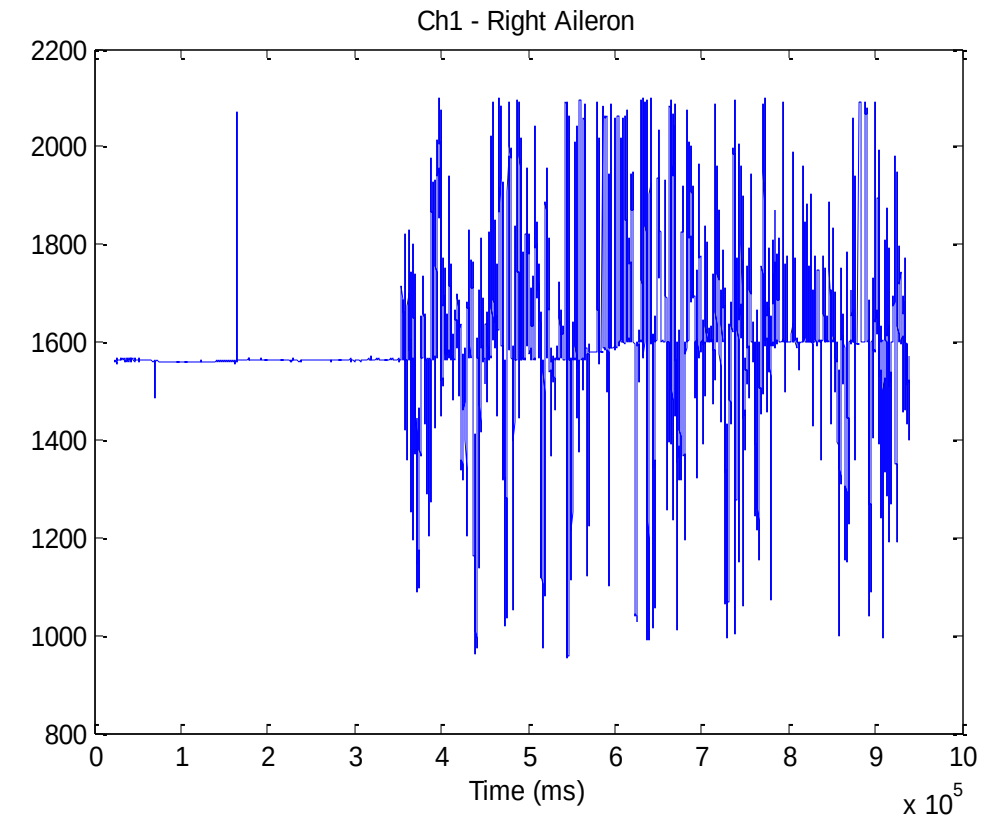
Ch1 - Right Aileron
2200
2000
1800
1600
1400
1200
1000
800
0
1
2
3
4
5
6
7
8
9
10
Time (ms)
x 10^5

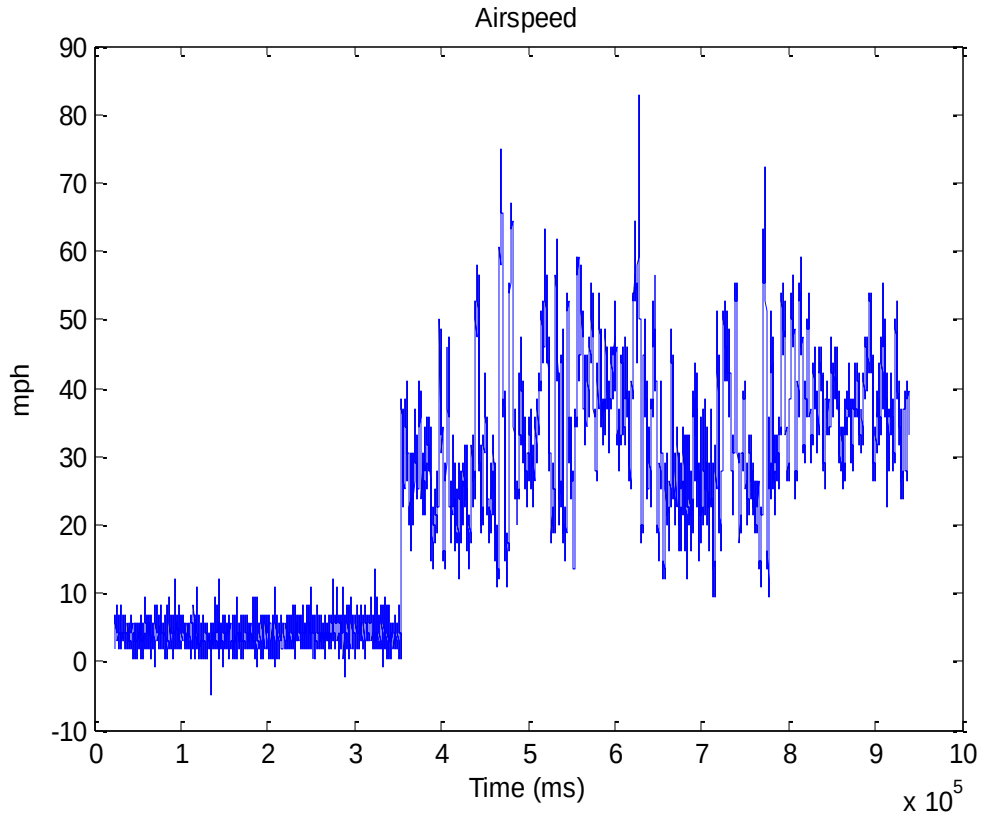
Airspeed
mph
90
80
70
60
50
40
30
20
10
0
-10
0
1
2
3
4
5
6
7
8
9
10
Time (ms)
x 10^5

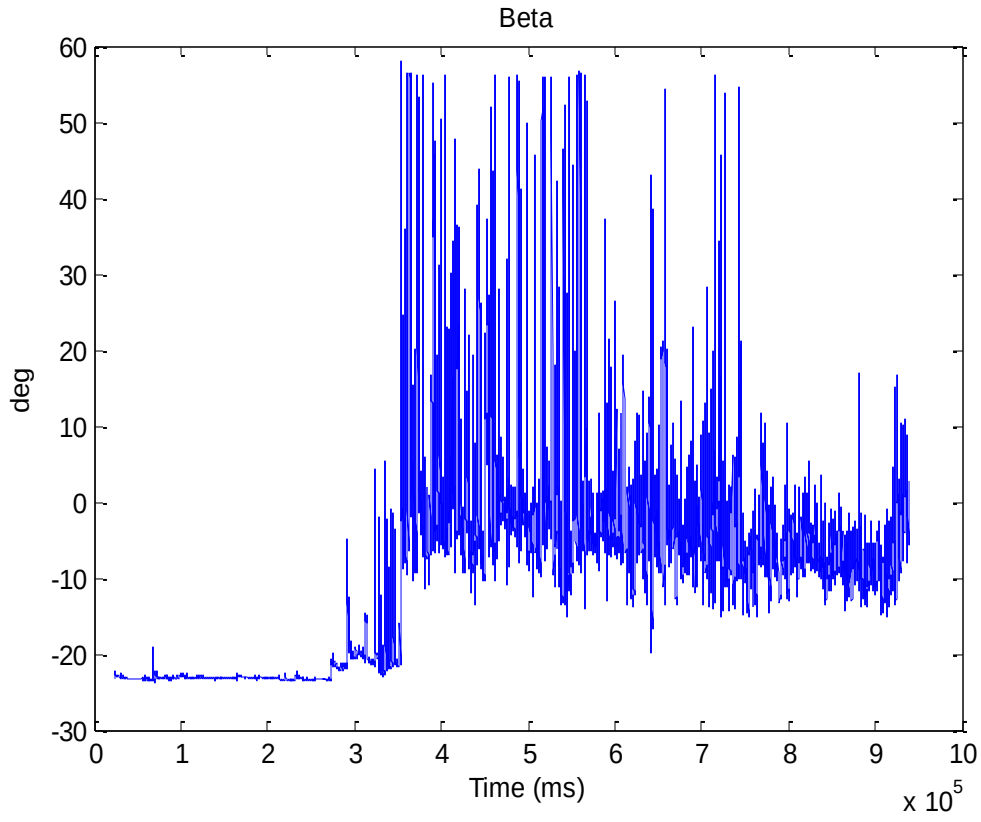
Beta
60
50
40
30
20
10
0
-10
-20
-30
deg
0
1
2
3
4
5
6
7
8
9
10
Time (ms)
x 10^5

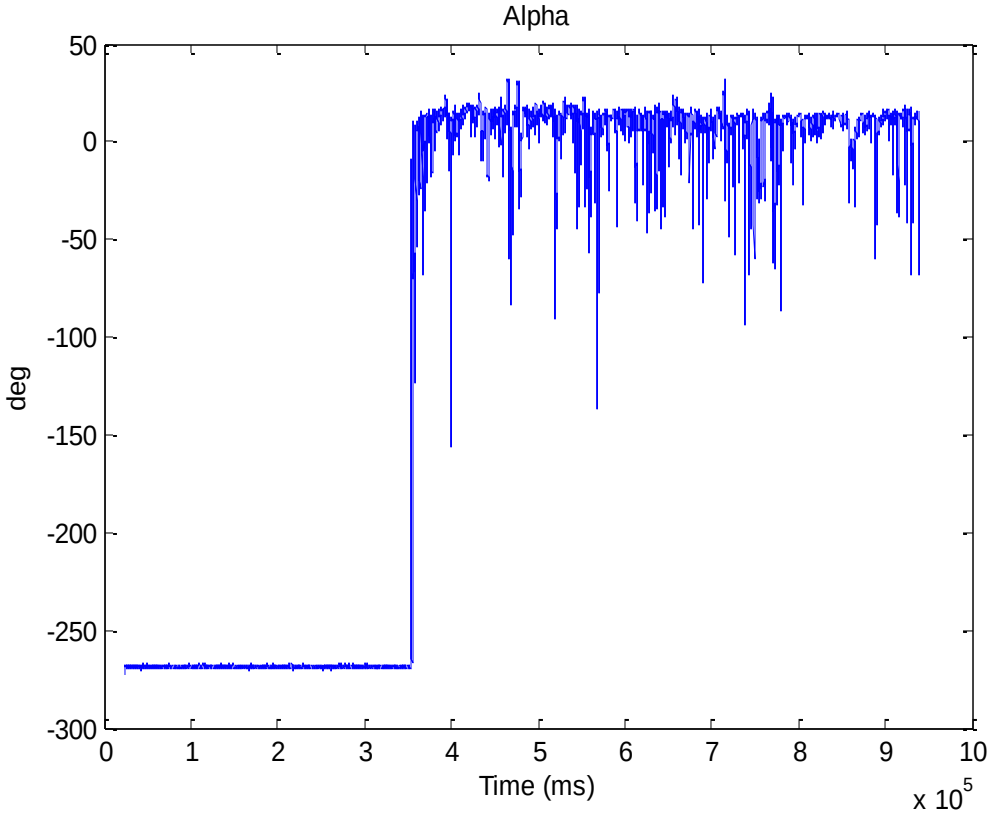
Alpha
50
0
-50
-100
-150
-200
-250
-300
deg
0
1
2
3
4
5
6
7
8
9
10
Time (ms)
x 10^5

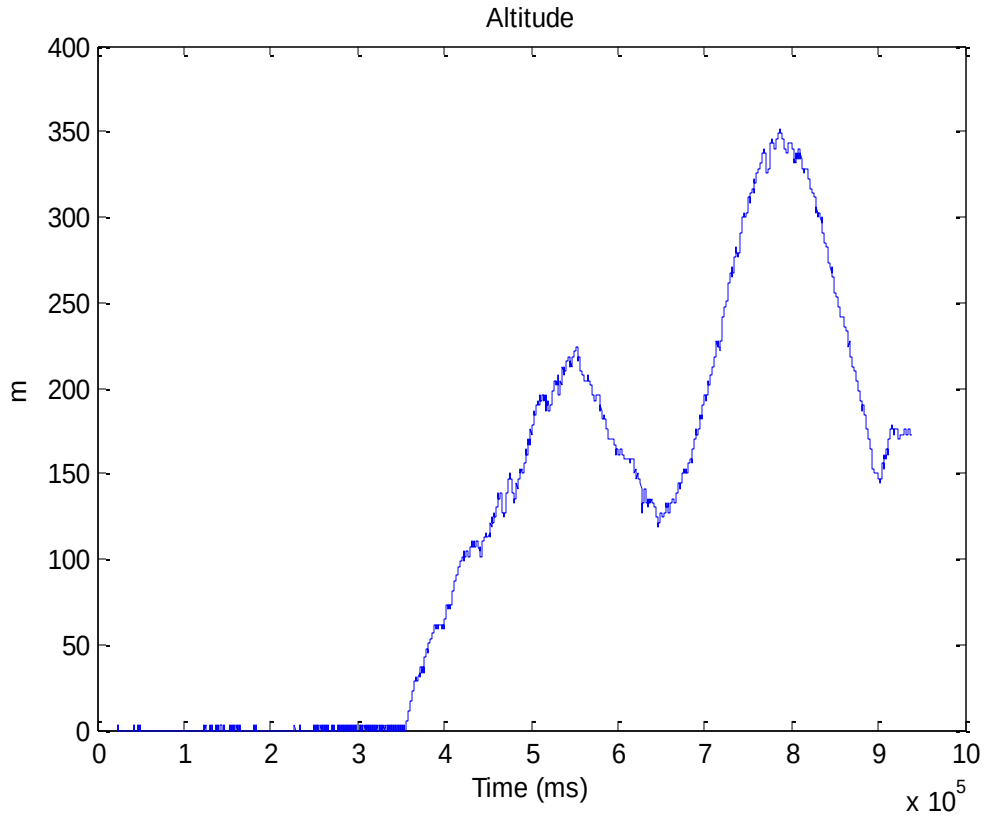
Altitude
m
400
350
300
250
200
150
100
50
0
0
1
2
3
4
5
6
7
8
9
10
Time (ms)
x 10^5

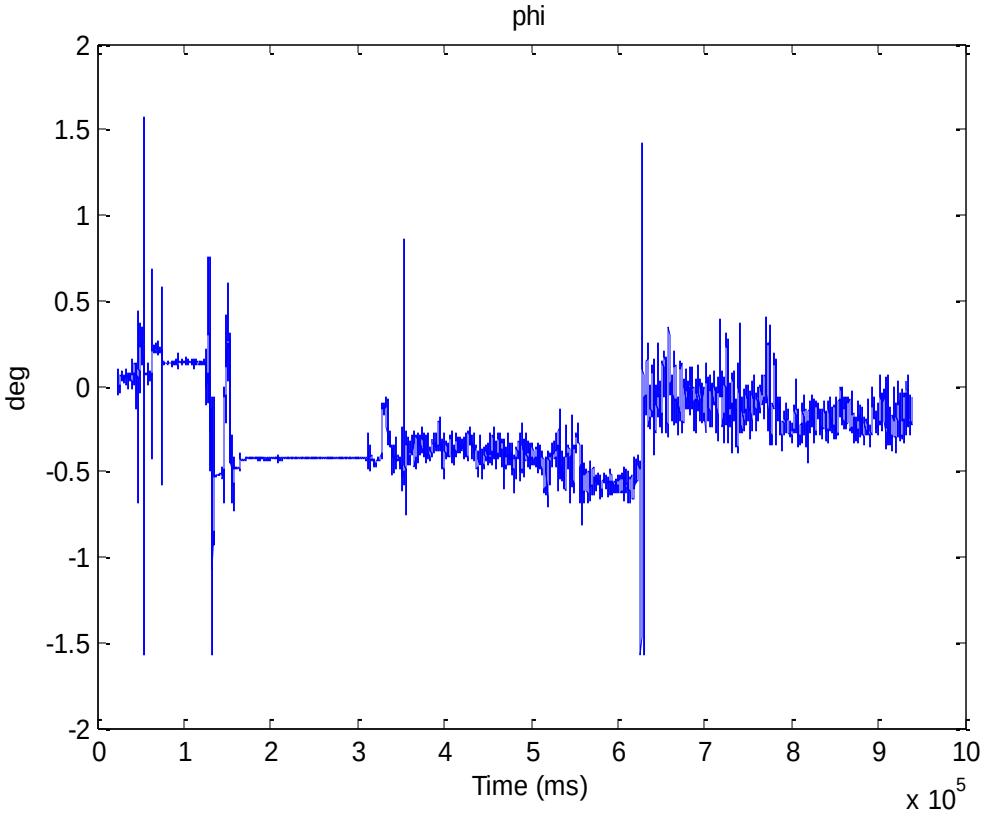
phi
deg
2
1.5
1
0.5
0
-0.5
-1
-1.5
-2
0
1
2
3
4
5
6
7
8
9
10
Time (ms)
x 10^5

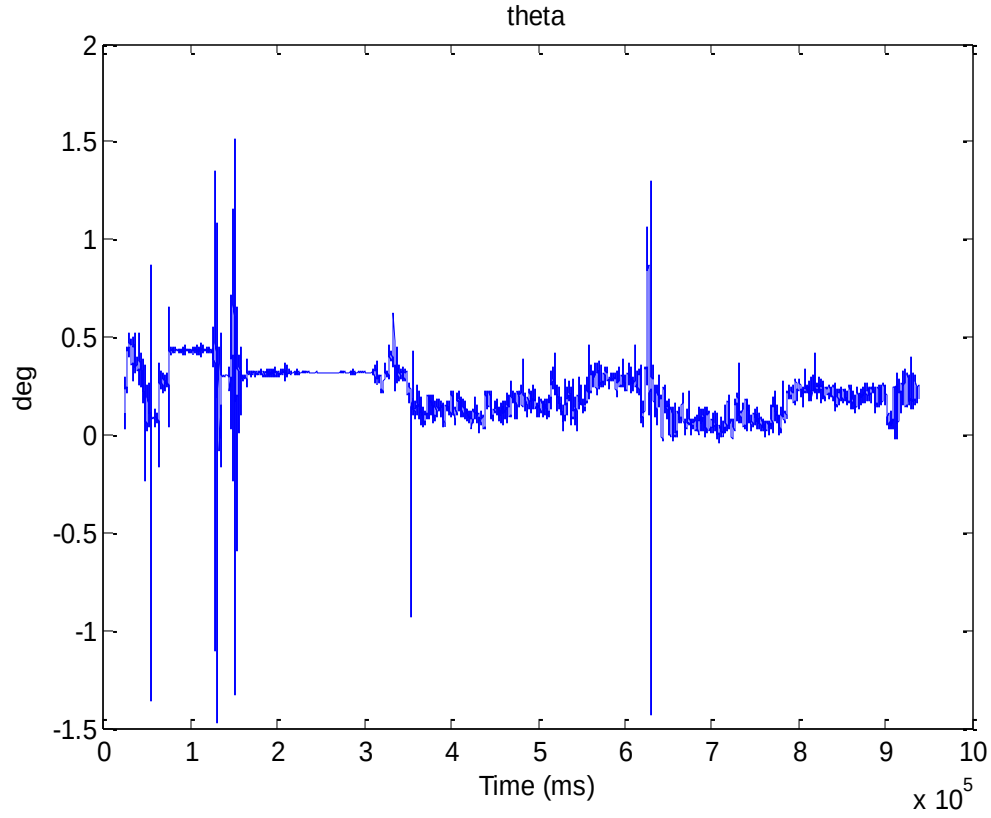
theta
deg
Time (ms)
x 10^5
2
1.5
1
0.5
0
-0.5
-1
-1.5
0
1
2
3
4
5
6
7
8
9
10

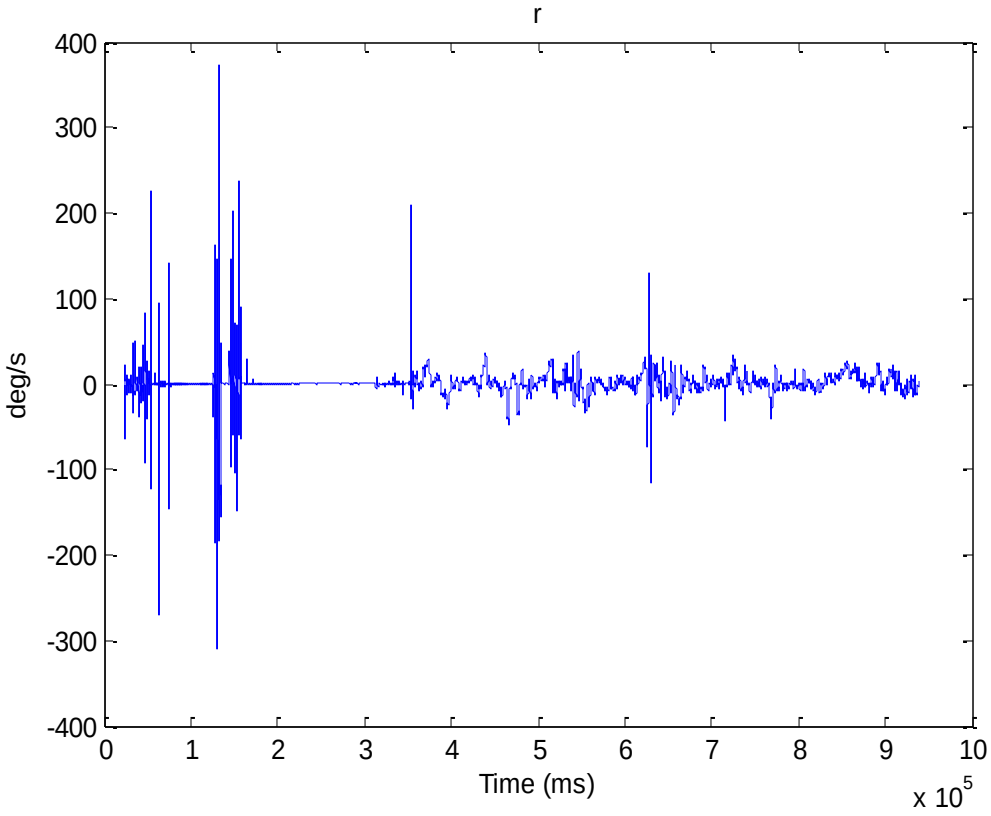
r
deg/s
Time (ms)
x 10^5
400
300
200
100
0
-100
-200
-300
-400
0
1
2
3
4
5
6
7
8
9
10

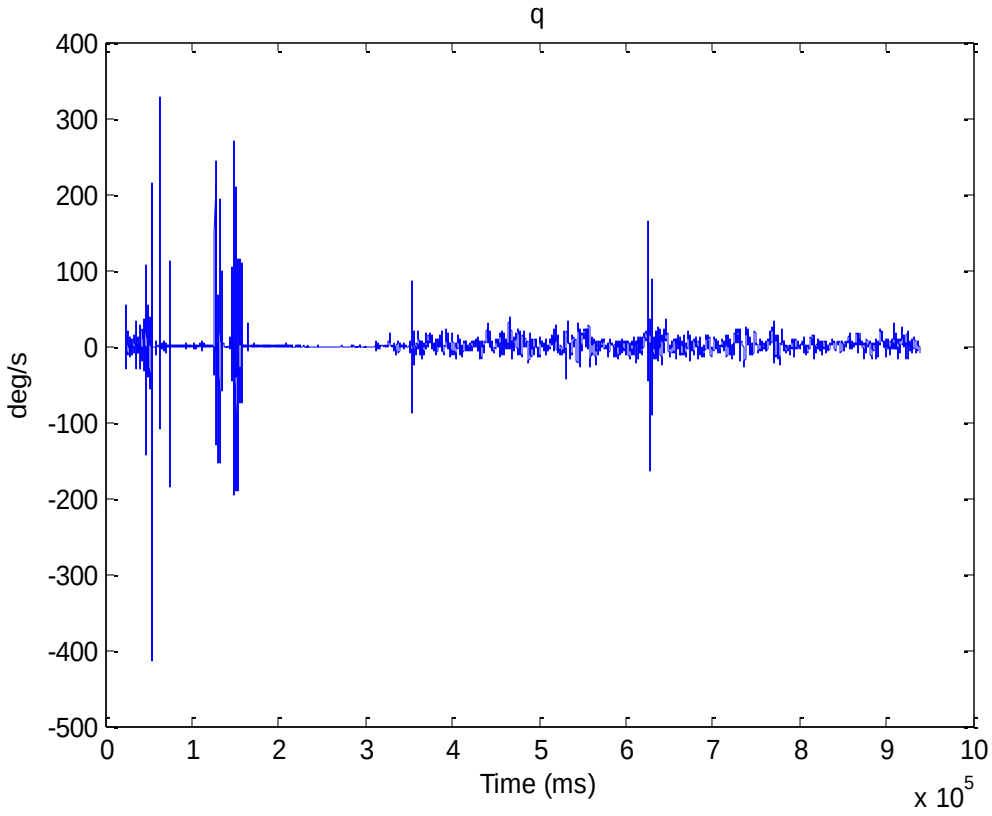
q
400
300
200
100
0
-100
-200
-300
-400
-500
deg/s
0
1
2
3
4
5
6
7
8
9
10
Time (ms)
x 10^5

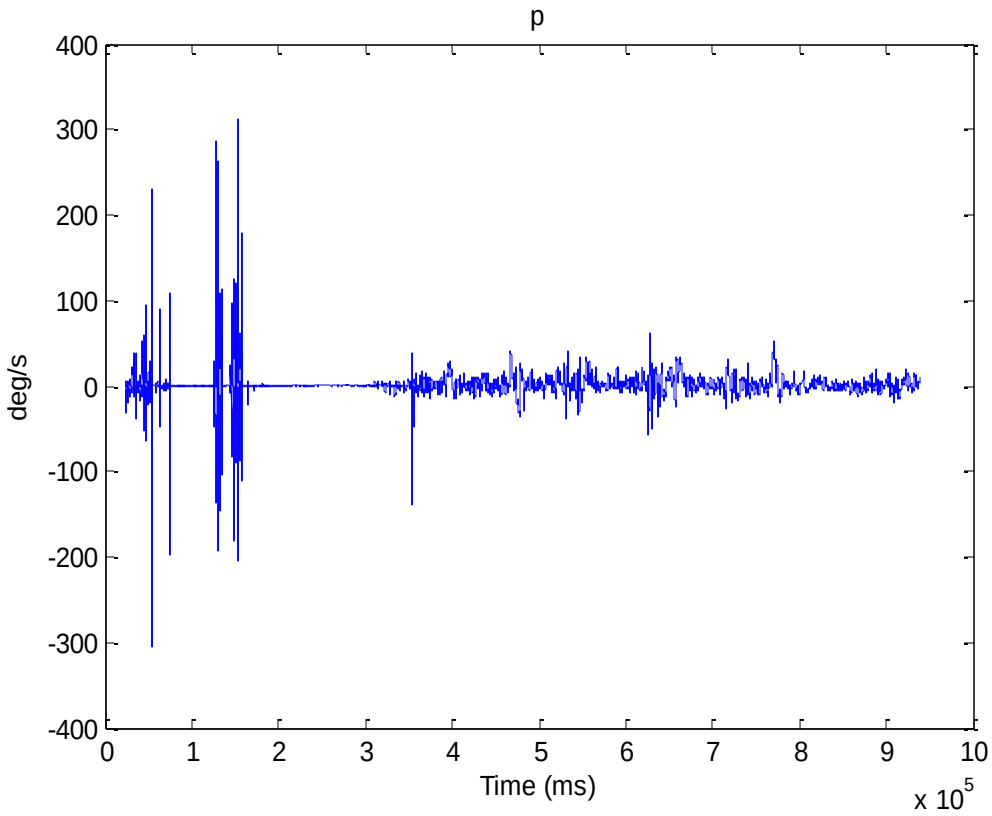
p
400
300
200
100
0
-100
-200
-300
-400
deg/s
0
1
2
3
4
5
6
7
8
9
10
Time (ms)
x 10^5

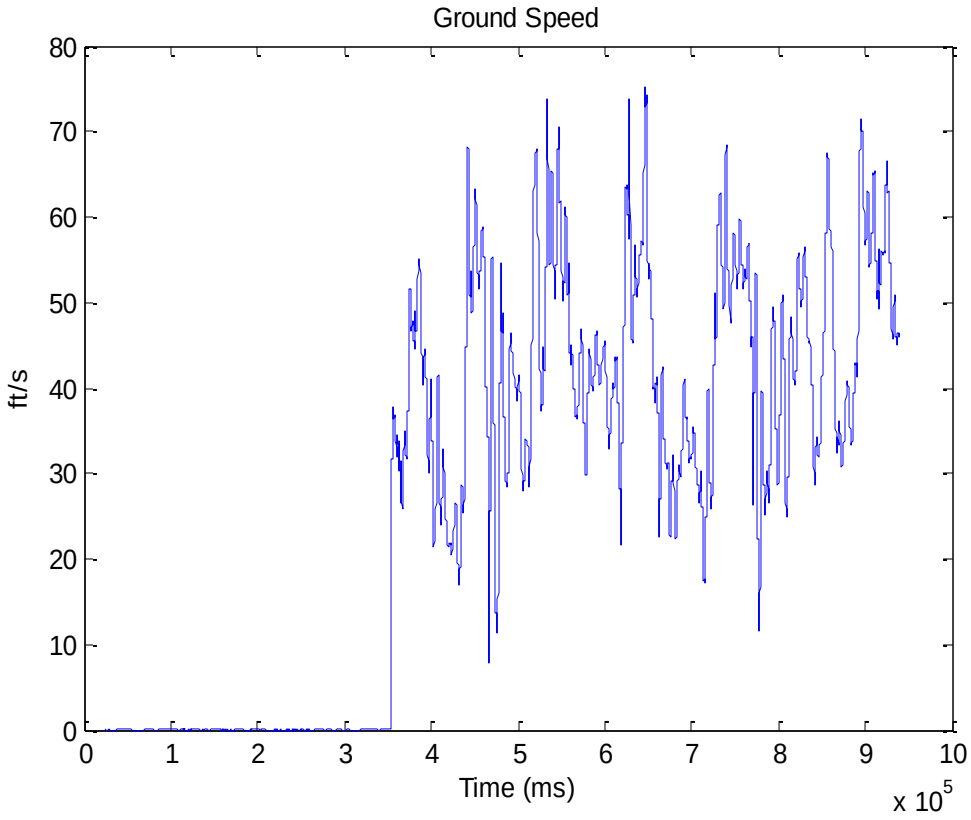

b. May 8th 2014 – 1

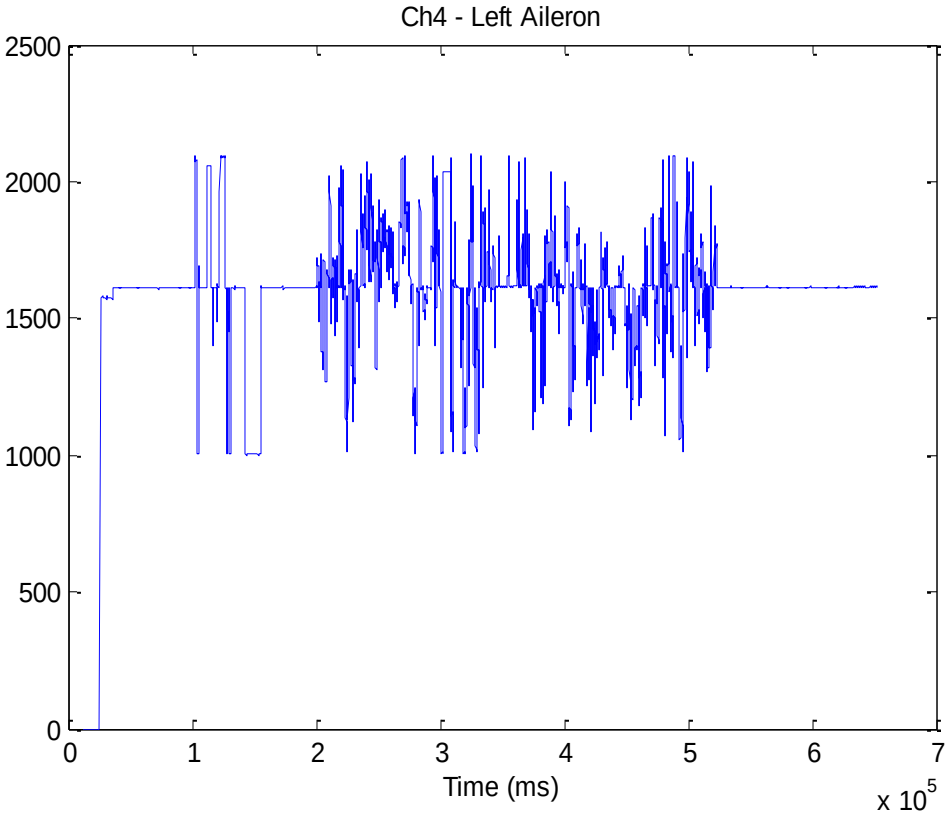

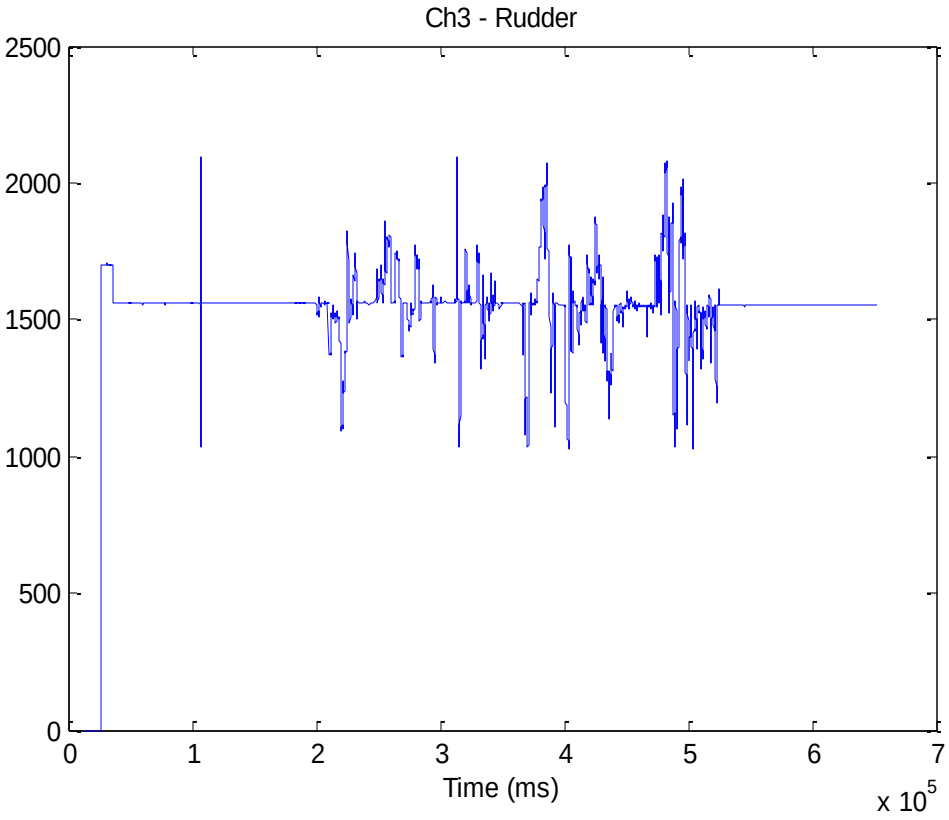
Ch3 - Rudder
2500
2000
1500
1000
500
0
0
1
2
3
4
5
6
7
Time (ms)
x 10^5

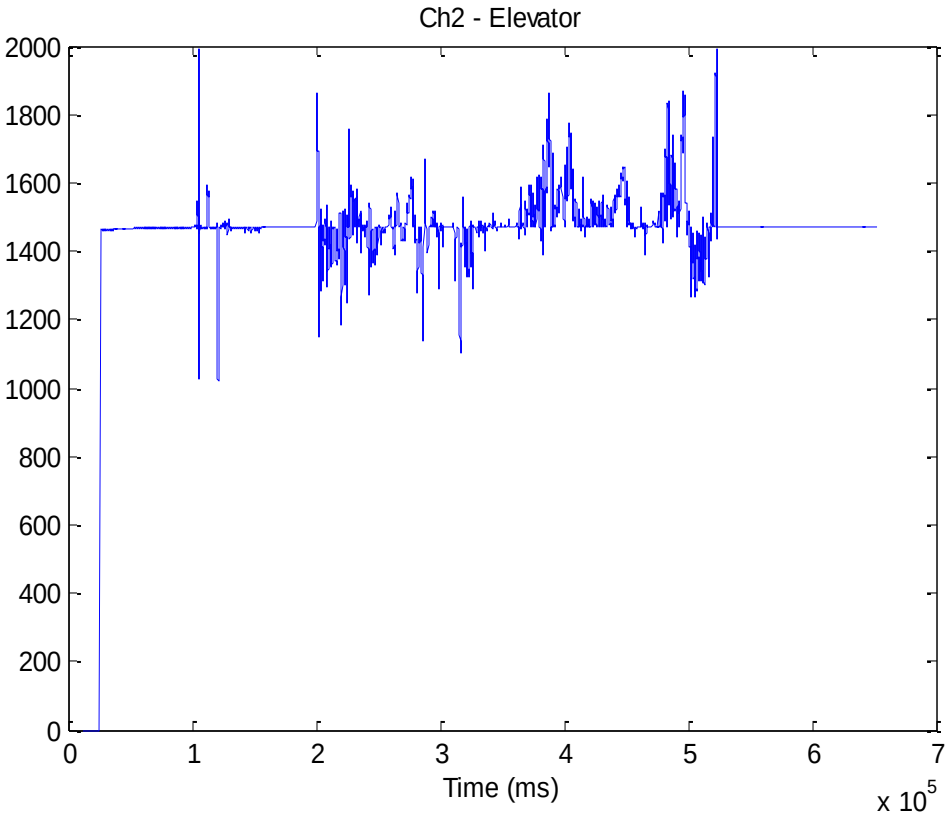
Ch2 - Elevator
2000
1800
1600
1400
1200
1000
800
600
400
200
0
0
1
2
3
4
5
6
7
Time (ms)
x 10^5

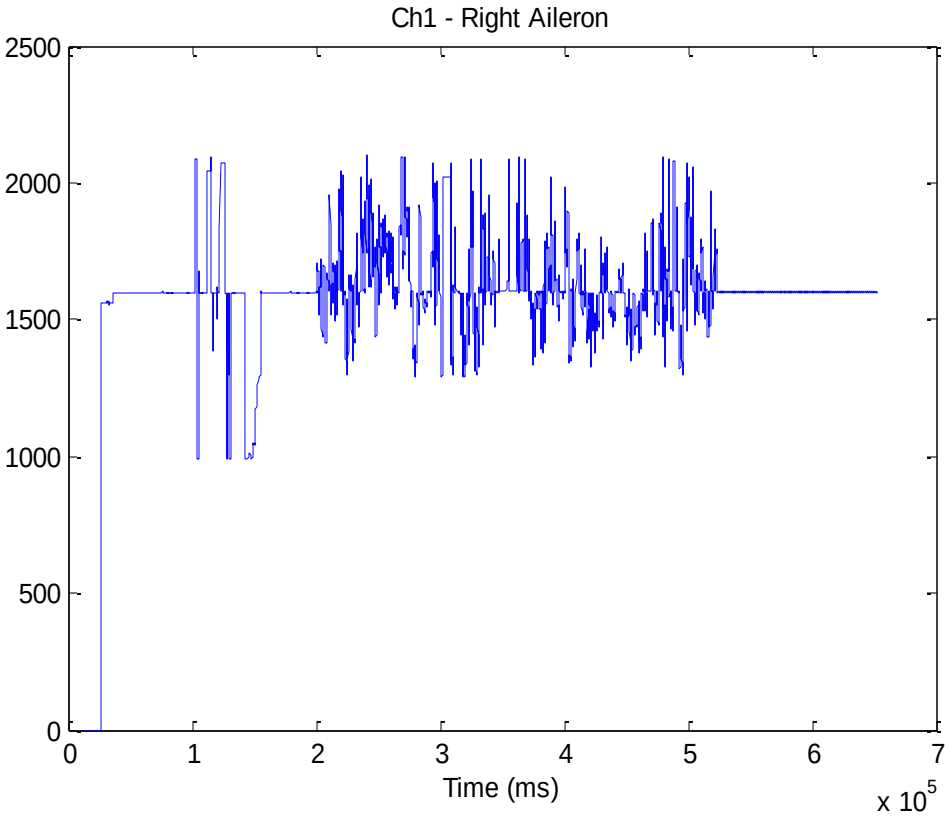
Ch1 - Right Aileron
2500
2000
1500
1000
500
0
0
1
2
3
4
5
6
7
Time (ms)
x 10^5

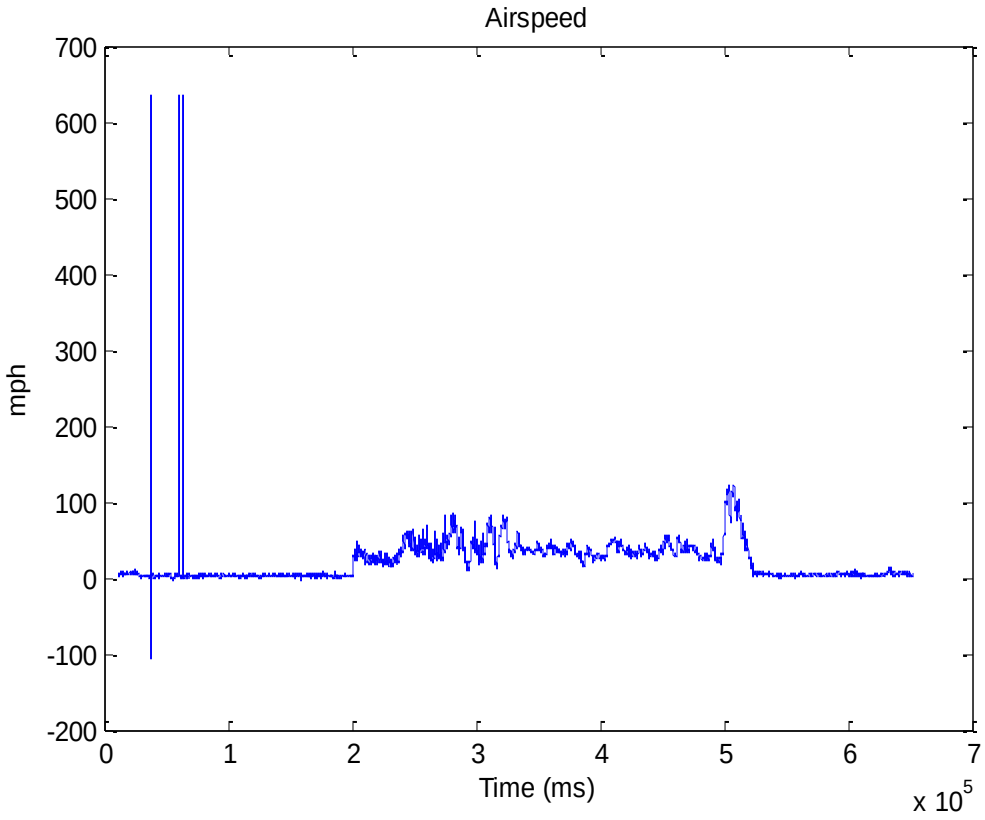
Airspeed
mph
700
600
500
400
300
200
100
0
-100
-200
0
1
2
3
4
5
6
7
Time (ms)
x 10^5

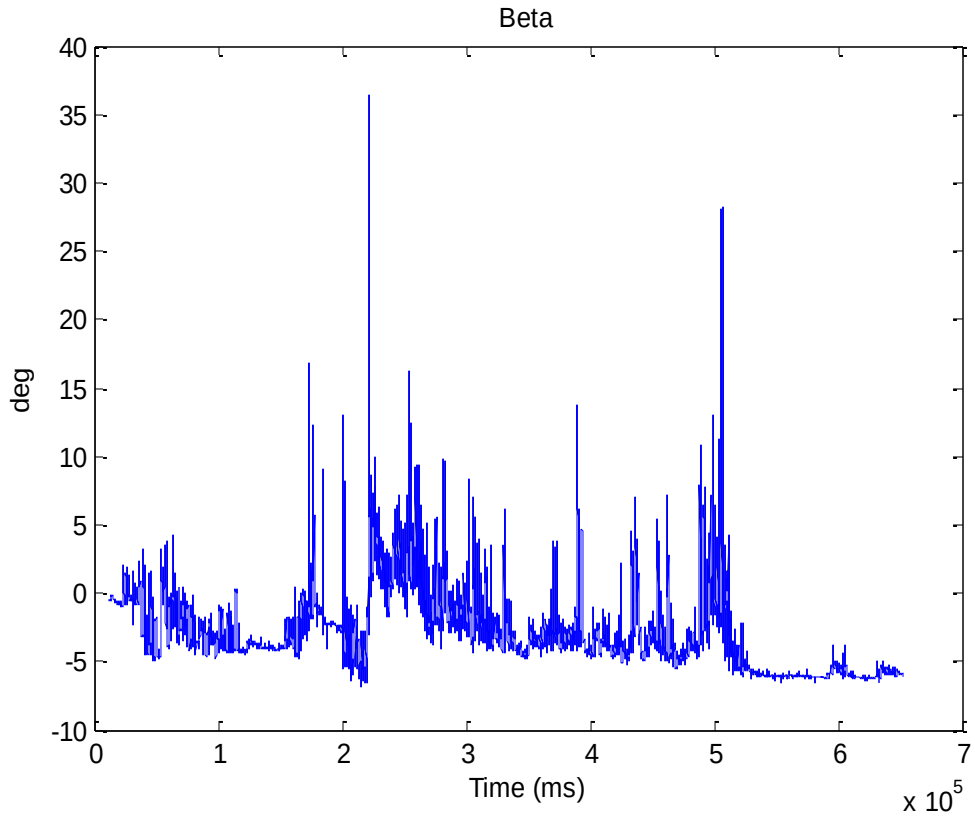
Beta
40
35
30
25
20
15
10
5
0
-5
-10
deg
0
1
2
3
4
5
6
7
Time (ms)
x 10^5

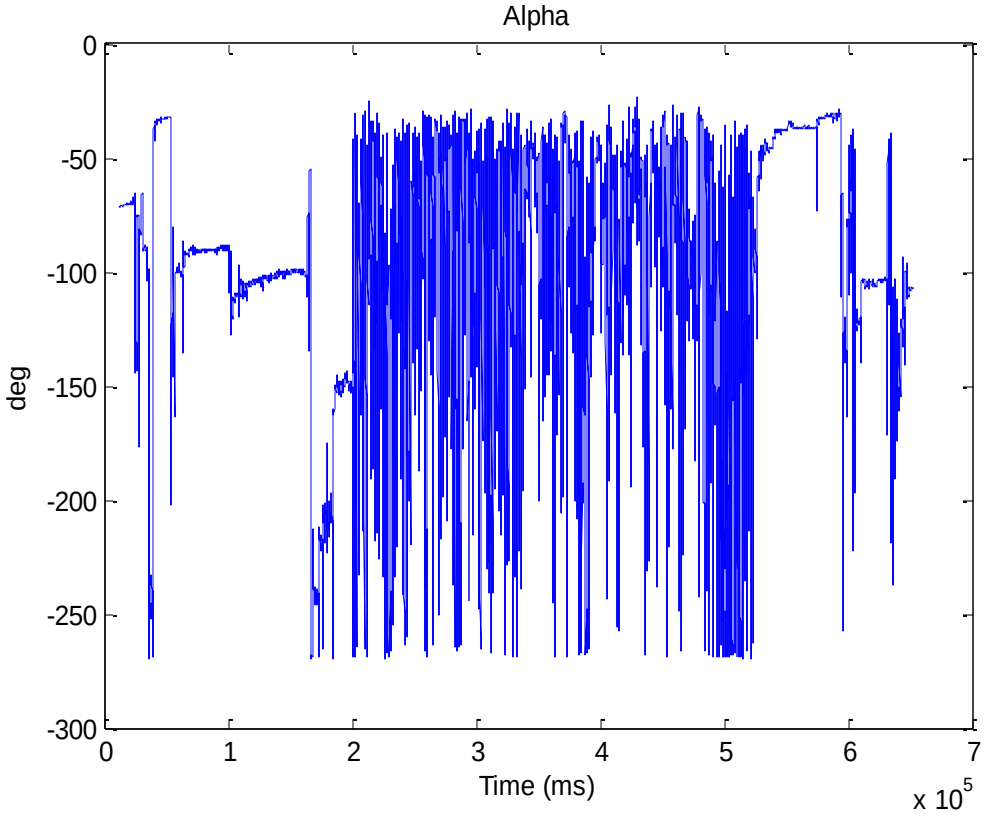
Alpha
0
-50
-100
-150
-200
-250
-300
deg
0
1
2
3
4
5
6
7
Time (ms)
x 10^5

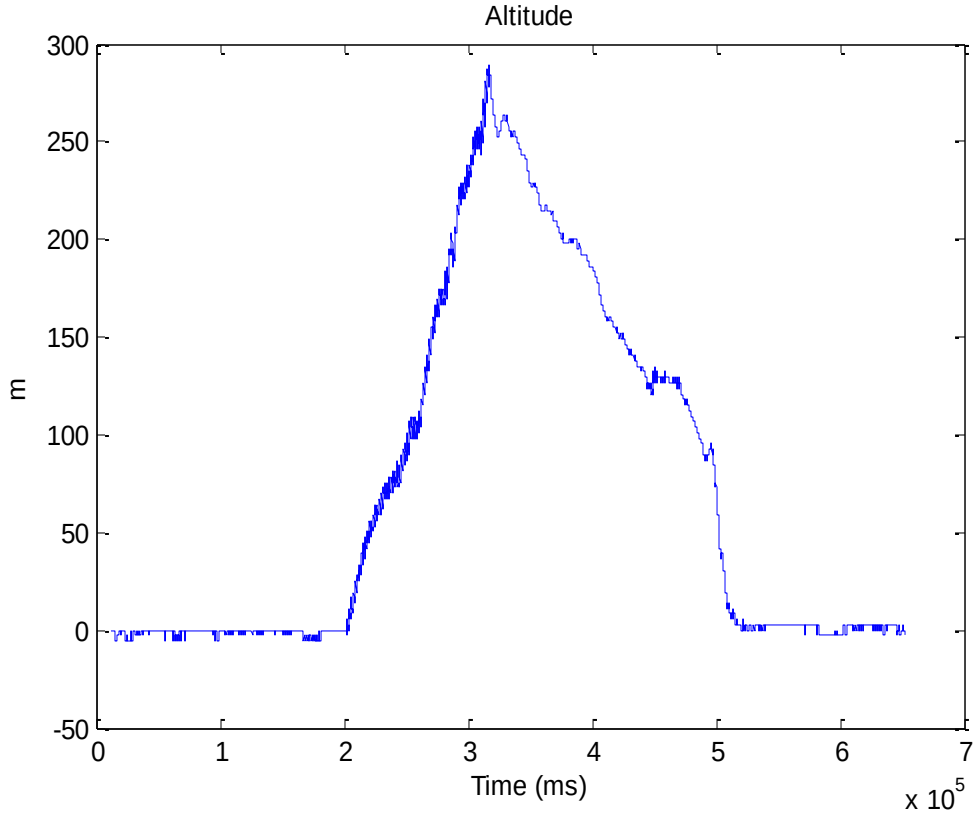
Altitude
300
250
200
150
100
50
0
-50
m
0
1
2
3
4
5
6
7
Time (ms)
x 10^5

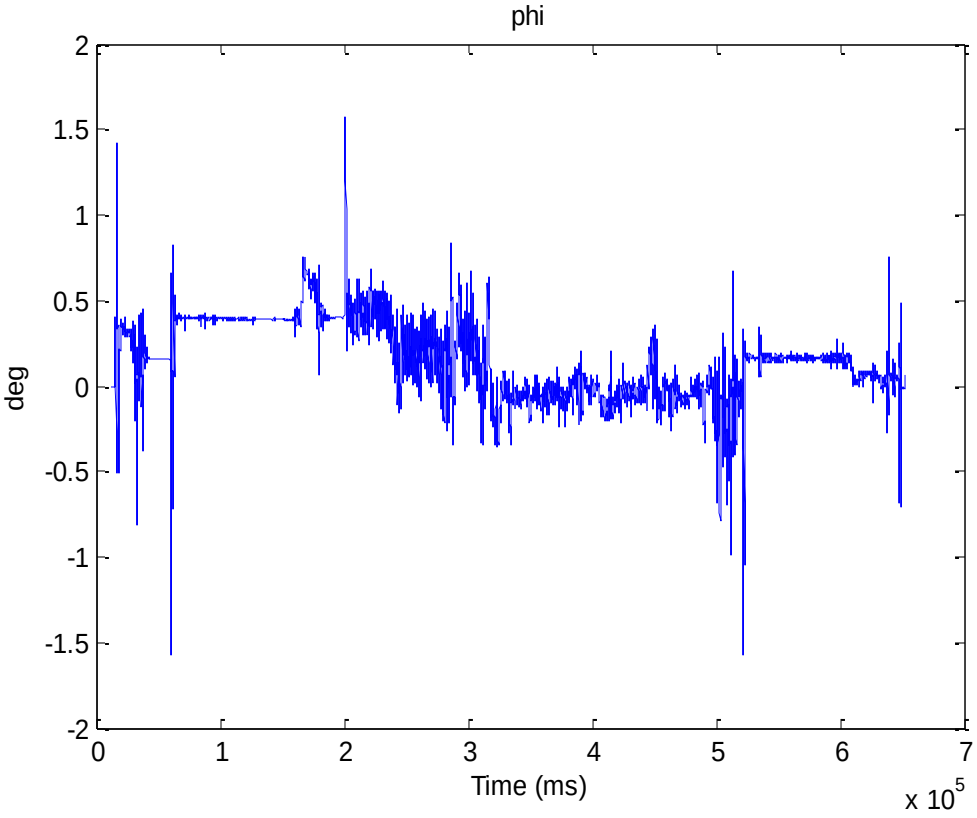
phi
2
1.5
1
0.5
0
-0.5
-1
-1.5
-2
deg
0
1
2
3
4
5
6
7
Time (ms)
x 10^5

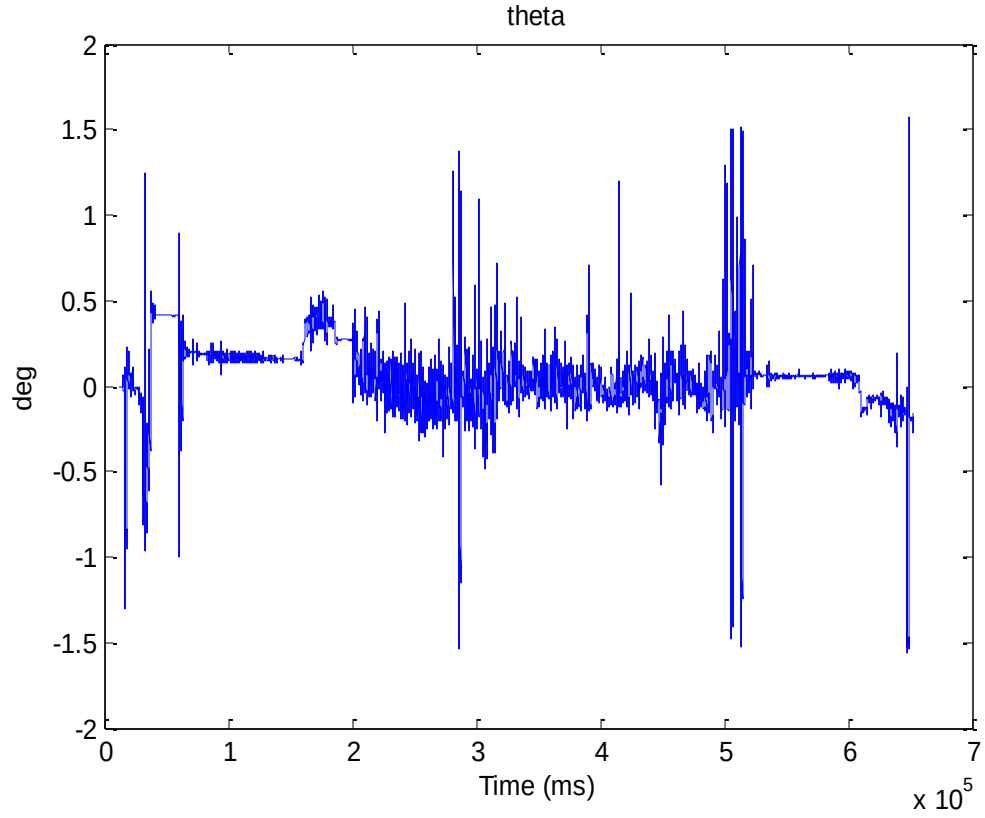
theta
deg
Time (ms)
x 10^5

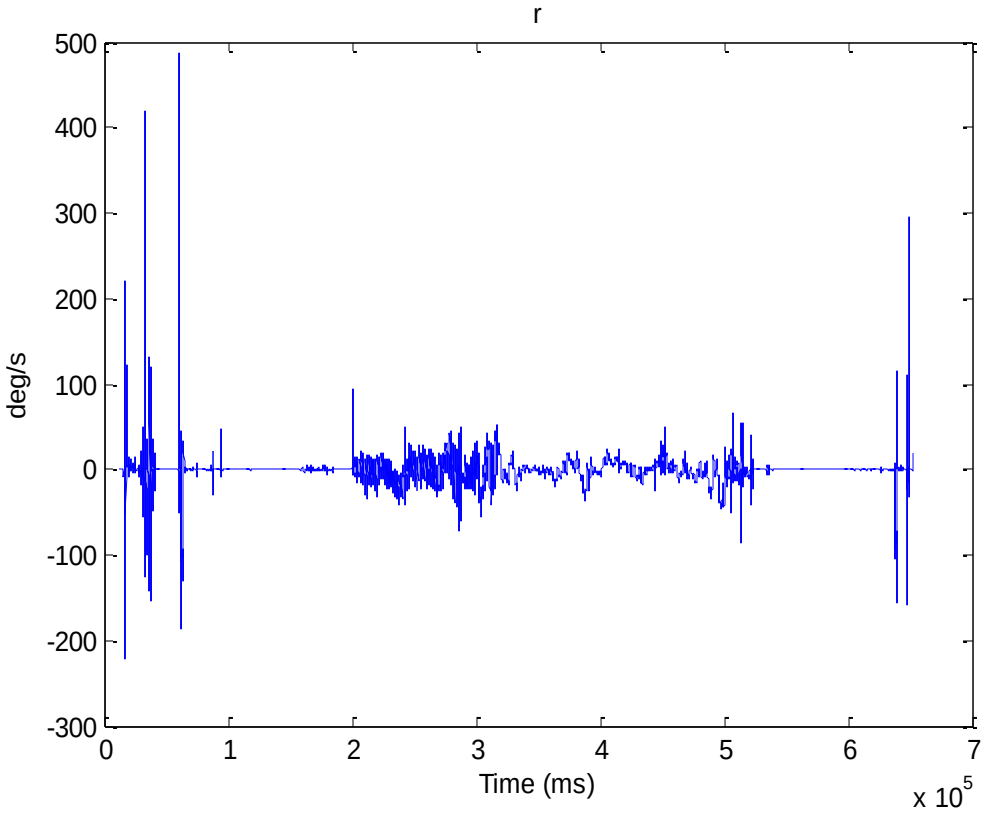
r
deg/s
Time (ms)
x 10^5

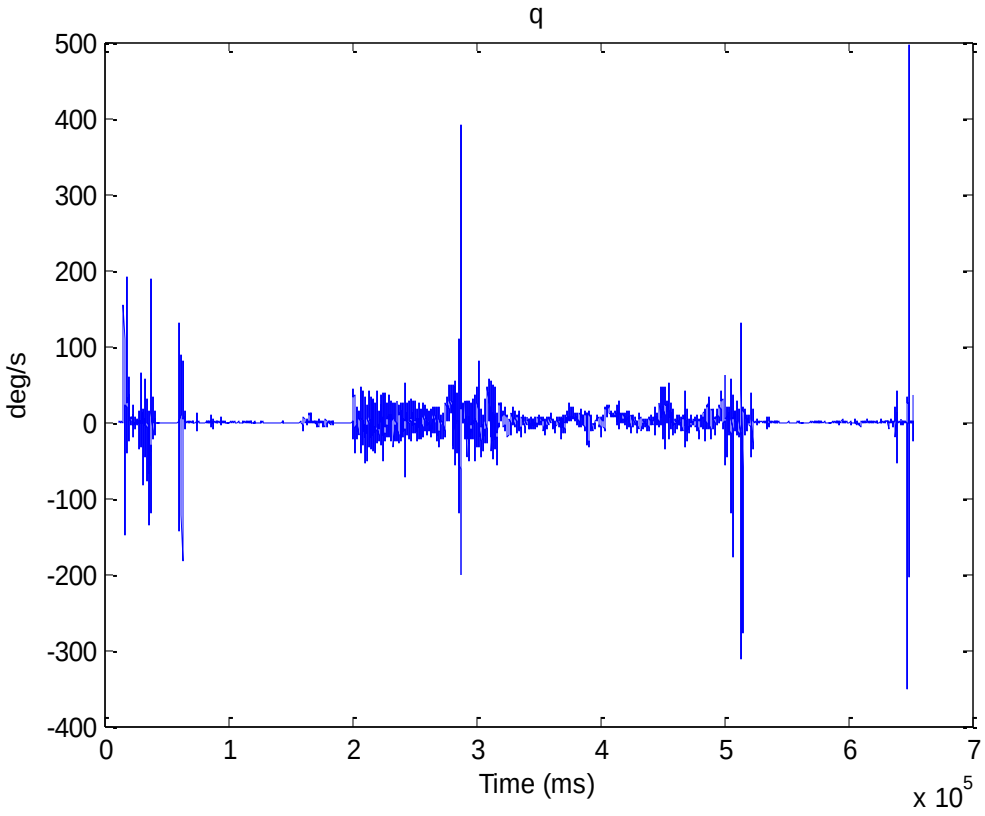
q
500
400
300
200
100
0
-100
-200
-300
-400
deg/s
0
1
2
3
4
5
6
7
Time (ms)
x 10^5

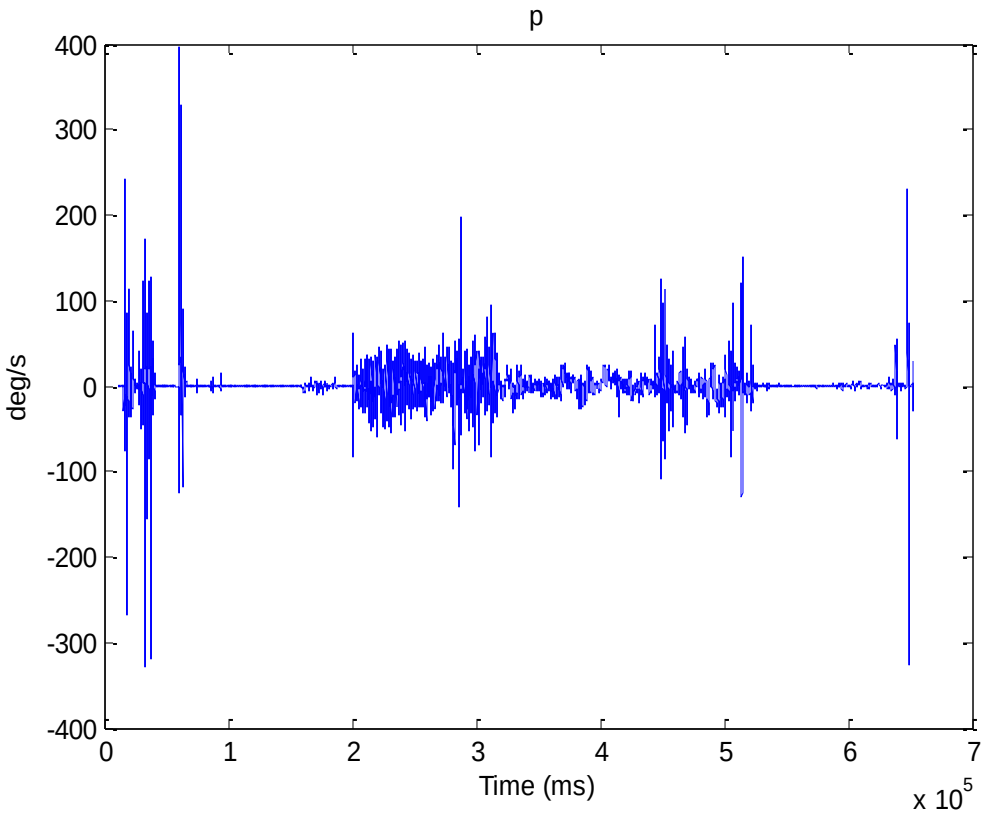
p
400
300
200
100
0
-100
-200
-300
-400
deg/s
0
1
2
3
4
5
6
7
Time (ms)
x 10^5

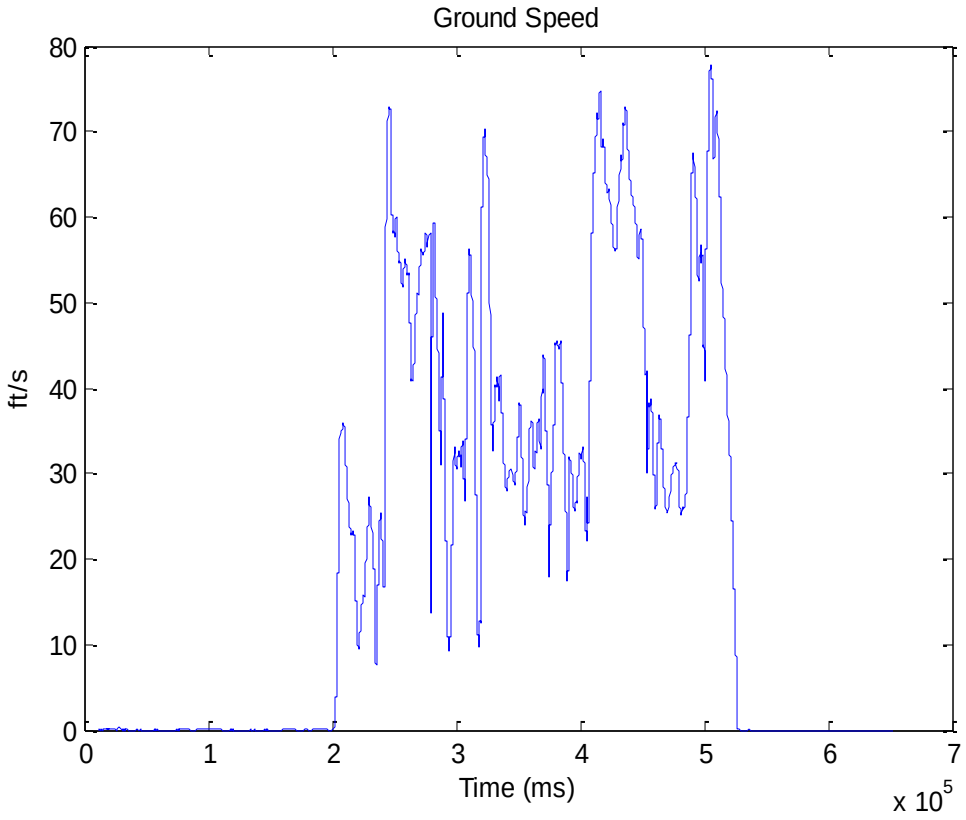

c. May 8th 2014 – 2

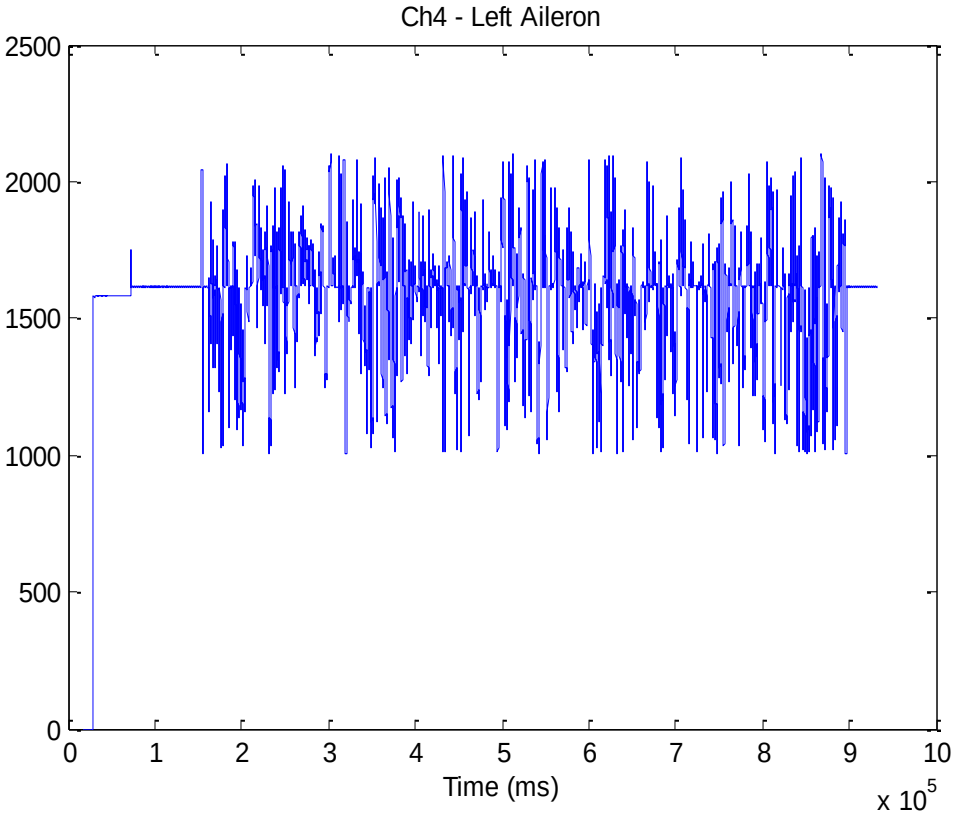

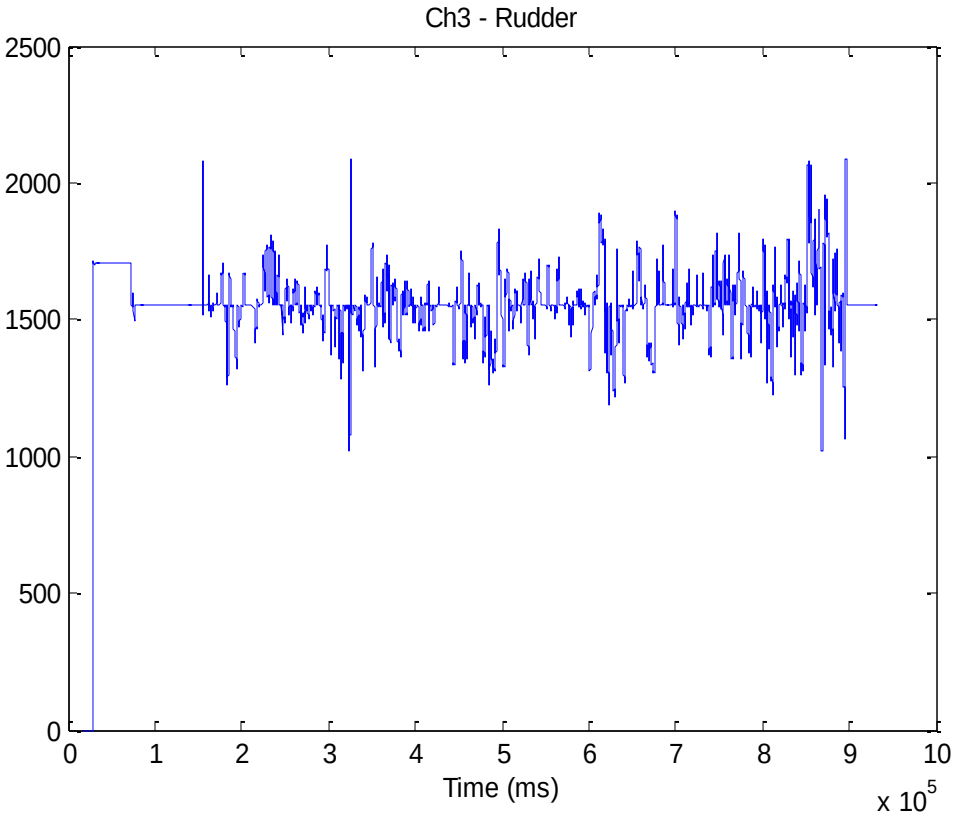
Ch3 - Rudder
2500
2000
1500
1000
500
0
0 1 2 3 4 5 6 7 8 9 10
Time (ms)
x 10^5

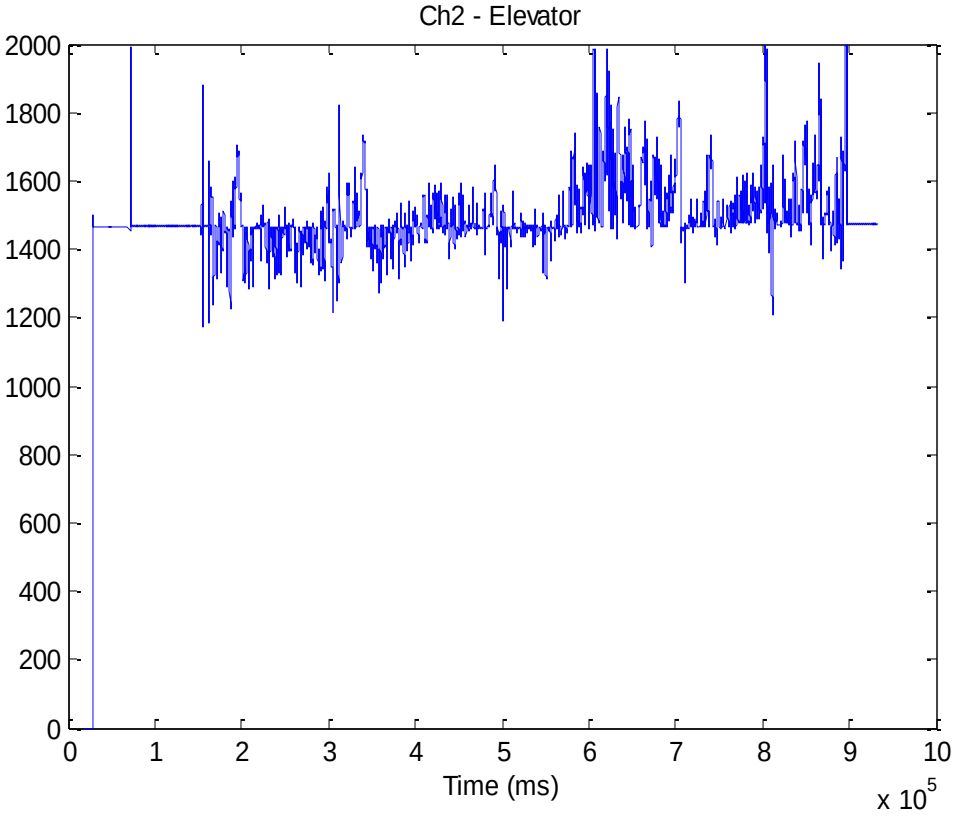
Ch2 - Elevator
2000
1800
1600
1400
1200
1000
800
600
400
200
0
0 1 2 3 4 5 6 7 8 9 10
Time (ms)
x 10^5

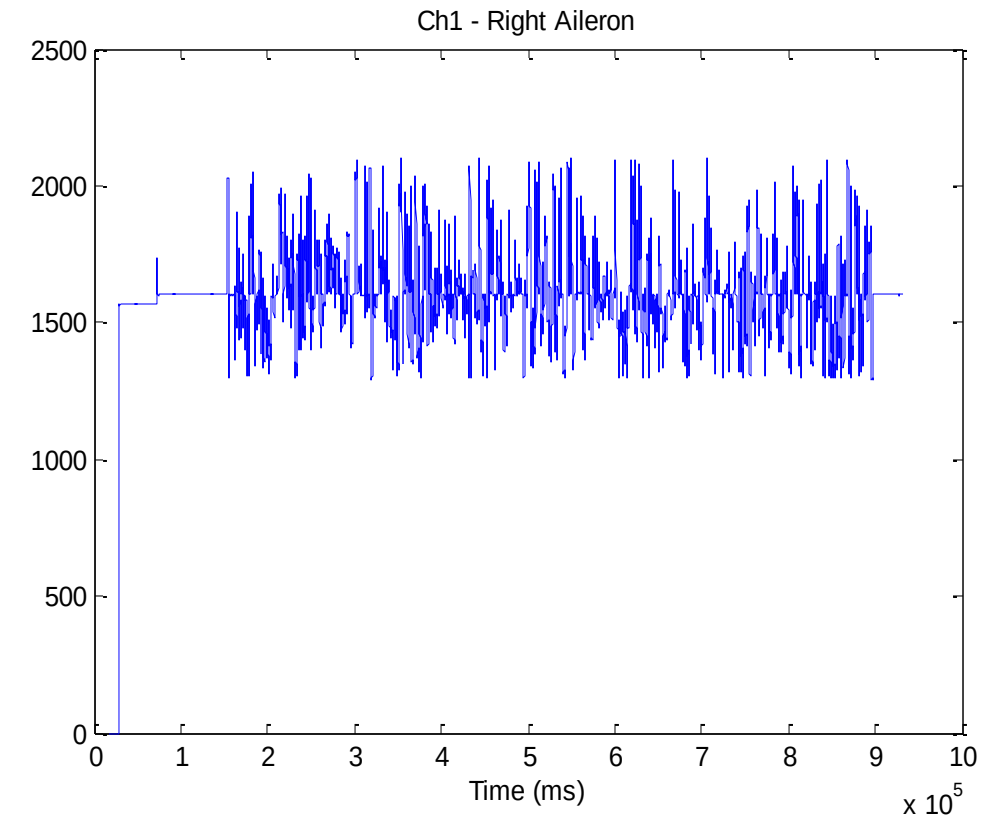
Ch1 - Right Aileron
2500
2000
1500
1000
500
0
0 1 2 3 4 5 6 7 8 9 10
Time (ms)
x 10^5

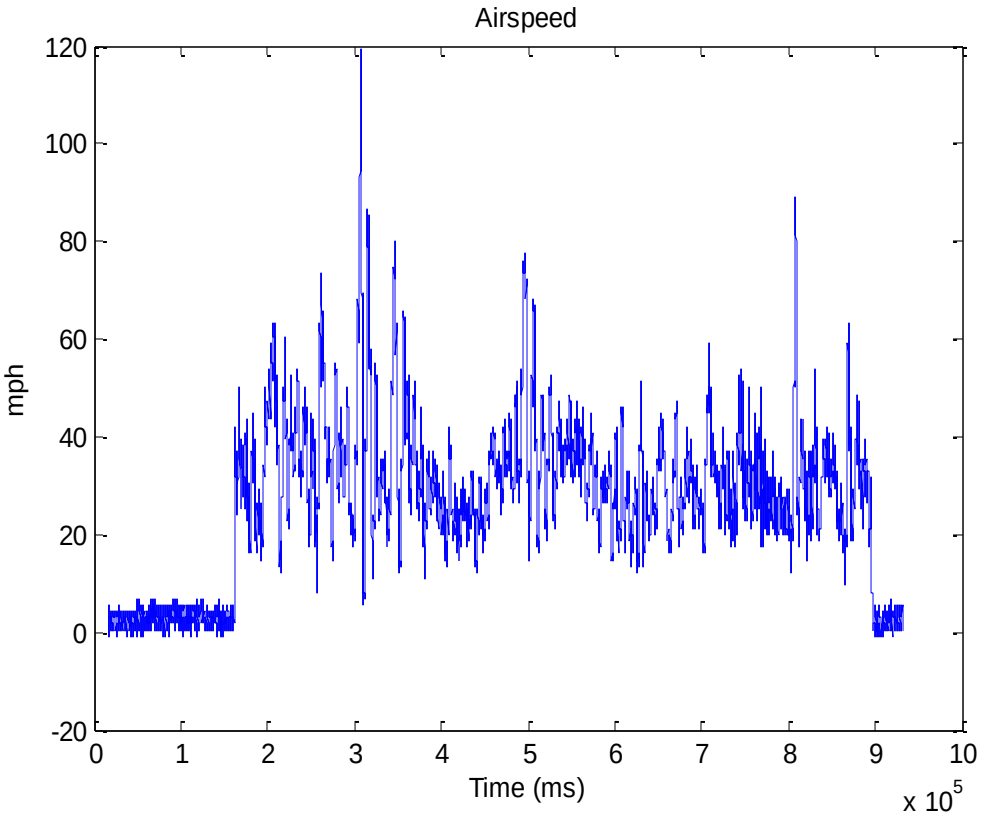
Airspeed
mph
120
100
80
60
40
20
0
-20
0 1 2 3 4 5 6 7 8 9 10
Time (ms)
x 10^5

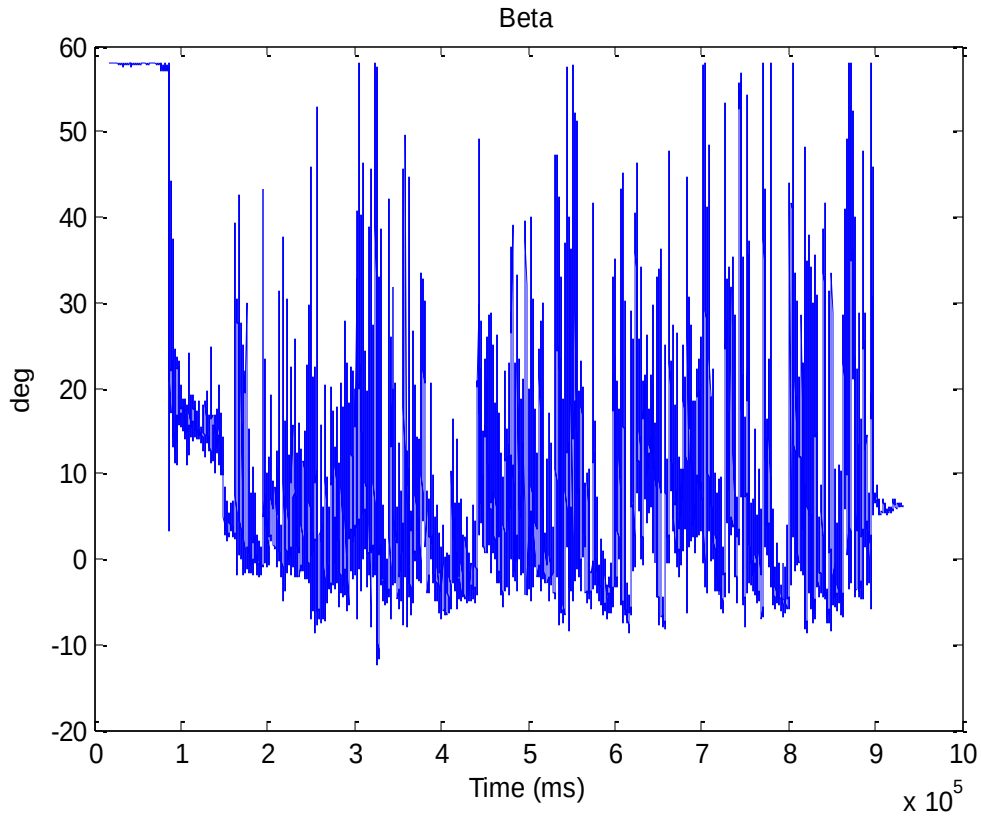
Beta
60
50
40
30
20
10
0
-10
-20
deg
0
1
2
3
4
5
6
7
8
9
10
Time (ms)
x 10^5

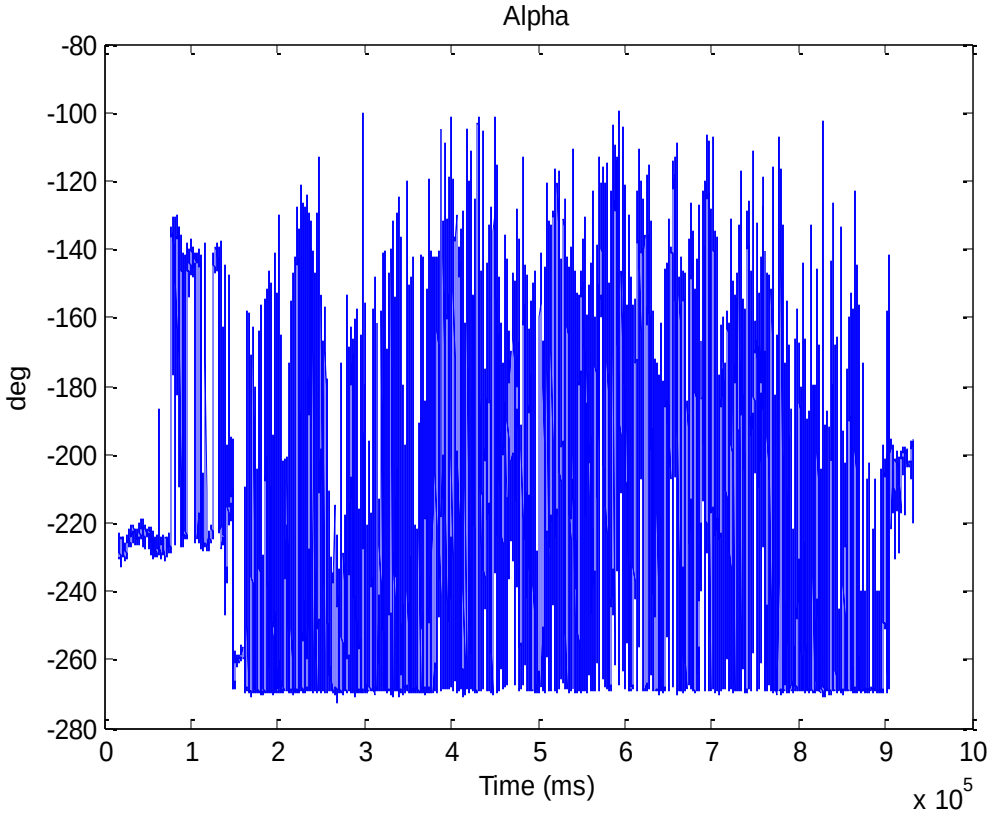
Alpha
-80
-100
-120
-140
-160
-180
-200
-220
-240
-260
-280
deg
0
1
2
3
4
5
6
7
8
9
10
Time (ms)
x 10^5

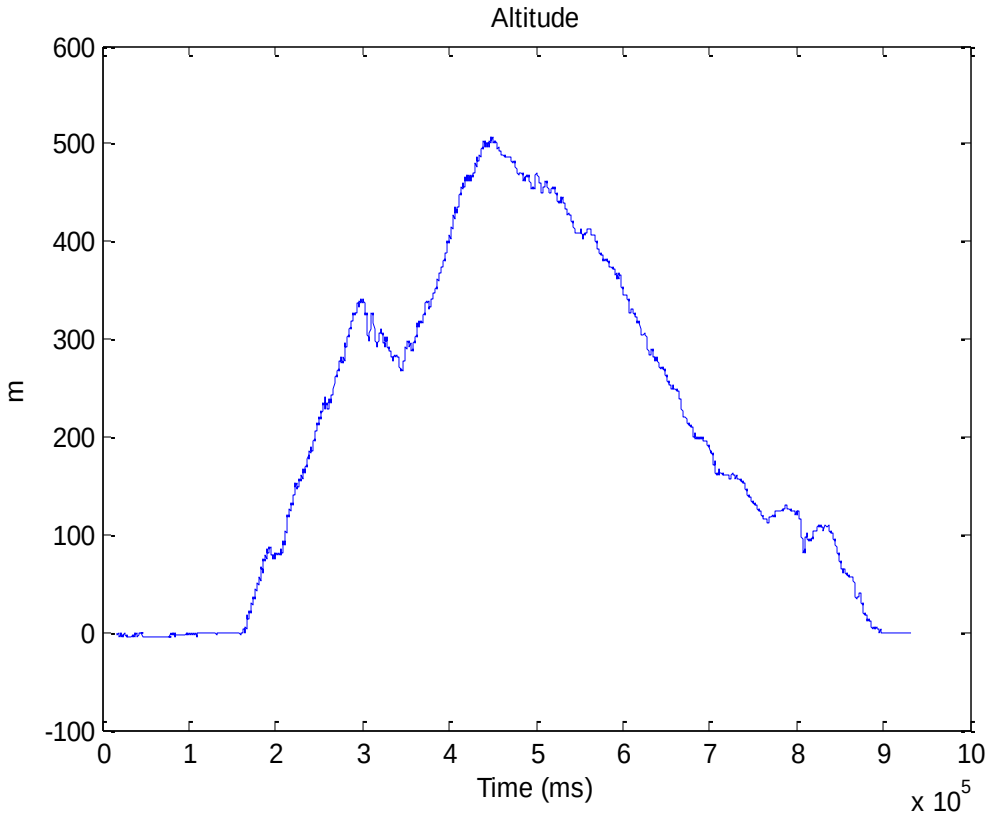
Altitude
600
500
400
300
200
100
0
-100
m
0
1
2
3
4
5
6
7
8
9
10
Time (ms)
x 10^5

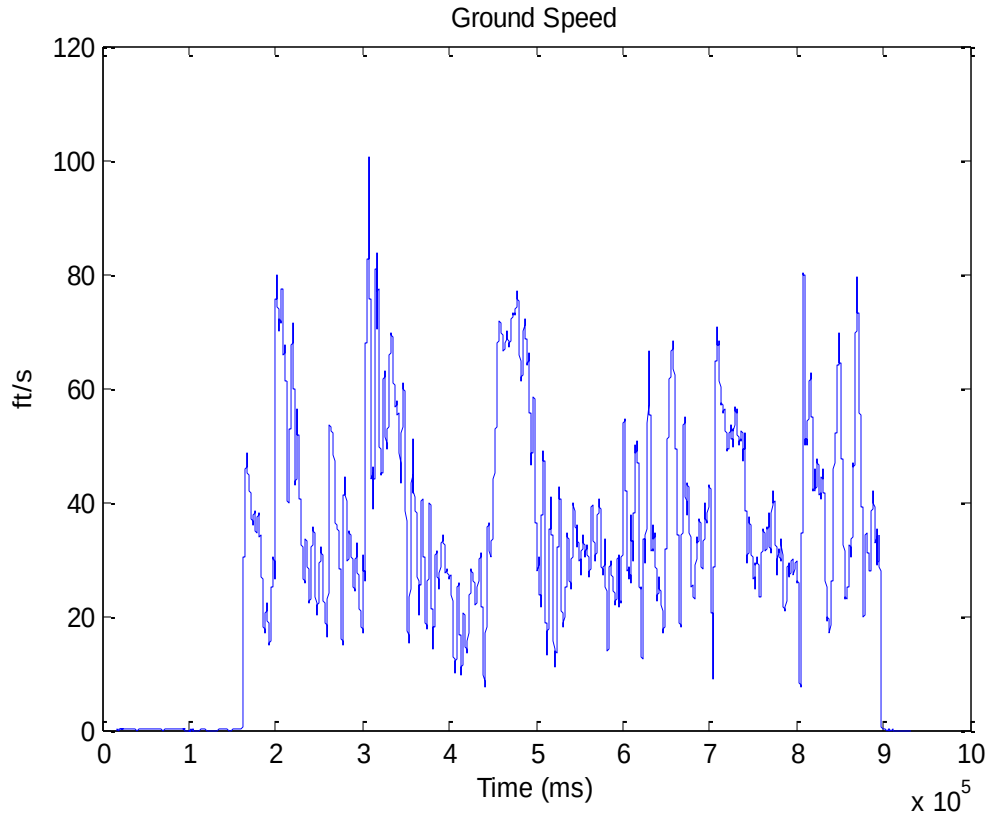
Ground Speed
120
100
80
60
40
20
0
ft/s
0
1
2
3
4
5
6
7
8
9
10
Time (ms)
x 10^5

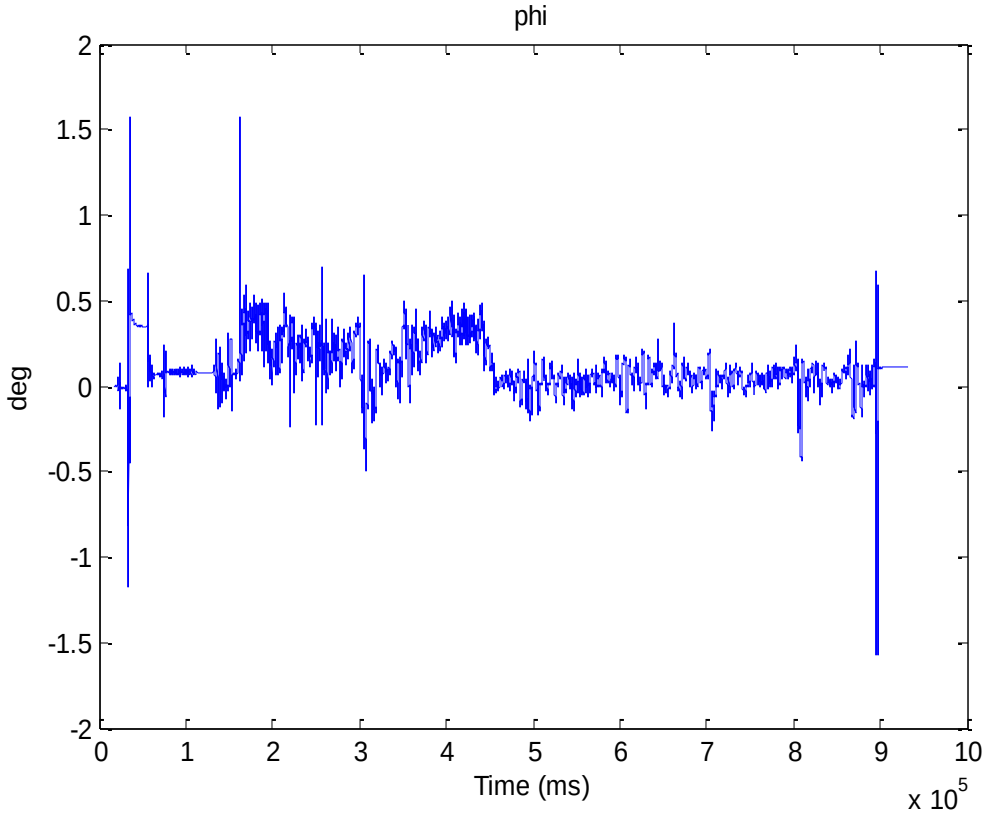
phi
deg
Time (ms)
x 10^5
2
1.5
1
0.5
0
-0.5
-1
-1.5
-2
0
1
2
3
4
5
6
7
8
9
10

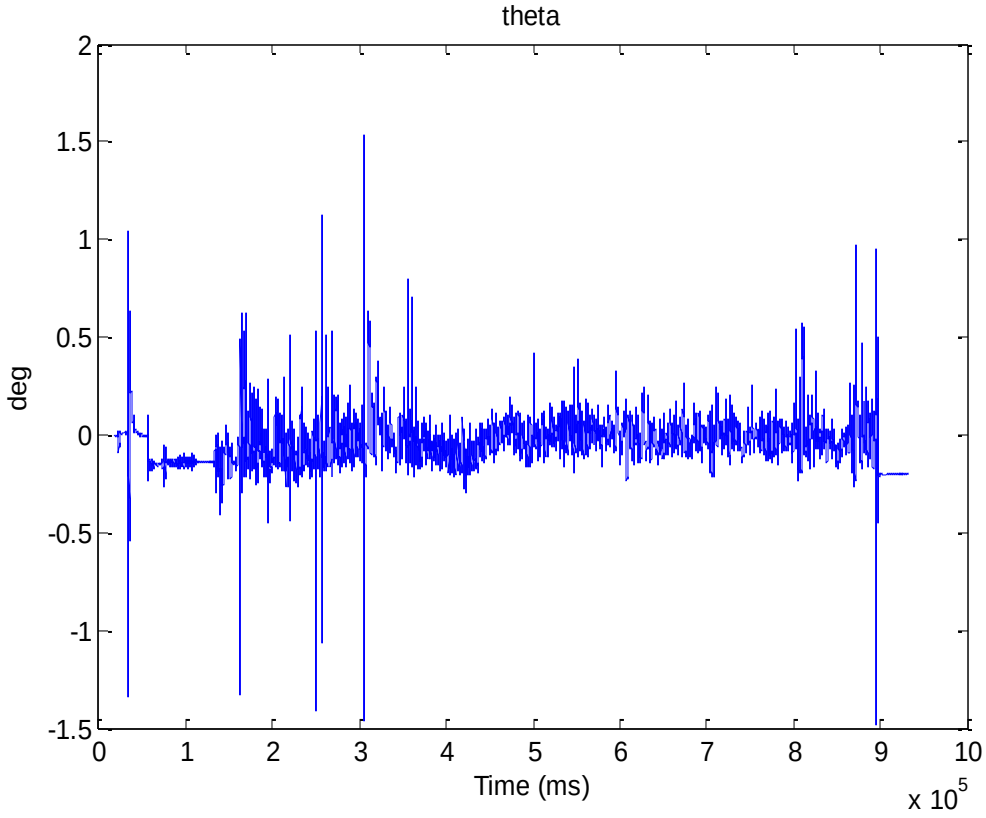
theta
deg
Time (ms)
x 10^5
2
1.5
1
0.5
0
-0.5
-1
-1.5
0
1
2
3
4
5
6
7
8
9
10

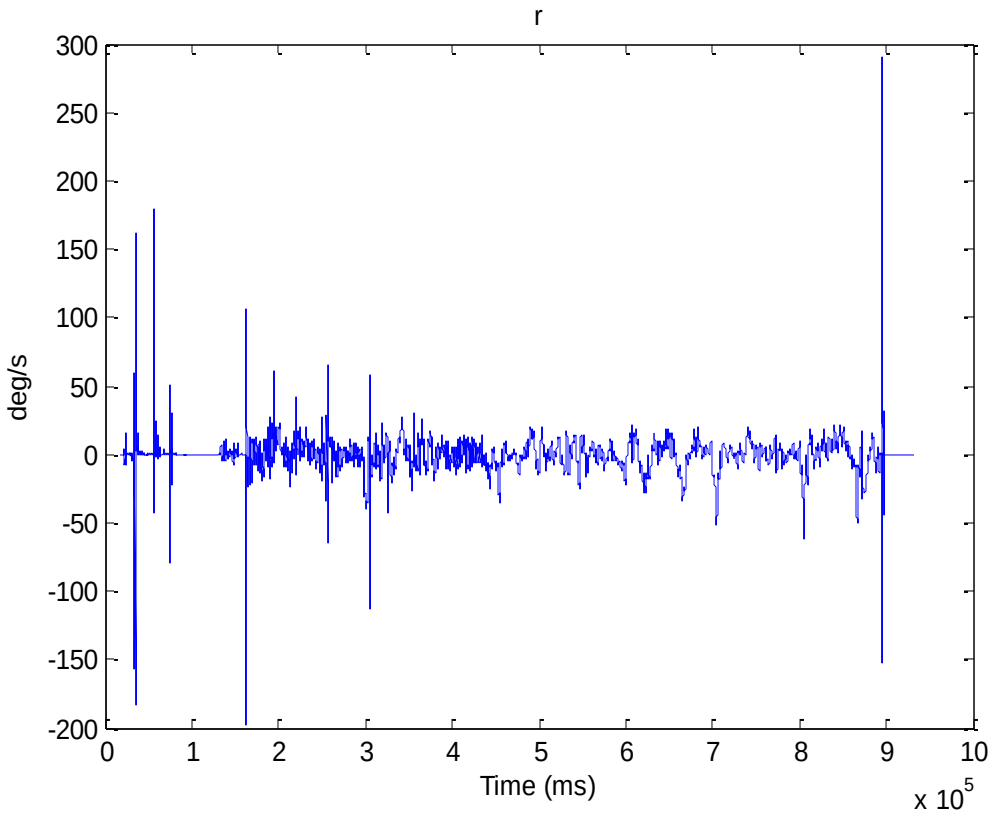
r
300
250
200
150
100
50
0
-50
-100
-150
-200
deg/s
0
1
2
3
4
5
6
7
8
9
10
Time (ms)
x 10^5

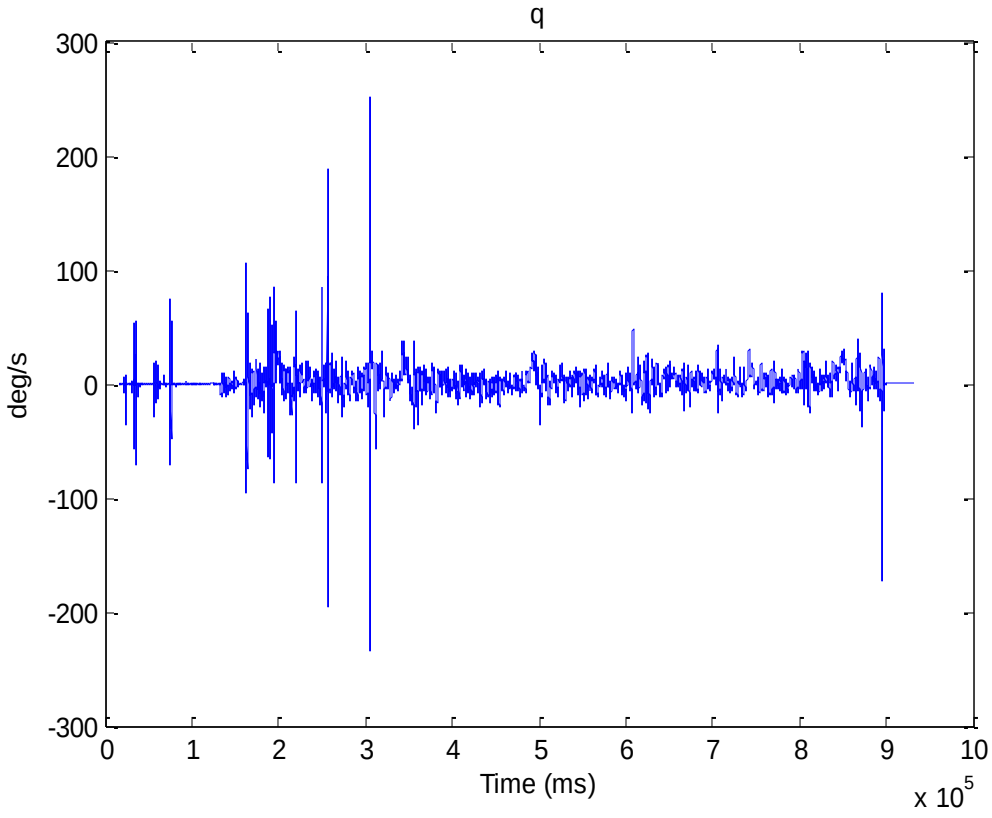
q
300
200
100
0
-100
-200
-300
deg/s
0
1
2
3
4
5
6
7
8
9
10
Time (ms)
x 10^5

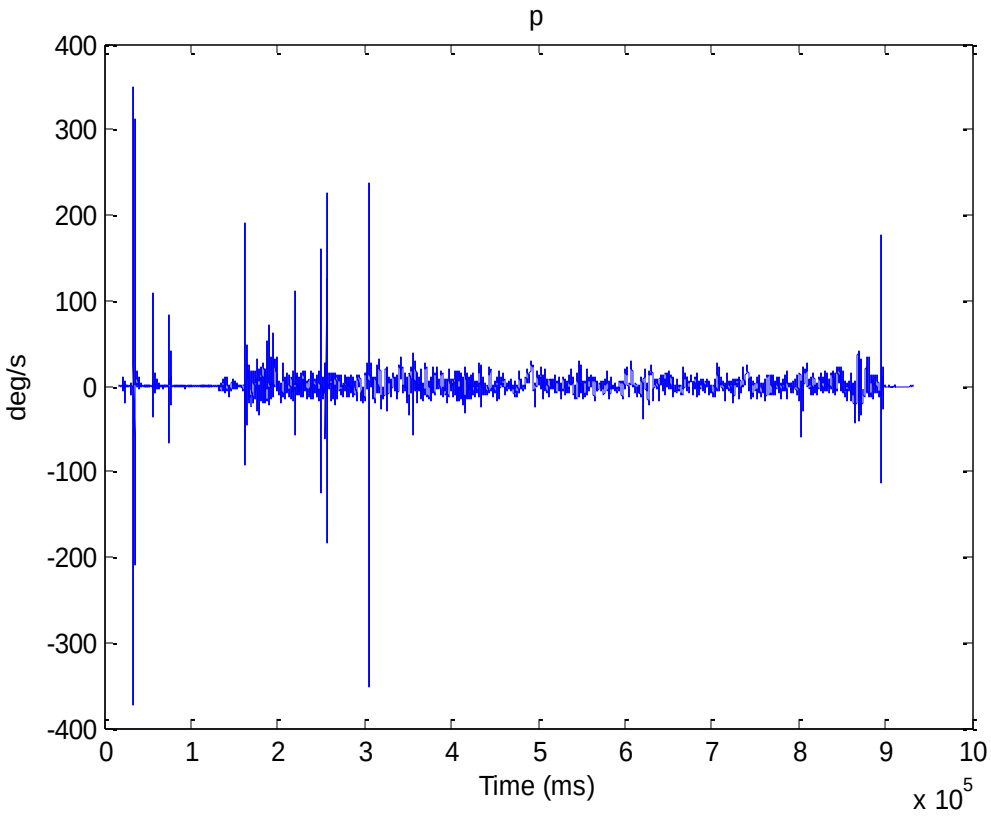
p
400
300
200
100
0
-100
-200
-300
-400
deg/s
0
1
2
3
4
5
6
7
8
9
10
Time (ms)
x 10^5

B. DATCOM Graphs

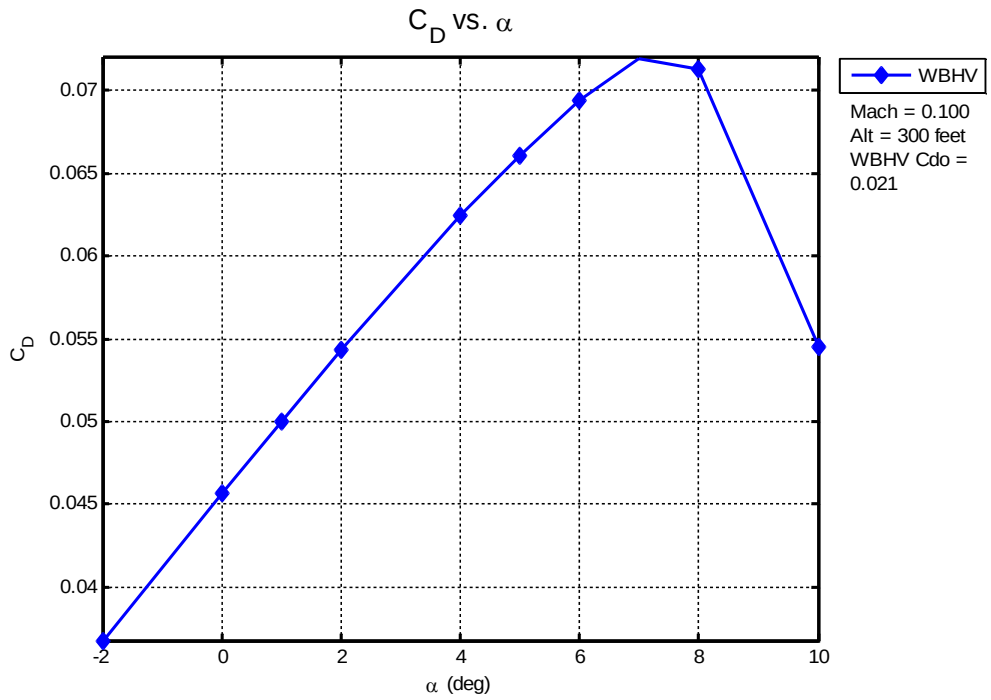

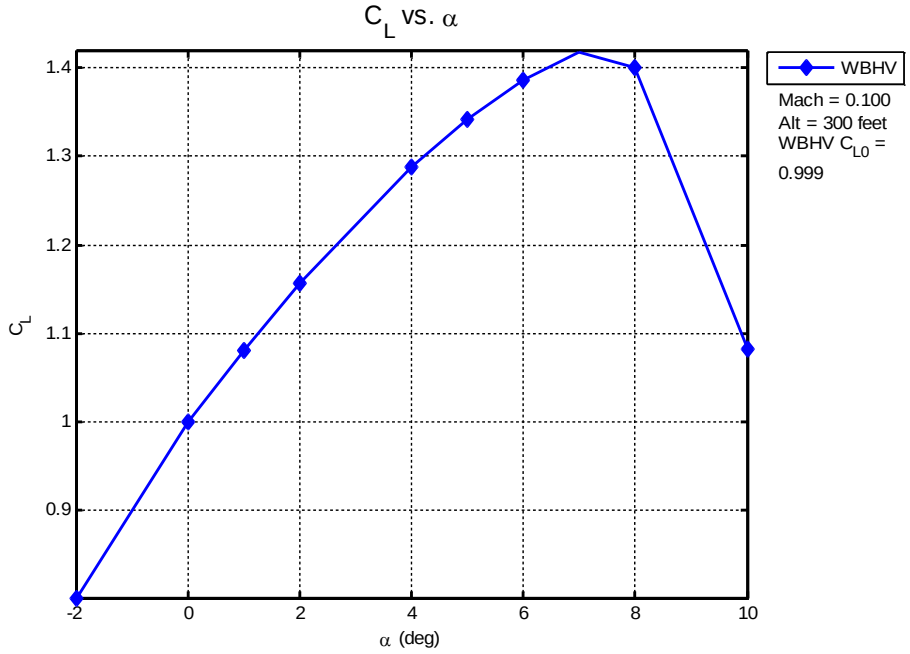

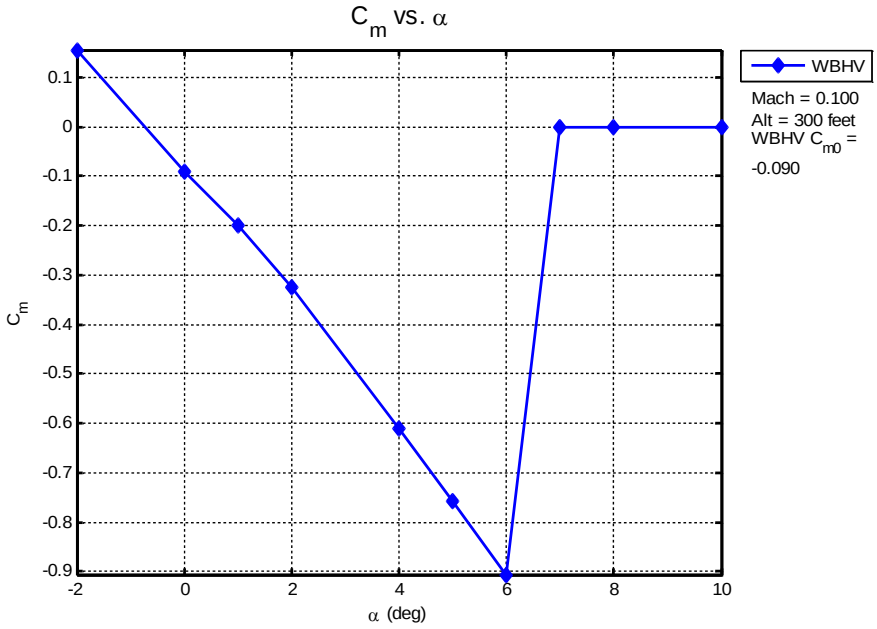
C_m vs. α
WBHV
Mach = 0.100
Alt = 300 feet
WBHV C_{m0} = -0.090
C_m
α (deg)

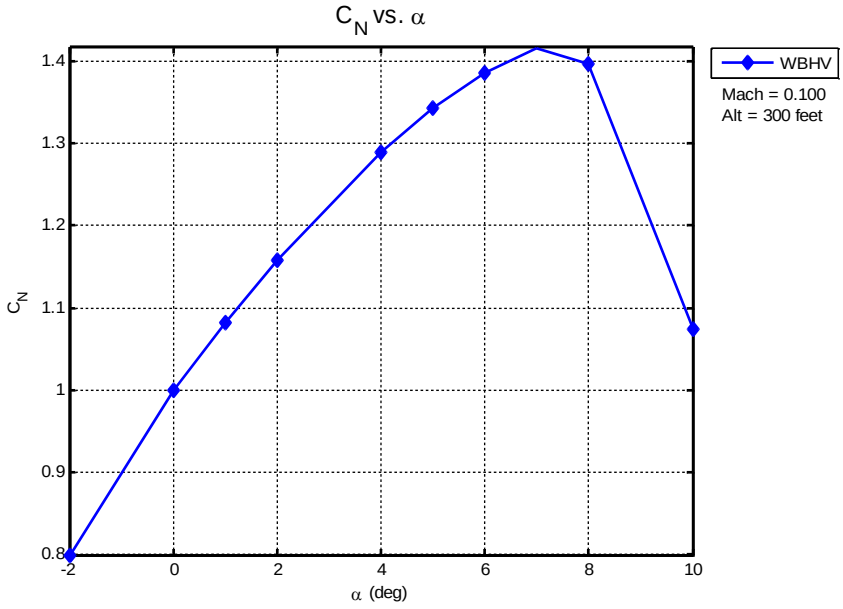
C_N vs. α
WBHV
Mach = 0.100
Alt = 300 feet
C_N
α (deg)

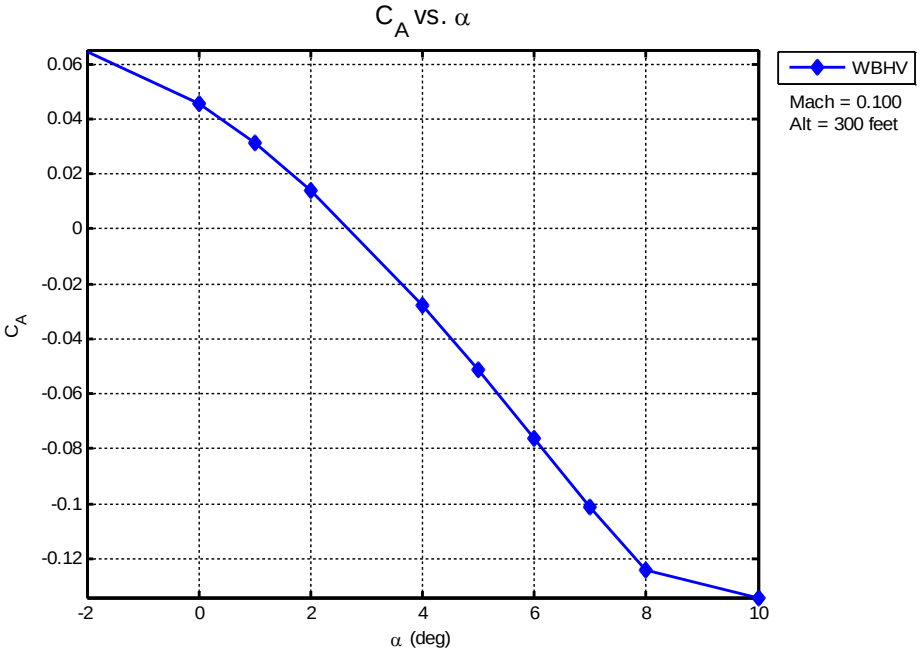
C_A vs. α
WBHV
Mach = 0.100
Alt = 300 feet
C_A
α (deg)
0.06
0.04
0.02
0
-0.02
-0.04
-0.06
-0.08
-0.1
-0.12
-2
0
2
4
6
8
10

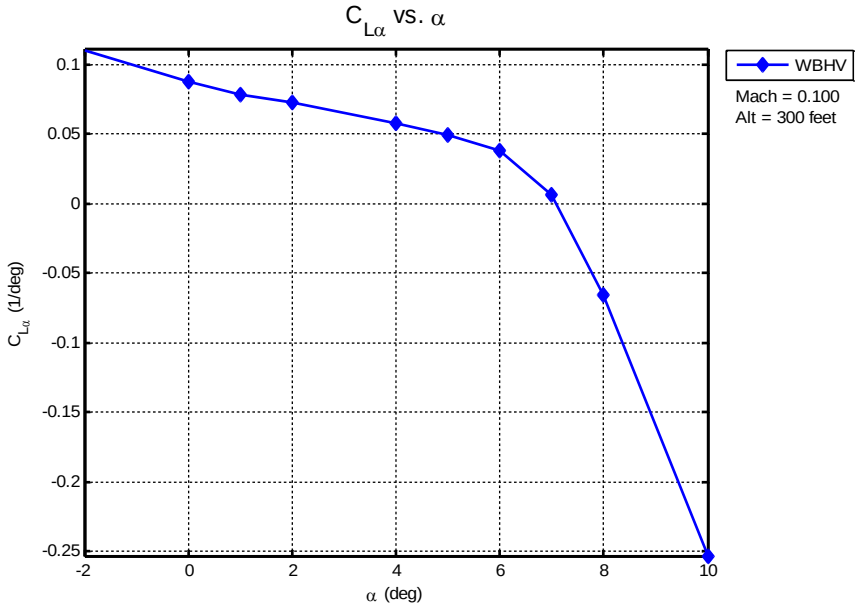
C_Lα vs. α
WBHV
Mach = 0.100
Alt = 300 feet
C_Lα (1/deg)
α (deg)
0.1
0.05
0
-0.05
-0.1
-0.15
-0.2
-0.25
-2
0
2
4
6
8
10

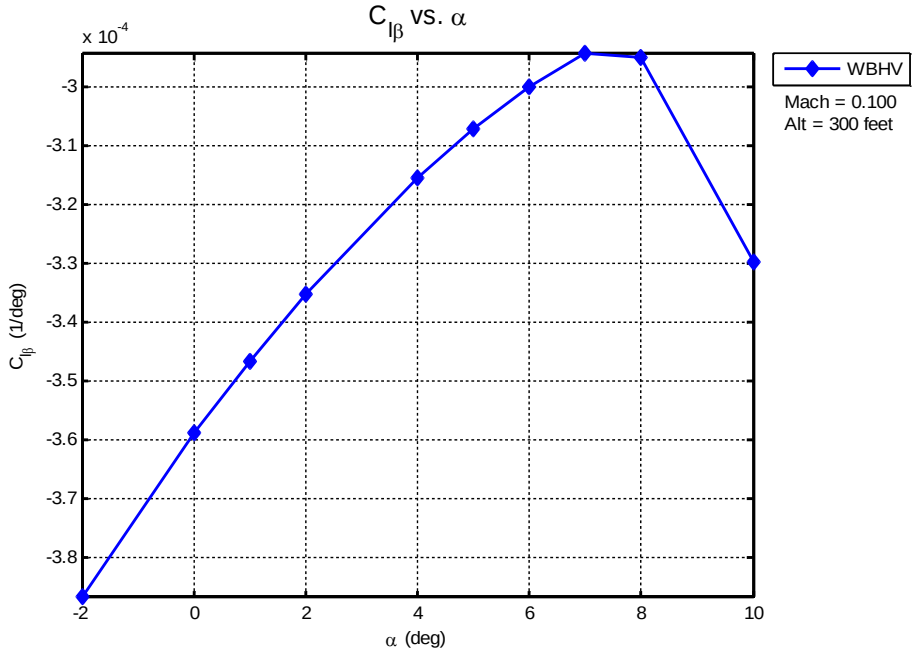
$C_{l\beta}$ vs. α
x 10^-4
-3
-3.1
-3.2
-3.3
-3.4
-3.5
-3.6
-3.7
-3.8
$C_{l\beta}$ (1/deg)
-2
0
2
4
6
8
10
α (deg)
WBHV
Mach = 0.100
Alt = 300 feet

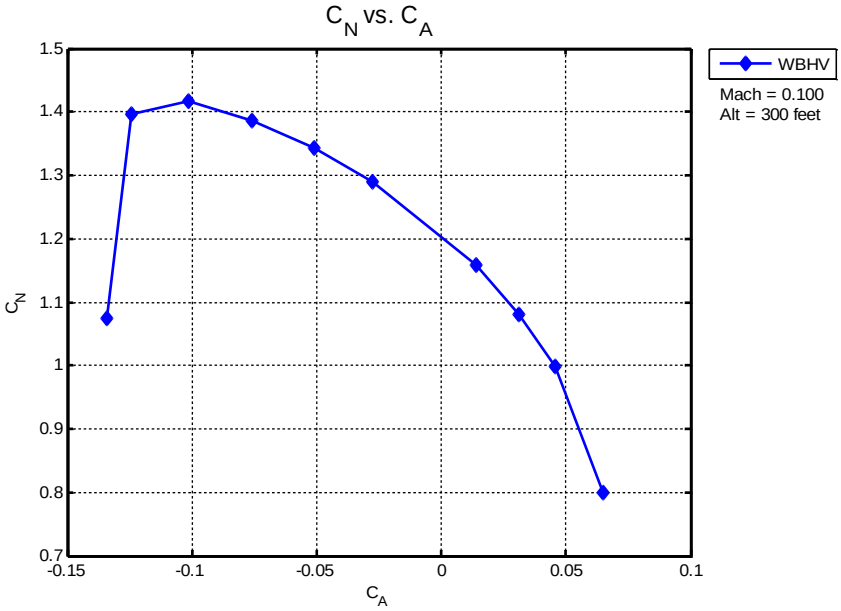
C_N vs. C_A
1.5
1.4
1.3
1.2
1.1
1
0.9
0.8
0.7
C_N
-0.15
-0.1
-0.05
0
0.05
0.1
C_A
WBHV
Mach = 0.100
Alt = 300 feet

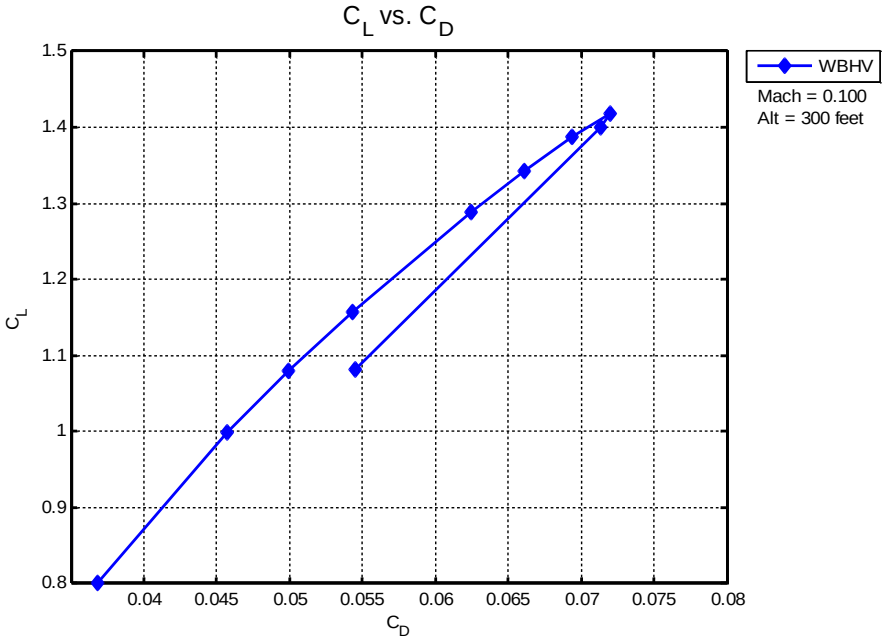
C_L vs. C_D
WBHV
Mach = 0.100
Alt = 300 feet
C_L
C_D
1.5
1.4
1.3
1.2
1.1
1
0.9
0.8
0.04
0.045
0.05
0.055
0.06
0.065
0.07
0.075
0.08

C. Pilot Inputs

a. Flight Test on April 30th 2014

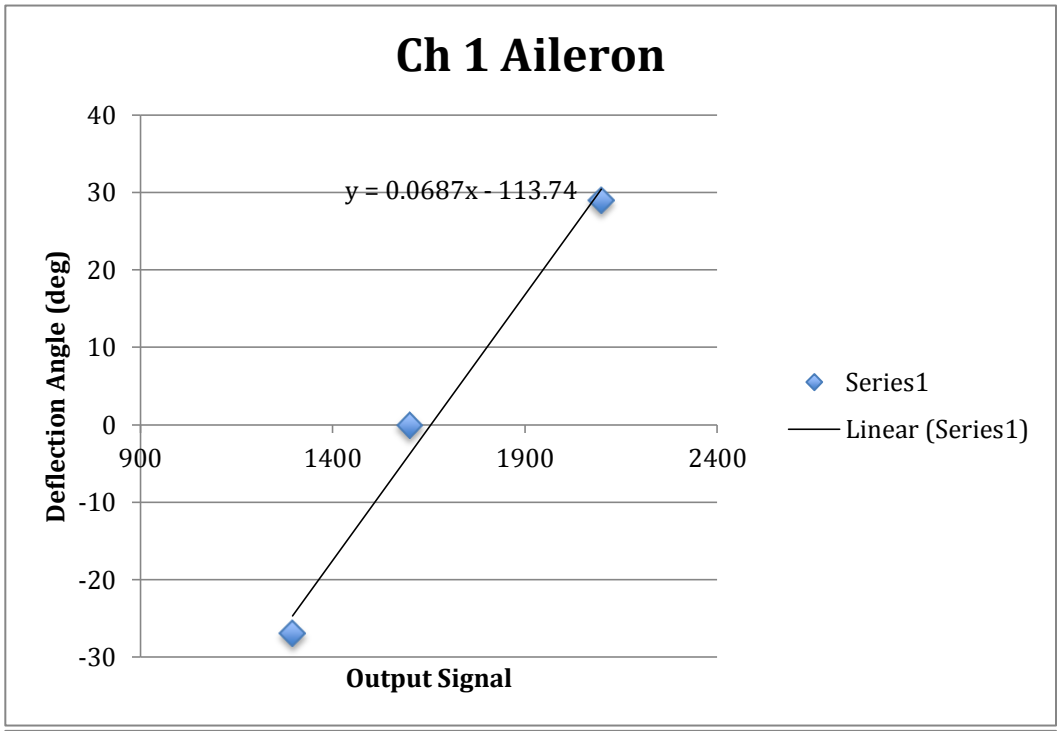

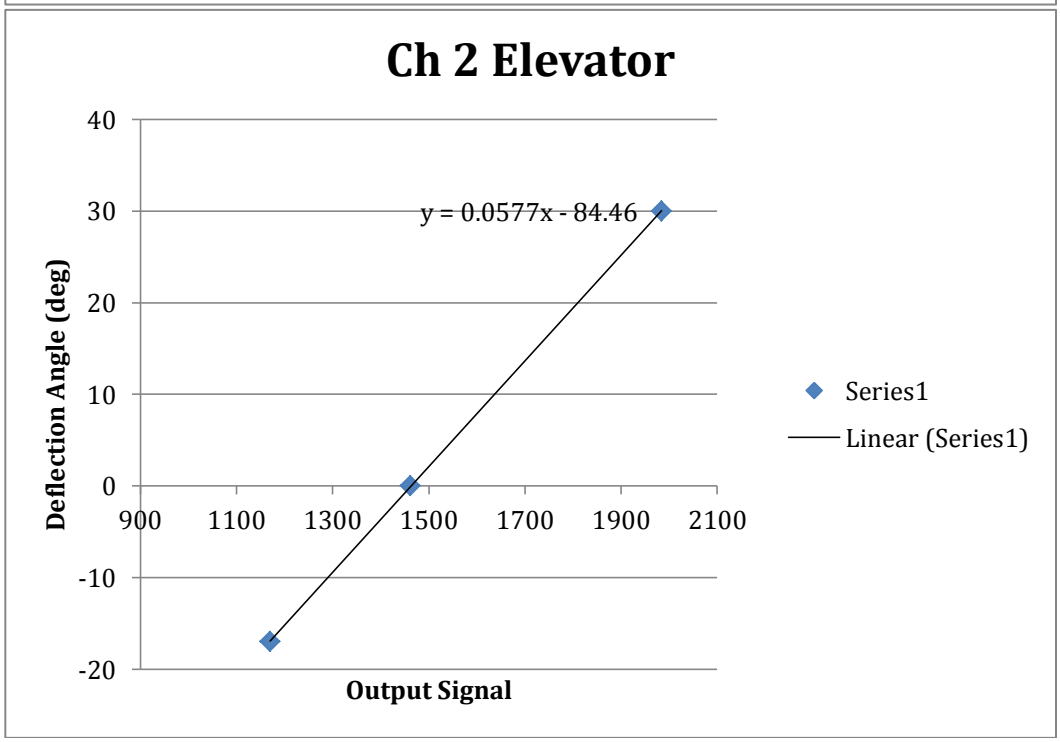

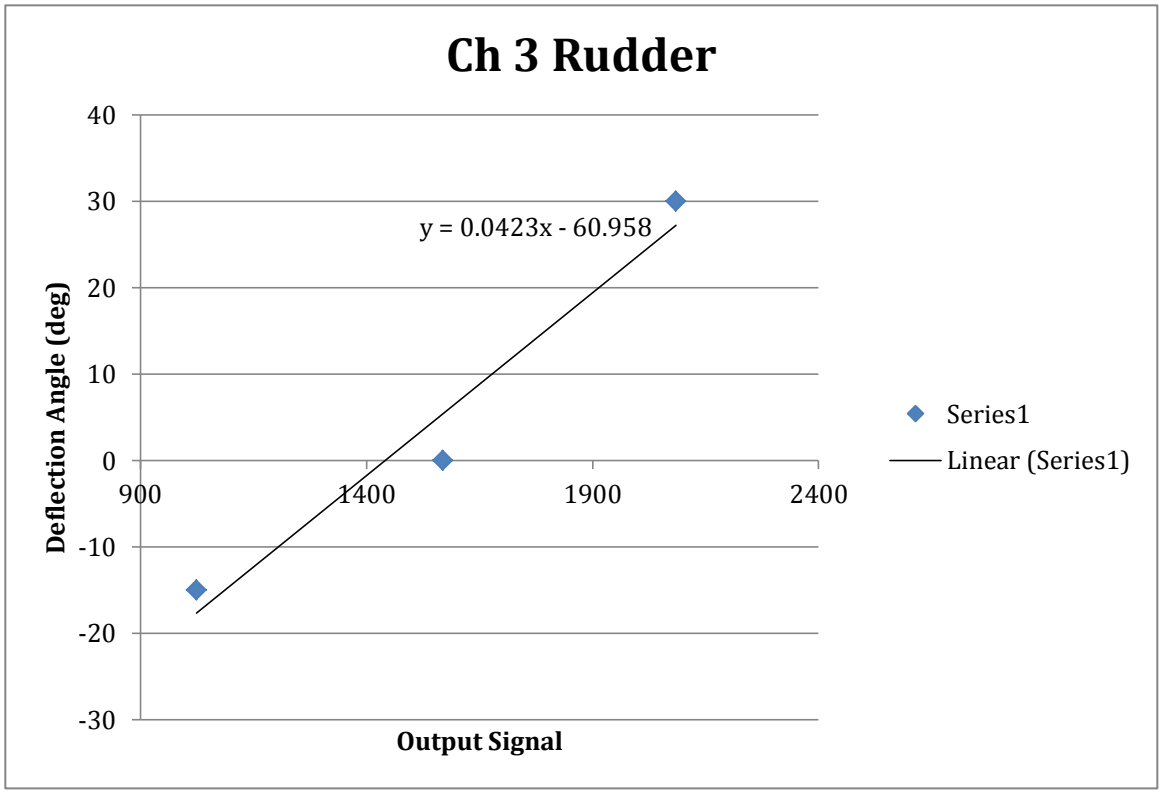

b. Flight Test on May 8th 2014 - 1

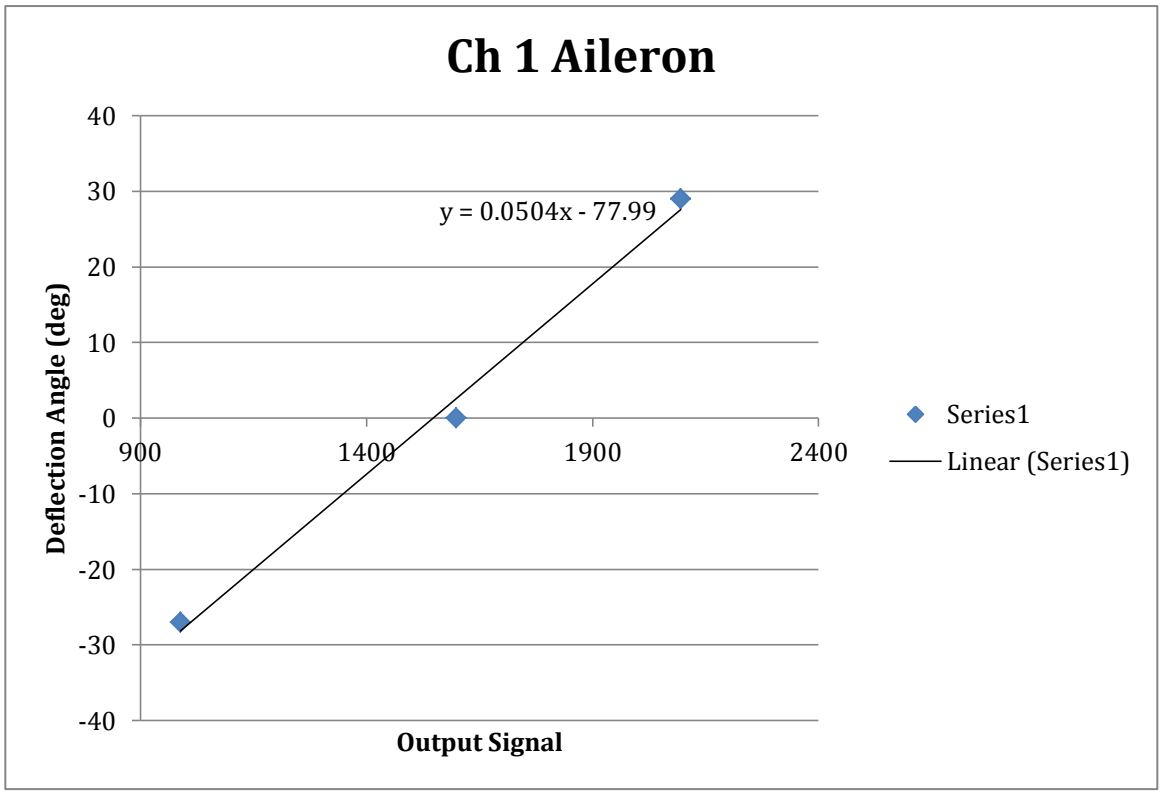

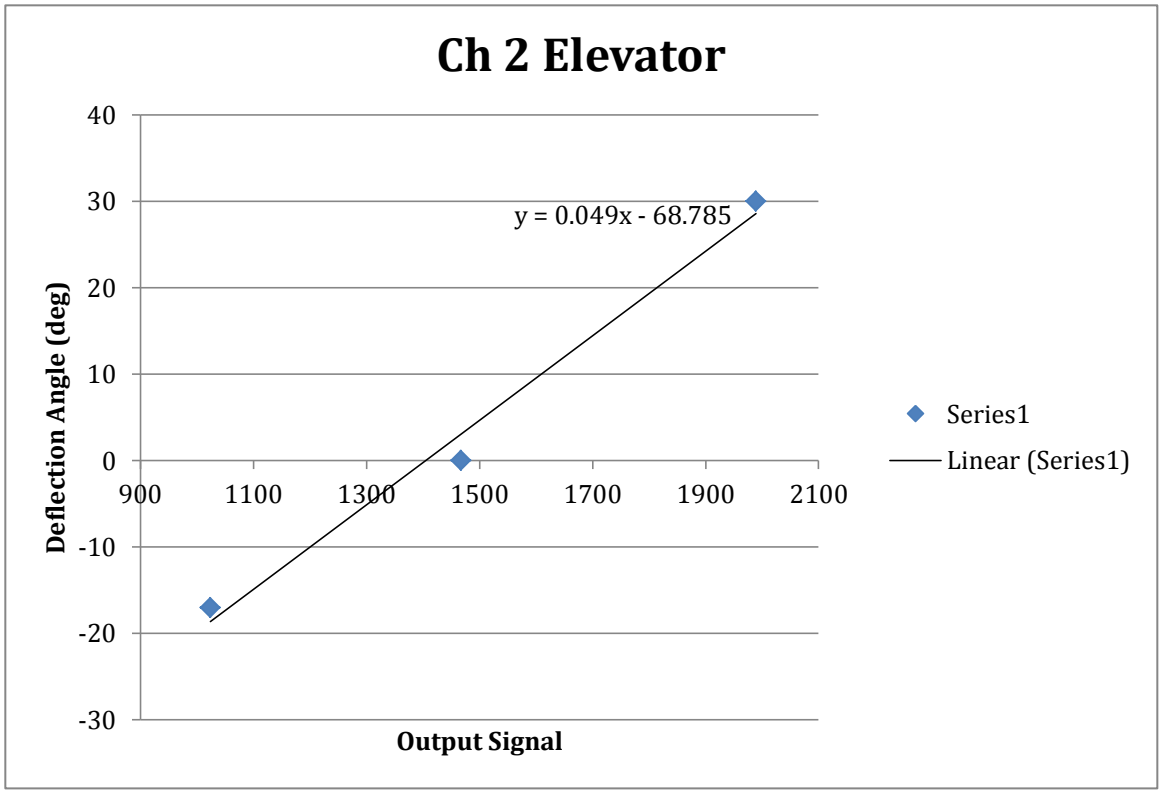
Ch 2 Elevator
40
30
20
10
0
-10
-20
-30
900
1100
1300
1500
1700
1900
2100
y = 0.049x - 68.785
Deflection Angle (deg)
Output Signal
Series1
Linear (Series1)

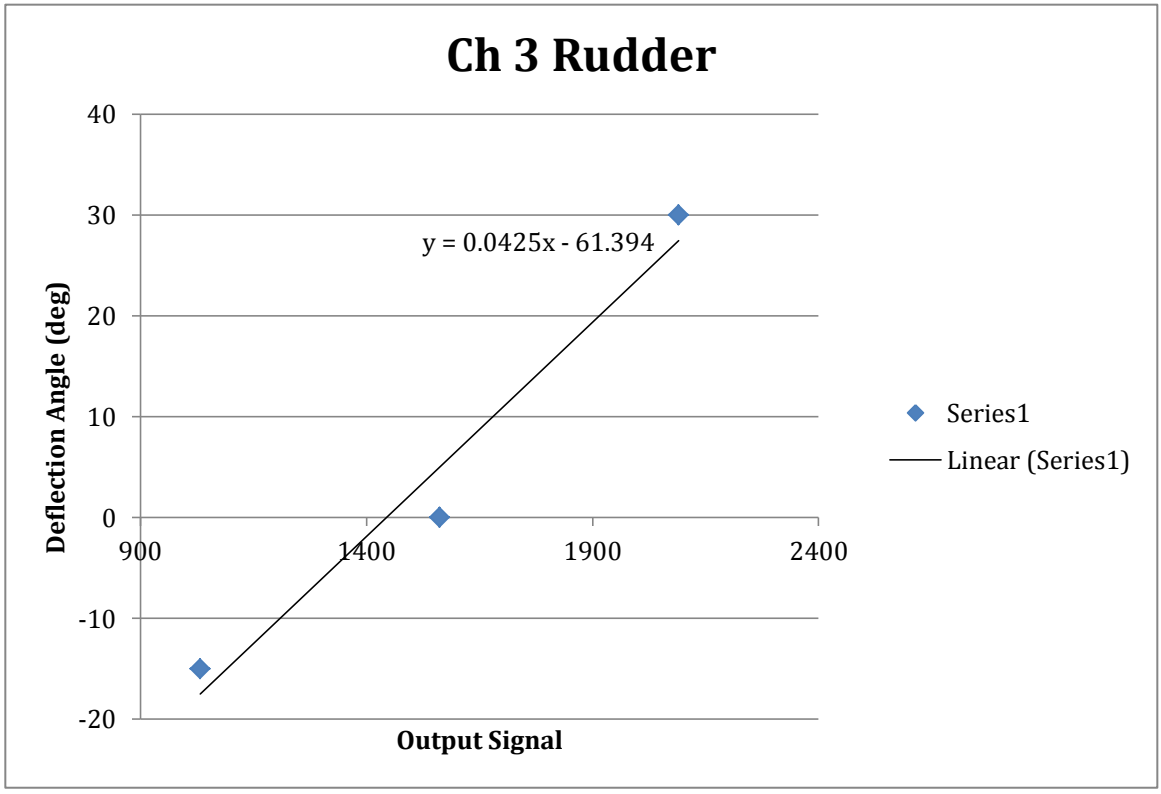
Ch 3 Rudder
40
30
20
10
0
-10
-20
900
1400
1900
2400
y = 0.0425x - 61.394
Deflection Angle (deg)
Output Signal
Series1
Linear (Series1)

c. Flight Test on May 8th 2014 - 2

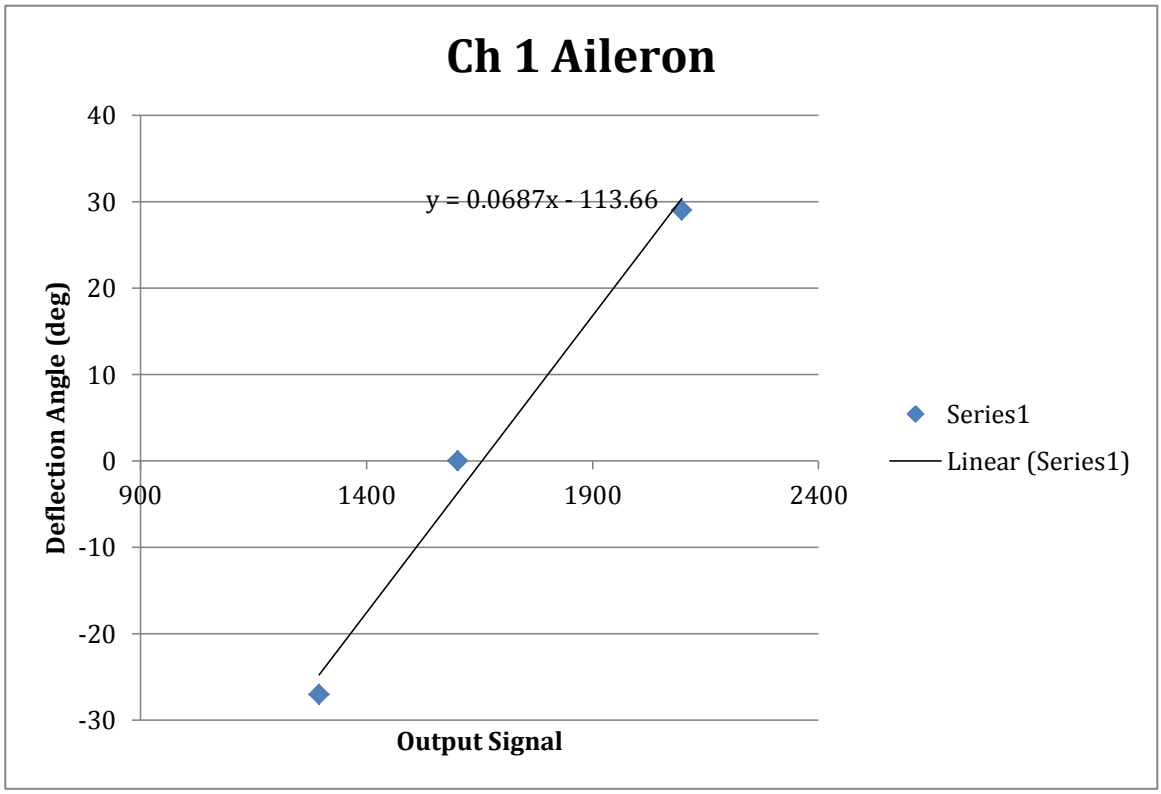

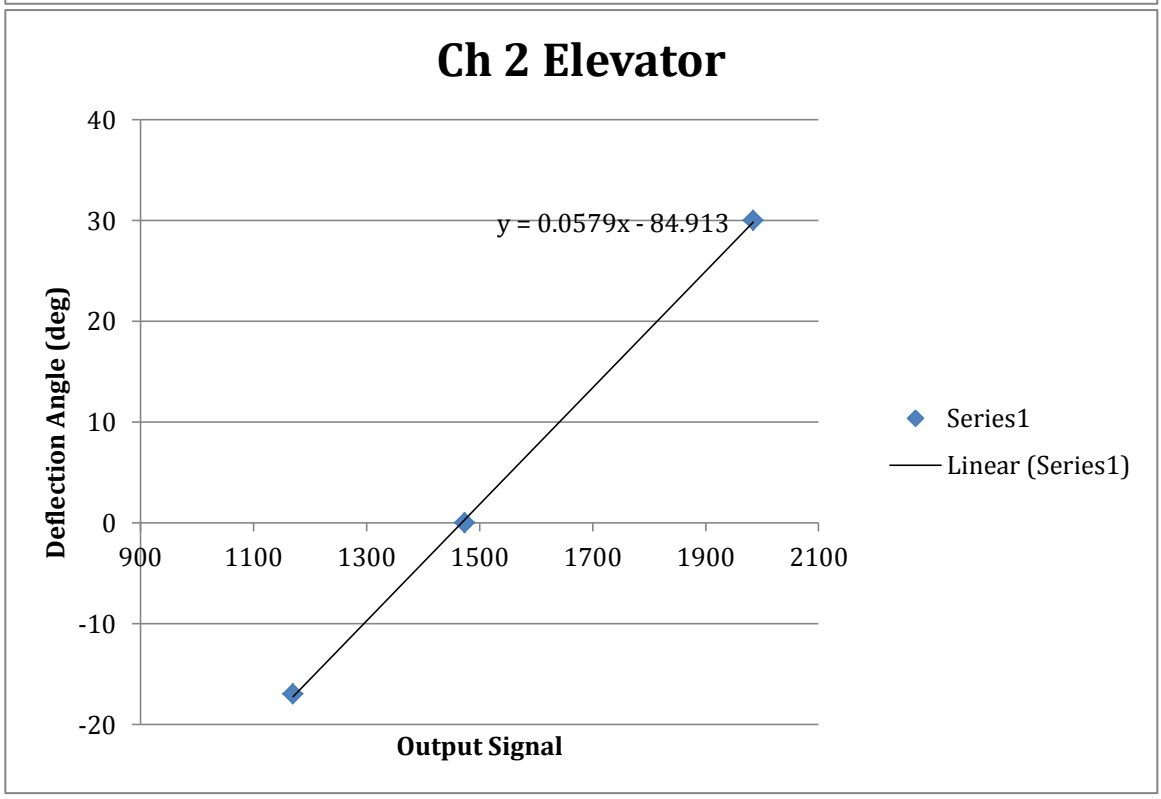

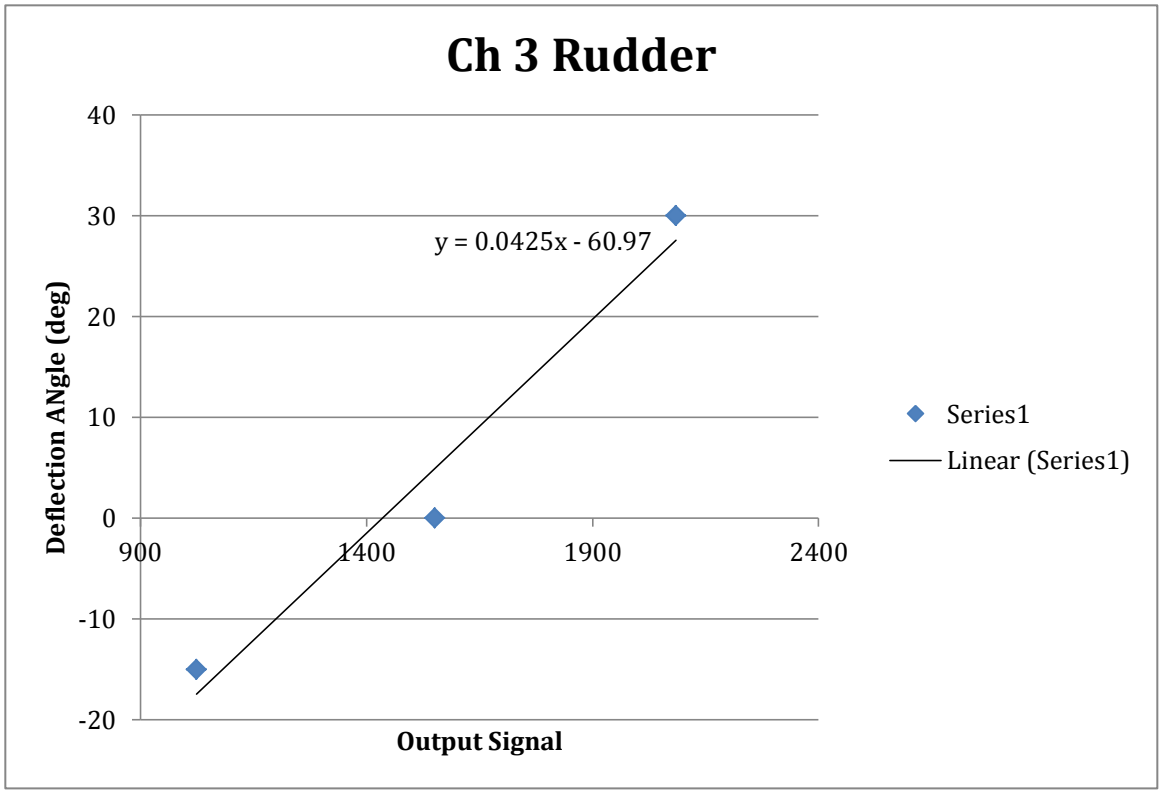
Ch 3 Rudder
40
30
20
10
0
-10
-20
900
1400
1900
2400
y = 0.0425x - 60.97
Deflection ANgle (deg)
Output Signal
Series1
Linear (Series1)

D. Graphs for Simulink Model

a. Stability Derivatives

Stability coefficient	Value	Unit
CL0	0.28	
CLa	5.65112	1/rad
CLq	7.5	1/rad
CLde	0.22735	1/rad
CLih	0	
CD0	0.0164	
CDa	0.37442	1/rad
CDde	-0.00462	1/rad
CDih	0	
CDq	0	
Cm0	0.048	
Cma	-.47318	1/rad
Cmq	-16.47972	1/rad/s
Cmde	-1.26278	1/rad
Cmih	0	
Cl0	0	
Clb	-0.9	1/rad
Clp	-0.65596	1/rad/s
Clr	0.18415	1/rad/s
Clda	-3.96308	1/rad
Cldr	0.39041	1/rad
Cn0	0	
Cnb	0.04641	1/rad
Cnp	-0.04016	1/rad/s
Cnr	0.03587	1/rad/s
Cnde	0.00462	1/rad
Cnda	0.40969	1/rad
Cndr	0.32189	1.rad
CY0	0	
CYb	-0.2595	1/rad
CYda	2.22584	1/rad
CYp	0.0075	
Cyr	0.146	
CYdr	-1.17913	1/rad

b. Trimmed Model Graphs

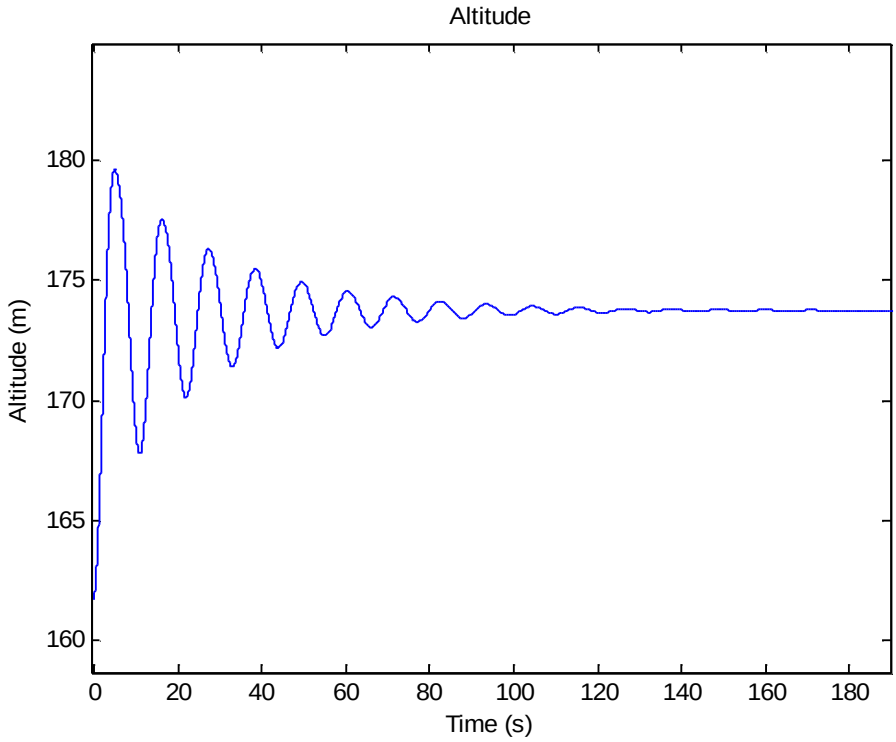

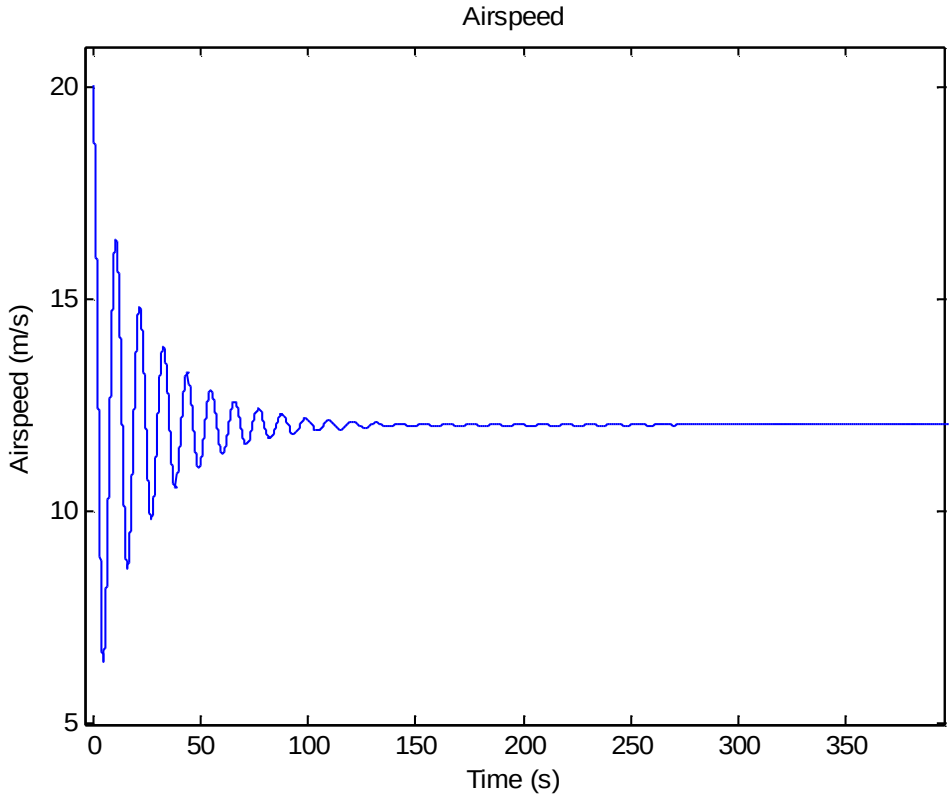

c. Doublet graphs

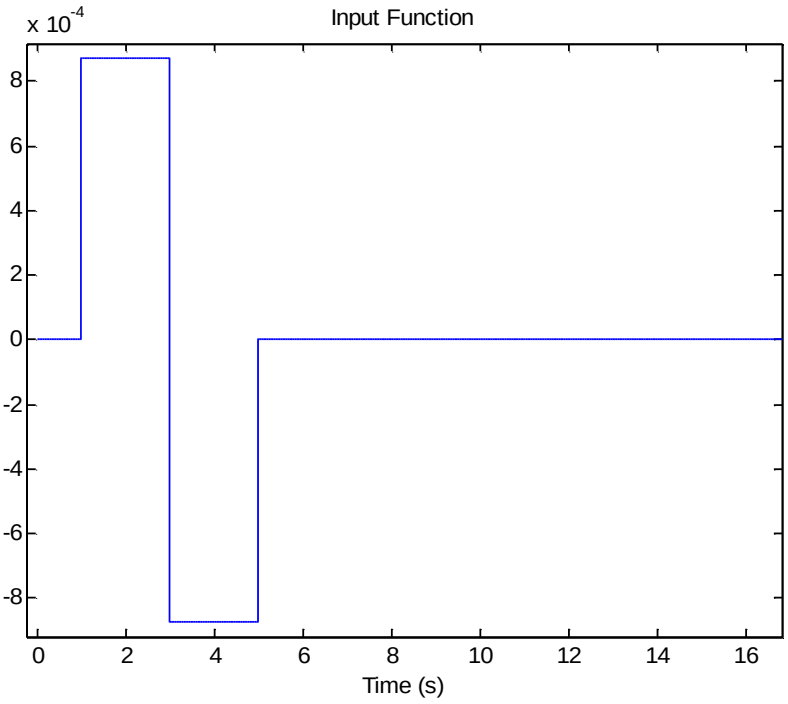

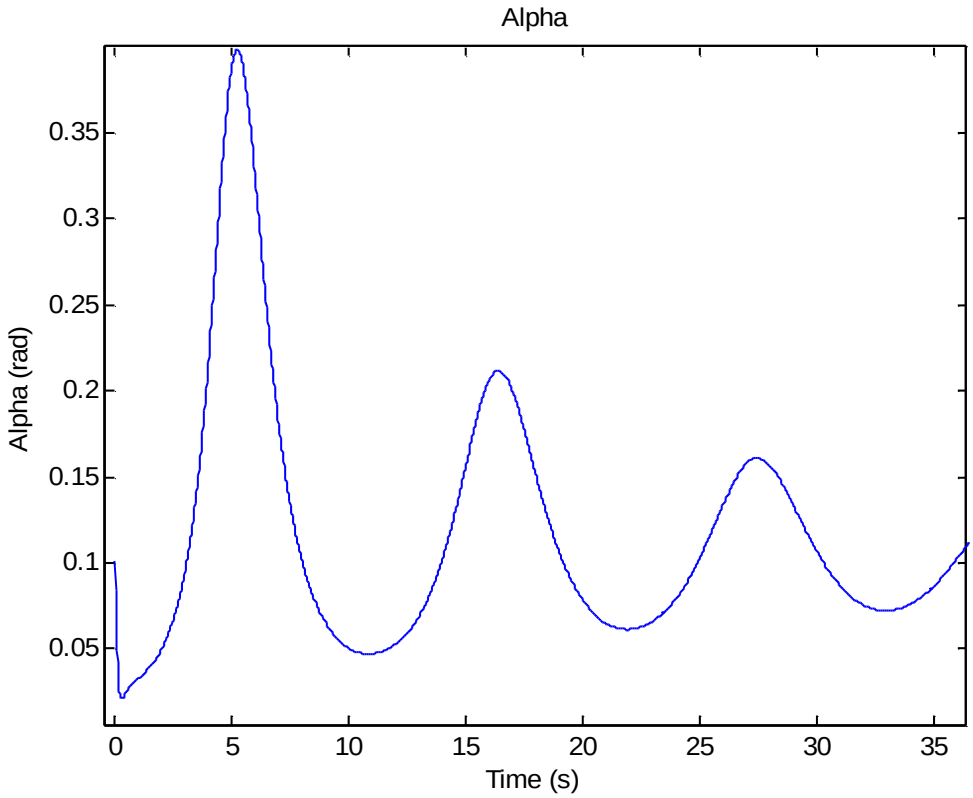

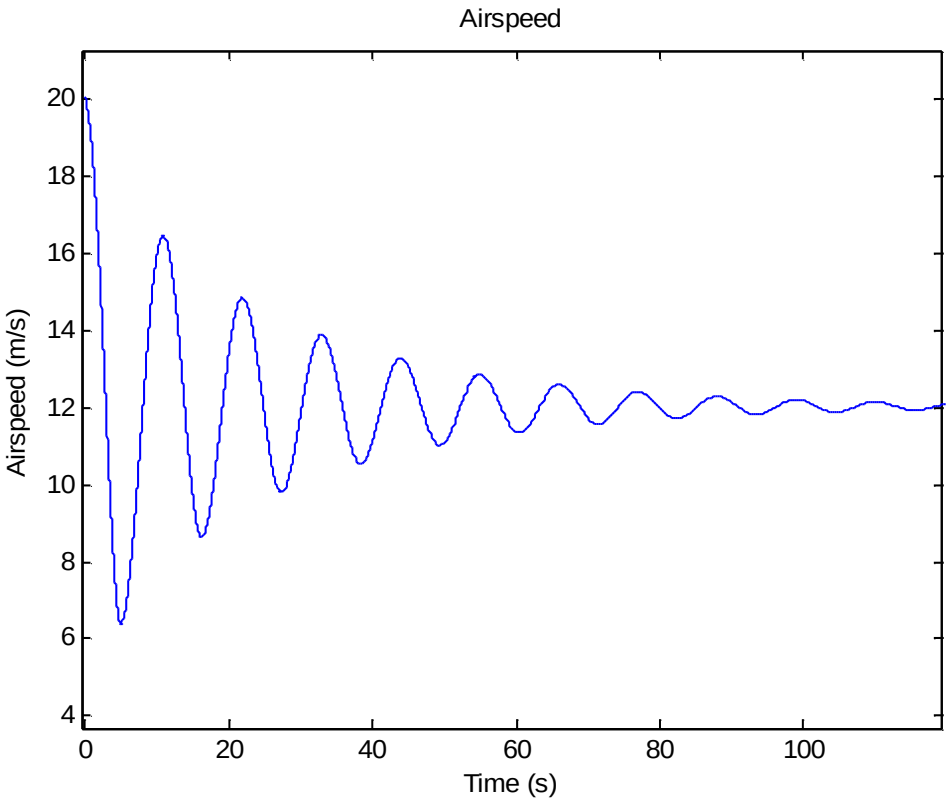
Airspeed
Airspeed (m/s)
20
18
16
14
12
10
8
6
4
0
20
40
60
80
100
Time (s)

E. Optimization

Iteration	F-count	alpha (min)	beta (min)	p (min)	q (min)	r (min)	theta (min)	phi (min)
0	1	3.52E+03	233.2719	96.7276	452.8464	120.5737	6.55E+06	319.5111
1	26	8.80E+03	1.90E+03	1.51E+03	3.09E+03	1.31E+05	6.54E+05	5.17E+06
2	29	1.11E+03	4.33E+03	3.94E+03	210.9835	2.77E+04	1.49E+06	2.13E+06
3	32	5.10E+03	1.28E+04	172.6951	1.11E+03	4.56E+04	2.45E+05	2.61E+06
4	36	5.09E+03	1.28E+04	171.3497	1.12E+03	4.58E+04	2.30E+05	2.55E+06
5	40	5.08E+03	1.27E+04	170.1352	1.12E+03	4.63E+04	2.10E+05	2.46E+06
6	53	5.08E+03	1.27E+04	170.1676	1.12E+03	4.62E+04	2.10E+05	2.46E+06
7	66	5.07E+03	1.27E+04	170.2327	1.12E+03	4.62E+04	2.10E+05	2.45E+06
8	79	5.06E+03	1.27E+04	170.7596	1.12E+03	4.62E+04	2.11E+05	2.45E+06
9	92	4.97E+03	1.24E+04	175.3959	1.07E+03	4.61E+04	2.16E+05	2.41E+06
10	124	4.94E+03	1.23E+04	174.4054	1.07E+03	4.59E+04	2.04E+05	2.35E+06
11	156	4.93E+03	1.23E+04	174.4729	1.07E+03	4.57E+04	2.04E+05	2.32E+06
12	214	4.93E+03	1.23E+04	174.4729	1.07E+03	4.57E+04	2.04E+05	2.32E+06
13	272	4.93E+03	1.23E+04	174.4729	1.07E+03	4.57E+04	2.04E+05	2.32E+06
14	330	4.93E+03	1.23E+04	174.4729	1.07E+03	4.57E+04	2.04E+05	2.32E+06
15	388	4.93E+03	1.23E+04	174.4729	1.07E+03	4.57E+04	2.04E+05	2.32E+06
16	402	3.01E+03	5.42E+03	276.9322	365.2483	4.53E+04	1.81E+05	1.16E+06
17	460	3.01E+03	5.42E+03	276.9322	365.2483	4.53E+04	1.81E+05	1.16E+06
18	467	2.85E+03	5.41E+03	267.7889	371.9185	4.55E+04	9.51E+04	8.49E+05
19	525	2.85E+03	5.41E+03	267.7889	371.9185	4.55E+04	9.51E+04	8.49E+05
20	583	2.85E+03	5.41E+03	267.7889	371.9185	4.55E+04	9.51E+04	8.49E+05
21	641	2.85E+03	5.41E+03	267.7889	371.9185	4.55E+04	9.51E+04	8.49E+05
22	699	2.85E+03	5.41E+03	267.7889	371.9185	4.55E+04	9.51E+04	8.49E+05
23	757	2.85E+03	5.41E+03	267.7889	371.9185	4.55E+04	9.51E+04	8.49E+05
24	761	2.86E+03	5.37E+03	265.175	368.6721	4.55E+04	8.43E+04	8.16E+05
25	819	2.86E+03	5.37E+03	265.175	368.6721	4.55E+04	8.43E+04	8.16E+05
26	848	2.87E+03	5.37E+03	261.9004	364.4361	4.59E+04	7.93E+04	7.99E+05
27	906	2.87E+03	5.37E+03	261.9004	364.4361	4.59E+04	7.93E+04	7.99E+05
28	965	2.87E+03	5.37E+03	261.9004	364.4361	4.59E+04	7.93E+04	7.99E+05
29	1003	2.83E+03	5.45E+03	261.2299	364.7912	4.57E+04	7.76E+04	7.96E+05
30	1062	2.83E+03	5.45E+03	261.2299	364.7912	4.57E+04	7.76E+04	7.96E+05
31	1122	4.54E+03	6.98E+03	9.41E+03	1.33E+04	9.13E+04	2.35E+07	4.12E+10
32	1182	4.54E+03	6.98E+03	9.41E+03	1.33E+04	9.13E+04	2.35E+07	4.12E+10
33	1242	4.54E+03	6.98E+03	9.41E+03	1.33E+04	9.13E+04	2.35E+07	4.12E+10
34	1302	4.54E+03	6.98E+03	9.41E+03	1.33E+04	9.13E+04	2.35E+07	4.12E+10
35	1362	4.54E+03	6.98E+03	9.41E+03	1.33E+04	9.13E+04	2.35E+07	4.12E+10
36	1422	4.54E+03	6.98E+03	9.41E+03	1.33E+04	9.13E+04	2.35E+07	4.12E+10
37	1482	4.54E+03	6.98E+03	9.41E+03	1.33E+04	9.13E+04	2.35E+07	4.12E+10
38	1542	4.54E+03	6.98E+03	9.41E+03	1.33E+04	9.13E+04	2.35E+07	4.12E+10
39	1602	4.54E+03	6.98E+03	9.41E+03	1.33E+04	9.13E+04	2.35E+07	4.12E+10

F. Stability Derivatives Comparison

Stability Characteristic	Variable	Flight Testing	Surfaces (deg)	Datcom (deg)	AVL (deg)
Lift coefficient	C_L		**1.18**	**0.999**	**1.12**
Lift curve slope	C_{La}		**0.0978**	**0.0872**	**0.1125**
Lifr curve variation wrt AoY	C_{Lb}		0	0	0
Lift variation wrt p	C_{Lp}		-0.000162	0	0
Lift variation wrt q	C_{Lq}		0.121	0	0.23975
Lift variation wrt r	C_{Lr}		0	0	0
Drag coefficient	C_{D0}		**.046**	**0.046**	.02235
Drag coefficient slope	C_{Da}		0.00673	0	0
Drag variation wrt p	C_{Dp}		0	0	0
Drag variation wrt q	C_{Dq}		0.00444	0	0
Drag variation wrt r	C_{Dr}		0	0	0
Basic pitching moment	C_{m0}		0	-0.0898	-0.2659
Pitching moment wrt AoA	C_{ma}		-0.00111	-0.1137	-0.0526
Pitching moment wrt AoY	C_{mb}		0	0	0
Pitching moment wrt p	C_{mp}		0	0	0
Pitching moment wrt q	C_{mq}		-0.280	0	-0.3971
Pitching moment wrt r	C_{mr}		0	0	0
Basic rolling moment	C_{l0}		0	0	0
Rolling moment wrt AoA	C_{la}		0	0	0
Dihedral effect	C_{lb}		-0.000116	-3.587E-04	-0.00104
Damping-in-Roll derivative	C_{lp}		-0.0113	0	-0.01243
Rolling moment wrt q	C_{lq}		0	0	0
Cross derivative due to yaw	C_{lr}		0.00318	0	-0.005066
Basic yawing moment	C_{n0}		0	0.999	0

Yawing moment wrt AoA	C_{na}		0	0	0
Directional stability	C_{nb}		0.000772	2.988E-04	0.001048
Cross derivative due to roll	C_{np}		-0.000683	0	-0.001825
Yawing moment wrt q	C_{nq}		0	0	0
Damping-in-Yaw derivative	C_{nr}		-0.000596	0	-0.001129
FY	C_{y0}		0	0	0
FY variation wrt to AoA	C_{ya}		0	0	0
Side force derivative	C_{yb}		**-0.00447**	-0.00296	**-0.004743**
Side force due to roll derivative	C_{yp}		0.000107	0	-7.565eE4
FY variation wrt to q	C_{yq}		0	0	0
FY variation wrt to r	C_{yr}		0.00247	0	0.003886
	Aileron				
Lift variation with roll	C_{lda}		-0.00112	0	0.011842
Drag variation with roll	C_{Dda}		0	0	0
FFY variation in roll	C_{yda}		0.000220	0	0.001426
MX variation in roll	C_{lda}		-0.00643	0	0.011631
MY variation in roll	C_{mda}		-0.000617	0	-0.003549
MZ variation in roll	C_{nda}		0.000530	0	-0.000237
	Elevator				
Lift variation with pitch	C_{lde}		0.00721	0	0.008957
Drag variation with pitch	C_{Dde}		0.000273	0	0
FY variation in pitch	C_{yde}		0	0	0
MX variation in pitch	C_{lde}		0	0	0
MY variation in pitch	C_{mde}		-0.0263	0	-0.035863
MZ variation in	C_{nde}		0	0	0

pitch					
	Rudder		(left)		
Lift variation with yaw	C_{Ldr}		-0.0000318	0	0
Drag variation with yaw	C_{Ddr}		0	0	0
FY variation in yaw	C_{ydr}		0.00375	0	-0.003293
MX variation in yaw	C_{ldr}		0	0	0
MY variation in yaw	C_{mdr}		0	0	0
MZ variation in yaw	C_{ndr}		-0.00109	0	0.001096

G. MATLAB Scripts

```
%Calculating the Sink Rate and Error for DAP Glider
%Alvydas Civinskas
%MSAE Thesis
%June 2014
clc
clear all
close all
load('DAP_TEST_CONV_2')                    %load test data
poly_num_user=1;                           %pick power of polynomial fit - 1 or 2
time=(1/1000)*(DAP(:,1)-DAP(1,1));         %convert to seconds
start_t=2.684e4;                           %start of selected time range
end_t=3.01e4;                              %end of time range
D=start_t:end_t;                           %making selected time range one variable
A=-(4611686018427387904*log(DAP(:,14)/101325))/546701353661673
+(4611686018427387904*log(DAP(1,14)/101325))/546701353661673; %converting 'in Hg' to m using
barometric formula and zeroing
A=A*3.28084;                               %converting from meters to ft
AA=A(D);                                   %selected altitudes in the tie range
BB=time((D));                              %selected time range vector
p=polyfit(BB,AA,poly_num_user); %using Matlab's polytfit function
%The next five lines were taken from the Mathworks website's
%example section of "Computing R^2 from Polynomial Fits"
%The next five lines were taken from the Mathworks website's
%example section of "Computing R^2 from Polynomial Fits"
%*********************************************************************
%Title: Linear Regression
%Author: Mathworks
%Date: 2014
%Code Version: MATLAB 2013
%Availability: http://www.mathworks.com/help/matlab/data_analysis/linear-regression.html
yfit=polyval(p,BB);                        %predicted y values using polyval MATLAB function
yresid=AA-yfit;                            %computing the residual values
SSresid=sum(yresid.^2);                    %computing residual sum squares
SStotal=(length(AA)-1)*var(AA); %total of sum squares of y
if poly_num_user==1                        %checking what order was used
rsq=1-SSresid/SStotal;                     %sumputing R^2 for linear regression
else
rsq=1 - SSresid/SStotal * (length(AA)-1)/(length(AA)-length(p)); %summing up R^2 for polynomial order
2
end
%*********************************************************************
err_h=8.2744;                              %calculated barometer error in feet
 err_vy_t=(2*err_h)/(BB(end)-BB(1))   %calculated average sink rate error in ft/s over time range from first
method analysis. . Multiply by 2 to add constant error
if poly_num_user==1                        %checking what order was used
vy_t=p(1);                                 %velocity of sink rate in ft/s based off of the derivative of the first order
trend line
else
vy_t=2*p(1).*BB+p(2);                      %velocity of sink rate in ft/s based off of the derivative of the trend line
end
V_air=DAP((start_t:end_t),17)*1.4667; %airspeed converted to ft/s
```

```
LD=abs(V_air./vy_t);                %instantaneous L/D
plot(BB,LD)                         %plotting instantaneous L/D
err_tot_LD=abs((LD.*((.4074./V_air)+(err_vy_t)./vy_t))); %calculating the error for L/D using the
equations #13
xlabel('Time (s)')
ylabel('L/D')
title('L/D')
LD_avg=sum(LD)/length(LD)                   %average L/D
hold on
EE=zeros(size(BB));
EE(:,:)=err_tot_LD;
errorbar(BB(1:100:end),LD(1:100:end),EE(1:100:end),'r') %creating error bars to be plotted for every
100th point
legend('Instantaneous L/D','Error')
figure(6)
plot(BB,DAP(D,11)-DAP(D,17)*1.4667)     %plotting the wind direction by taking the difference between
ground and airspeed
xlabel('Time (s)')
ylabel('Velocity(ft/s)')
title('Wind Direction')
figure(2)                           %plotting the total altitude data set and the selected range
plot(time,A)
hold on
plot(BB,yfit,'r')
legend('Entire Data Set','537.0470 s to 602.2820 s')
title('Atltitude')
xlabel('Time (s)')
ylabel('Altitude (ft)')
figure(4)
plot(BB,yresid,'-+')                %plotting the residuals for each point
title('Residuals')
xlabel('Time (s)')
ylabel('Residual')
figure(5)
plot(BB,err_tot_LD)                 %plotting the error in L/D at each point
title('Error in L/D')
ylabel('Error')
xlabel('Time (s)')
SUM_err_tot=sum(err_tot_LD)/length(err_tot_LD); %calculating the average error associated with the L/D
```

```
%Calculating the L/D with average Airspeed
%Alvydas Civinskas
%MSAE Thesis
%June 2014
clear all
clc
close all
load('DAP_TEST_CONV_2');
%%%WARNING: Using a filter will change the values of the data depending on the order and cut off
frequency %%%
[BB,AA]=butter(9,5/50);        %figuring out the nth order butterworth filter denominator and numerator
DAP(:,:)=filtfilt(BB,AA,DAP(:,:));  %using MATLAB's filtfilt to create filtered data using the respective
numerator and denominator

P=DAP(:,14)*3386; %converting from in Hg to Pa
P_0=101325; %Pa
g=9.807; %m/s^2
M=0.02896; %kg/mol
T=288.15; %K
R=8.3143; %(N*m)/(mol*K)
n=0;
for i=1:length(P)
   n=n+1;
   h(n)=-(461168601842738790 4*log(P(n)/101325))/546701353661673
+(461168601842738790 4*log(P(1)/101325))/546701353661673; %finding the altitude using the
barometric formula
end
figure(1)
h=h*3.28084;
plot(DAP(:,1),h)                %plotting the total altitude data set or comparison to selected ranges
xlabel('Time (ms)')
title('Altitude')
ylabel('Altitude (ft)')
% hold on
% plot(DAP([2.648e4:3.01e4],1),h(2.648e4:3.01e4),'r')       %plotting the selected range in red
% hold on
% plot(DAP([2.8e4:3.01e4],1),h(2.8e4:3.01e4),'k')          %plotting the selected range in black
% legend('Entire Data Set','5.5344e5 - 6.2388e5 ms','5.8386e5 - 6.2388e5 ms')
A=input('Start time')
B=input('End time')
figure(2)
D=[A:B];                        %selected time range as single variable
plot(DAP(D,1),h(D))
Time=(DAP(D(end),1)-DAP(D(1),1))/1000;
dh=h(D(1))-h(D(end));              % difference in altitude
V_s=dh/Time;                    %sink rate in ft/s by taking the difference in altitude
Airspeed=sum(DAP(D,17)/length(D));  %finding the average airspeed
Airspeed=Airspeed*1.46667;         %converting to ft/s
L_D_Ratio=Airspeed/V_s
xlabel('Time (ms)')
ylabel('Altitude (ft)')

figure(3)          %plotting the ground speed and the airspeed
plot(DAP(D,1),DAP(D,17)*1.4667)
hold on
```

```
plot(DAP(D,1),DAP(D,11),'r')
xlabel('Time (ms)')
ylabel('Velocity (ft/s)')
legend('Airspeed','Ground Speed')

figure(4)          %plotting the total data set and selected range
title('Specified Altitude ')
plot(DAP(:,1),h)
hold on
plot(DAP(D,1),h(D),'r')
xlabel('Time (ms)')
ylabel('Altitude (ft)')
legend('Entire Data Set','Selected Range')

figure(5)
plot(DAP(D,1),DAP(D,19))        %plotting the elevator deflection angle
xlabel('Time (ms)')
ylabel('Deflection Angle (deg)')
title('Ch 2 - Elevator Inputs')

figure(6)
plot(DAP(D,1),DAP(D,11)-DAP(D,17)*1.4667) %plotting the difference in ground speed and airspeed
xlabel('Time (ms)')
ylabel('Velocity(ft/s)')
title('Wind Direction')

figure(7)
plot(DAP(D,1),DAP(D,15))          %plotting selected range angle of attack
xlabel('Time (ms)')
ylabel('Alpha (deg)')
title('Angle of Attack')
```